STUDIES IN THE THEORY OF LASER MODELOCKING

A Thesis submitted in partial fulfilment of the requirements for the degree of Doctor of Philosophy

by

JOHN MICHAEL CATHERALL

Imperial College of Science and Technology

University of London

1983

"Studies In The Theory Of Laser Modelocking"

ABSTRACT

This thesis describes theoretical investigations of the modelocking of cw organic dye lasers with particular reference to the prediction of steady state operating parameters in synchronously pumped modelocking.

A detailed re-analysis of a standard technique for predicting steady state pulse shapes is presented. In this "self-reproducing profile" method, first applied to active modelocking, a simple analytic form for the profile is assumed and solutions are obtained for the free parameters by considering the dynamic equilibrium at steady state. The treatment describes the population inversion by a rate equation and requires numerous approximations.

In the above method, the presence of spontaneous emission is ignored. Consideration of this leads to a new approach which allows accurate profiles to be computed directly under certain circumstances while modelling the finite bandwidth in a particularly simple fashion. A striking similarity appears between this formulation and the Wagner- Lengyel equation for the time evolution of giant pulsing: a process which occurs under very different conditions. The rate equation approximation is again used together with a simple noise model, but no further significant simplifications are needed. The predictions differ from those of the preceeding treatment and indicate the possibility of important defects in the latter.

The evolution of the pulse from a weak start signal is followed in computer simulations, confirming the direct prediction and its stability to perturbation. Empirical consideration of the effect of noise fluctuations indicates limits to the validity of the technique.

The application of the model to passive and hybrid modelocking is considered and a large scale fluctuating regime is found for the latter. Finally, the prospects for the method without making the rate equation approximation are investigated.

CONTENTS

Chapter 1: **Introduction**

Chapter 2: **The development of synchronously pumped dye laser modelocking**

2.1 Introduction
2.2 Early developments
2.3 Consolidation
2.4 CW ion laser pumping of other dyes
2.5 Detailed investigations of pulse structure (A)
2.6 Detailed investigations of pulse structure (B)
2.7 Active stabilisation
2.8 Unidirectional ring systems
2.9 Hybrid modelocking
2.10 Hybrid rings and colliding pulses
2.11 Below 100 fs
2.12 Cavity dumping
2.13 Other synchronously pumped experiments
References

Chapter 3: **Existing theoretical treatments of synchronous pumping**

3.1 Introduction
3.2 The closed form gaussian solution
References

Chapter 4: **Direct stepping calculation of steady state profiles**

4.1 Introduction
4.2 The foundation of the stepping model
4.3 The stepping model for positive cavity detunings
4.4 Dependence of the solutions on the principal parameters
4.5 Matched cavities and the etalon filter
4.6 Stepping profiles with the filter
4.7 Noise and the filter
References

Chapter 5: **Negative mismatch : numerical evolutions**

5.1 Failure of direct stepping
5.2 Solution by matrix elimination
5.3 Numerical evolutions
References

Chapter 6: **The complete picture**

6.1 The transition from +ve to -ve mismatch
6.2 Further parameter variations
6.3 A simple analytic solution
6.4 Other theoretical treatments
References

/ctd..

Chapter 7: **Stepping model extensions**

7.1 Introduction
7.2 The etalon filter
7.3 Feedback & iteration
7.4 Hybrid Modelocking
7.5 Active Modelocking
References

Chapter 8: **Numerical evolutions**

8.1 Introduction
8.2 Pump & loss modulation
8.3 Modulation of cavity mismatch
8.4 Cavity dumping
8.5 Substantial parameter modifications
8.6 Hybrid modelocking and self-pulsation
8.6 Noise burst evolution
References

Chapter 9: **Conclusion**

Acknowledgements

1

INTRODUCTION

A normal laser oscillator contains an amplifying medium in a cavity formed by mirrors aligned for standing wave propagation or for ring operation in one or both directions. Cavity lengths vary from $10^{-5}-10^{-4}$ m (ultrashort dye lasers and some semiconductor lasers) to ~10 m (high power gas lasers) but are betweeen 50 cm and 2 m in many systems. When the time variation of the radiation is slow, propagation in the system is conveniently analysed through the cavity modes, the self-transforming field distributions. In stable confocal resonators, these have transverse amplitude profiles which are tightly confined to the axis of propagation and diffraction losses at the apertures – often the mirrors – are small. The standing wave condition also constrains the frequency to discrete values separated by c/2L (the absolute values being offset by an amount that depends on the transverse mode numbers). The time variation of the laser output depends on the relative sizes of the characteristic times T_{cav} (=[cavity length]/c), the longitudinal and transverse amplifier relaxation times T_1 & T_2, and the time dependence of the pumping.

The laser flux evolves from, and is continuously perturbed by, spontaneous emission. When the fluorescence bandwidth is large compared to the mode spacing the radiation filling the cavity can contain a large number of random fluctuations, with corresponding random the phasing of the modes. In this case the system can support a radiation profile consisting of one or more short pulses. To this imposition of order in the time domain corresponds increased order in the mode phases – the modes become "locked", by which term the effect is now known. Roughly speaking, the pulse duration is shortest when the phase profile is flat. The simplest way to organise the noisy time variation is to apply a synchronous "gate", for example, a time varying loss driven at the cavity round trip rate or a harmonic of it. Because the gate is inside the cavity and the pulse, in effect, sees it many times, the steady-state pulse duration can be shorter than the "aperture time" of the gate. Although response times of ~10ps are available from laser-driven semiconductor switches, the loss or frequency modulation is typically derived from electrically driven modulators

at frequencies of ~100 MHz and the aperture time is too long to make full use of the very large bandwidths available from some materials.

Intrinsically faster modulation is possible if the gate is driven by the signal fluctuation itself. "Spontaneous modelocking" can arise through nonlinearities in the amplifier alone, but the process is unreliable and, although much investigated in the past, the technique is not now used. Much more effective gating can be achieved using passive modelocking by a saturable absorber with a recovery time which is faster than the round trip time. The equilibrium state, in which a uniform laser signal keeps the absorber continuously bleached, can be unstable, leading to the growth of an isolated large fluctuation from the noise while the rapid absorber recovery holds down the level of other, smaller, spikes. The aperture time is then given by the absorber lifetime, T_{1b} – typically ~100 ps. In giant pulse lasers, where the amplifier population has a high intertia because of the long upper state lifetime, this process is intrinsically unreliable when the noise bandwidth is much larger than $1/T_{1b}$ (the gate can then let through more than one spike and the overall evolution can depend on the initial noise profile).

In "quasi-continuous" systems, the population lifetime of the amplifier, T_{1a}, is $\simeq T_{cav}$, and the amplification can therefore respond significantly within the round trip time. Strikingly effective pulse compression can occur when passive modelocking is applied to a quasi-continuous laser through the combined action of amplifier and absorber saturation. The passively modelocked dye laser, with $T_{1a} \simeq T_{cav} \simeq 1$ ns and $T_{1b} \simeq 100$ ps, can produce stable pulses a thousand times shorter than the absorber recovery time. The system now has two strong linearities and several characteristic parameters, different relative sizes of which lead to output which is continuous, "deterministic chaos" or continuously pulsing. For appropriate parameter values, the formation of the pulse from noise fluctuations is extremely rapid and "fully modelocked" pulses are formed with bandwidths that approach the system limit.

Useful modulation is also possible in quasi-continuous systems by direct modulation of the gain. In the synchronously pumped dye laser this is achieved by pumping with another modelocked laser, typically producing pulses which are less than $1/10^{th}$ of the duration of the round trip time of the dye laser. Successful operation requires extremely precise matching of the pump repetition rate to the round trip time of the slave cavity and performance comparable to that of passive modelocking was not achieved for some time. Nevertheless, pulse

durations of 1–2ps (100 times shorter than the pump) can be achieved, and with very careful alignment and some modification to the system this can be reduced to around 0.1 ps.

This thesis is primarily concerned with a theoretical investigation of the synchronously pumped dye laser, and, in particular, the development of a simple method of predicting the steady-state pulse profile (ch.4). The very large number of modes which are implicitly "locked" in a subpicosecond pulse makes a frequency domain analysis impractical. The time domain analysis here makes the rate equation approximation throughout and simulates the finite system bandwidth through a simple linear device. The analysis differs in approach from most existing treatments, giving results which are less complicated and generally more accurate, and underlines the equivalence between the equations of the steady-state for the dye laser pulse and the time evolution of the intensity in lasers with very different characteristic times. The precise importance of several experimental parameters is still unclear, and the published experimental reports are reviewed in detail. Existing theoretical treatments are also summarised (chs.3&6) together with a reworking of one of them. Extensive computer simulations of perturbed pulse evolution in a simple numerical model are presented (ch.8) and applications to related systems are considered (ch.7).

2

THE DEVELOPMENT OF SYNCHRONOUSLY PUMPED DYE LASER MODE LOCKING

2.1 Introduction

The technique of dye laser modelocking by synchronous gain modulation has developed steadily since the first demonstration in 1967, achieving to date a minimum pulse duration that is almost three orders of magnitude shorter than the early results. The early phase, in which pumping by short bursts of modelocked pulses showed that such modulation could indeed be reflected in the dye laser output, has been succeeded by the gradual improvement of continuously pumped systems and the reduction of the pulse durations obtained from them. It has become clear that the successful generation of ultrashort pulses imposes stability and synchronism requirements which are extremely, and perhaps unexpectedly, stringent. Furthermore, the techniques available for evaluating the pulse profiles are either of inadequate resolution (streak cameras) or are significantly ambiguous (nonlinear autocorrelations). Although the accumulation of performance data is in reasonable agreement on certain qualitative features, direct comparison of experiments is difficult.

The behaviour of the laser depends sensitively on several parameters, none of which can be subjected to accurate absolute determination. There is growing evidence that the system now widely used, pumped by acousto-optically modelocked argon or krypton ion lasers, often generates pulses with substantial sub-structure which is largely obscured by the normal diagnostic techniques. Some reports contain pointers to this, but direct comparison is often prevented by the omission of a parameter value which at the time may not have seemed to be of interest (e.g. the level of the pumping relative to threshold). The reduction of the pulse durations obtained from typical CW systems has reached a limit at a value which is significantly longer than that imposed by the bandwidth of the dyes. The performance has been improved by incorporating saturable absorbers and, more recently, through "colliding pulse" operation - the mechanisms of which are still obscure.

This chapter reviews much of the experimental literature, treating the mainstream of the development as the search for stable pulses of the shortest duration. Many papers report the observation of bandwidth-limited pulses with profiles of simple analytic form, such as gaussian or single-sided exponentials, together with an appropriate value of the time-bandwidth product. These claims are reproduced in this summary but the substructure picture, mentioned above, means that they must be viewed with caution in many cases.

2.2 Early developments

The development of synchronously pumped modelocking began with the first successful modelocking of the dye laser itself. In 1967 Glenn, Brienza and de Maria [1] used the second harmonic of the ouput from a modelocked Q-switched Nd:glass laser to pump solutions of rhodamine 6G (Rh-6G) and rhodamine B (Rh-B). The broad absorption bands of the dyes allowed efficient use of the pump energy while it was hoped that the broad emission spectra might allow the production of picosecond pulses over a wide range of visible wavelengths. Lasing was observed when the dye cavity length was equal to 1,1/2 and 1/3 times the pump cavity length "satisfying the modelocking condition". The narrowness of the observed spectra was attributed to the fact that the laser was operated close to threshold.

Soffer and Lin [2] also used Nd:glass pumping of Rh-6G and found laser action for various integral cavity length ratios. Noting that the fluorescence lifetime of the dye was longer than the pulse separation, they felt that the dye would be ineffective as a bleachable absorber and viewed the modelocking, as did Glenn et al., in terms of the periodic gain modulation by the pump. (Both of these observations are of limited validity: the work of New [3,4,5] has shown that USP generation does not require fast absorber lifetimes while the work presented here will place the role of gain modulation in different perspective). Pulse durations were measured by the two photon fluorescence technique which was then known to have lead to erroneous conclusions concerning contrast ratios and there were already indications that full achievement of the modelocking potential of the dyes was not going to be simple. Pulse widths of ca. 10 ps were not affected by variations in the cavity configuration or substantial increases in the pump power. The authors considered the possibility that the observed pulse widths might be affected by frequency sweeping and by averaging over fluctuations within the pulse train.

Although rhodamines have remained the most widely used dyes, a number of others have been used successfully, and, indeed, some of the first experimental results were obtained from carbocyanines. Bradley and Durrant [6] pumped a dicarbocyanine solution with pulses from a Q-switched modelocked ruby laser and again observed lasing at integral cavity ratios while the high gain resulted in broader spectra. At infrared wavelengths, Derkachyova et al. [7] pumped polymethylene dyes directly with a modelocked Nd:glass laser, observing appropriate pulse separation for several cavity length ratios, and concluded that the spectral width indicated pulse durations of 0.1 ps "in the case of complete modelocking".

During the early 1970's experimental effort was concentrated on saturable absorber modelocking and pulse diagnostic techniques improved in step. In 1974 Royt et al. [8] returned to synchronous pumping and published streak camera investigations of individual pulses from a Rh-6G laser pumped by frequency doubled Nd:glass pulses. The streak camera allowed them to measure the relative delay of the pump and signal pulses as well as the effect of cavity length changes on the pulse duration. Although not a precision experiment by recent standards, the results were significant. When the cavities were matched, the dye pulses closely followed the pump pulses, being about 50% longer. The pulses doubled in length for cavity mismatches as short as 0.5 mm. For short cavities the pulses developed a long leading edge ahead of the pump pulse and a shorter trailing edge following the pump. In contrast, when the cavity was lengthened the signal pulses were substantially delayed relative to the pump. For large positive detunings a periodic spike structure, related to the mismatch, appeared. The former observations are in reasonable agreement with our (and certain other) numerical models while the latter was probably the first evidence for the importance of noise fluctuations in mismatched cavities.

Goldberg and Moore [9] used frequency-doubled Nd:YAG to pump a thin jet of solutions of a number of dyes and achieved tunable transform-limited pulses as short as 12 ps using intracavity etalons. Streak camera photographs of single pulses yielded the same result as Royt et al. [8]: for cavities shorter than match, the dye pulse overlapped with the pump and stretched ahead of it while for longer cavities the pulse arrived after the pump. Oscilloscope displays of the transmitted pump and dye pulse trains showed evidence for recycling of the amplifier population. For longer cavities, when the dye pulse arrived at the amplifier after the pump, a significant fraction of the pump pulse was

transmitted, while for shorter cavities the pulse overlap allowed greater extraction of energy from the pump resulting in a substantial drop in the transmitted pump power.

These early methods all used the output from Q-switched solid-state lasers which produce pulse trains lasting for tens of nanoseconds. This is not long enough to produce well modelocked pulses even though the gain in the dye may be substantial. In 1974 Dienes [10] published the first account of the CW technique which is now widely used. Following the successful passive modelocking of dye lasers pumped by CW argon ion lasers (Ippen et al. [11]), they used acousto-optic modelocking of an argon laser to provide continuous synchronous pumping of Rh-6G. Dye pulses of 125 ps from 160 ps pump pulses were reported but no details were given. The first details came from Chan and Sari [12]. The dye solution was now in a thin free-flowing stream instead of the closed cells of the early experiments, with the consequent improvement in stability and optical qualtity. Resonance was seen for dye cavity lengths of 1,2 and 3/2 times the one metre length of the Ar^+ cavity although mismatch tolerances were not specified. One important feature was established, however. The durations of the dye pulses were measured by autocorrelation using second harmonic generation of the first kind and showed a pulse width of approximately 3 ps. The SHG contrast indicated complete modelocking which was supported by simple spectral measurements (the intracavity bandwidth was controlled by a prism). The system was therefore able to produce pulses which were substantially shorter than the 160 ps pump pulses.

The results of Chan and Sari were quickly followed by those of Harris et al. [13]. Again Rh-6G was pumped by Ar^+ pulses, but this time a low loss oscillator was cavity-dumped by a Bragg deflector and could be tuned with a Lyot filter from 570 nm to 590 nm. The cavity lengths had to be matched to within 0.5 mm, which, although surprising in view of the pump pulse duration, was explained in terms of the amplification of small mismatches during the long cavity lifetime. As Chan and Sari had noted, the energy conversion was good and the system did not suffer from the wavelength tuning restrictions imposed on passively modelocked systems by the dye spectra.

2.3 Consolidation

Chan et al. [14] presented the first detailed autocorrelation measurements of the effect of length tuning. From Ar^+ pulses as long as 1 ns they obtained

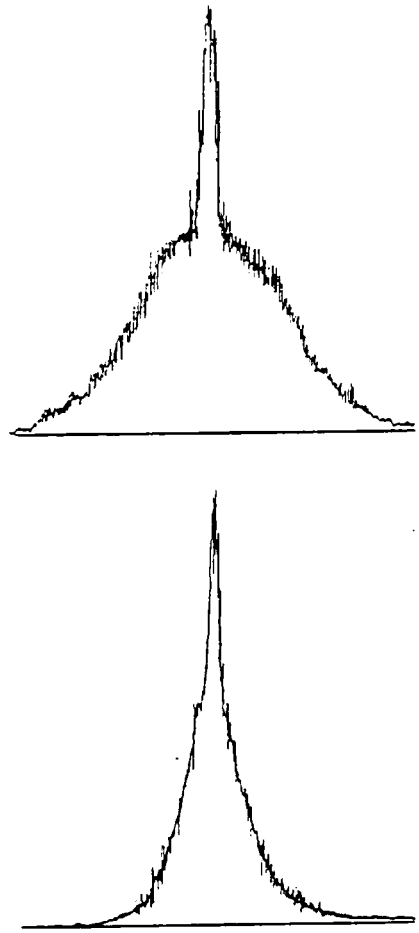


FIG. 2.1 : Typical Background-free Autocorrelations

rhodamine pulses down to about 50 ps in duration, although SHG autocorrelations (1st kind) showed incomplete modelocking. The pulse duration was found to increase with pump power but this was thought to be an effect near threshold. They also found that the cavity length had to be tuned to within 10μ to obtain the sharpest pulses and noticed, as have a number of subsequent workers, that the cavity length for the sharpest pulses (measured by the maximum 2^{nd} harmonic generation) differed from the length giving the maximum average power. The pulse width was much more sensitive to length detuning then was the average power. It was also found that the addition of a very small amount of the saturable absorber DODCI to the dye stream seemed to stabilise the laser power while larger amounts raised the pumping threshold without affecting the pulse durations. This incorporation of small quantities of saturable absorber, now referred to as hybrid modelocking, has become increasingly important but its effect has not yet been satisfactorily explained: we shall return to it later.

By now the typical cavity configuration comprised a 3-mirror folded cavity (Kogelnik et al. [15]) 1 to 2 metres in length. The pump pulses, with durations between 80 and 200 ps, were focussed into a jet stream of the dye, typically a few hundred μ thick. It had been found neccessary to limit the lasing bandwidth with intracavity devices such as prisms or etalons to obtain good modelocking. de Vries et al. [16] found that their pulse durations depended critically on the cavity matching but were ultimately limited by the tuning element. Using a 3-element Lyot filter they obtained pulses of 7.5 ps duration (which were transform-limited assuming gaussian profiles) while the duration reduced to 4.5 ps with a 2-element filter. A sampling oscilloscope showed that there was a single pulse circulating in the cavity and that, under optimum conditions, the pulse first passed through the jet stream between 50 and 150 ps later than the peak of the pump. Fluorescence measurements indicated that this resulted in roughly equal gain for the pulse on its two passages through the amplifier.

Frigo et al. [17] conducted a detailed investigation of the pulse forming process in a typical Rh-6G system. Pulses as short as 10 ps, tunable from 570 to 650 nm, were obtained with conversion efficiencies as high as 40%. The laser output was used to probe both the dye fluorescence and the pump pulse itself by sum frequency up-conversion in ADP. The dye pulses were short enough to resolve clearly the major features of the evolution of the gain (via the fluorescence), shown in fig. 2.2. From a low background level, caused by residual inversion from the preceeding transit, the gain rose rapidly, closely following the

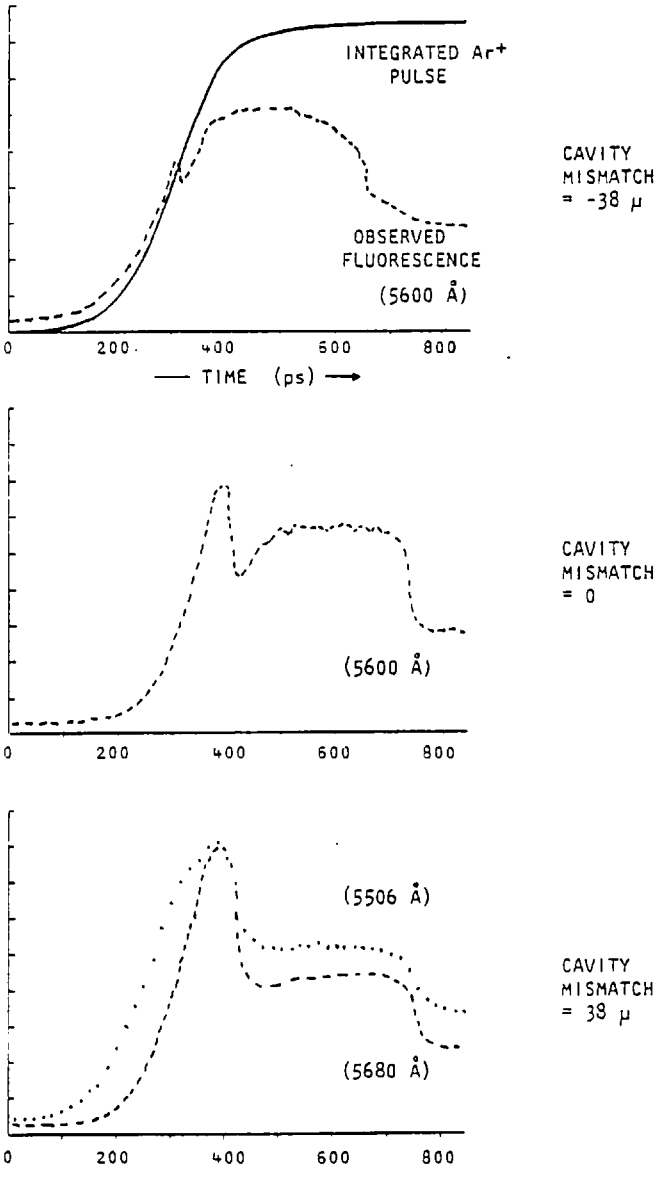


FIG. 2.2 : Gain Fluorescence

(from Frigo et al. [17])

computed integral of the pump. A sharp dip towards the end of the pump indicated the first passage of the dye pulse, followed 300 ps later by a second dip as the pulse returned from one of the mirrors. The absence of other dips indicated that only one pulse circulated in the cavity. This was confirmed by autocorrelations of the pulse which showed the presence of satellites only at extreme operating conditions such as large shortening of the cavity. Under these conditions mode-locking was incomplete. Satellite pulses also arose at high pumping powers when the pulse was followed by a low pedestal or even a second pulse.

The effect of cavity mismatch on the relative delay of the pump and signal pulses could be seen clearly. For a cavity 38 μ shorter than optimum (determined by the maximum 2^{nd} harmonic power), a weak signal pulse arrived early in the pumping and the autocorrelation showed the pulse to have a long tail. At optimum, the pulse arrived towards the end of the pump pulse and was further delayed when the cavity was lengthened by 38 μ. Good modelocking, producing bandwidth-limited pulses, was limited to this range. The time shift in the pulse relative to the pump was considerably greater than the cavity mismatch causing the shift.

The first generation of subpicosecond pulses by synchronous pumping of rhodamines came in 1978 from Heritage and Jain [18] who used a tandem arrangement to reduce the duration of the pump pulses. A standard synchronously pumped Rh-6G system drove a similar Rh-B laser, the former using 4-prism tuning and a substantial output coupling of 70% to give 55 ps pulses from the 100 ps Ar^+ pump. Rh-B pulses of 0.8 ps were tunable over a limited range with a prism or Lyot filter. The authors attributed the pulse compression to the short duration of the pump pulses, although they noted that they had been able to generate Rh-6G pulses of just 1.7 ps directly from the Ar^+ pump. Moreover, the use of shorter Rh-6G pulses in the tandem arrangement did not further shorten the Rh-B output, suggesting that factors such as dispersion were also important.

It was soon demonstrated that pulses of the same duration could be obtained from direct Ar^+ pumping if greater attention was paid to stability, both of the resonator and the ion laser modelocker. Ferguson et al. [19] obtained 0.85 ps pulses at 600 nm from 150 ps Ar^+ pumping with 20% output coupling. The pulses were almost bandwidth-limited and the best autocorrelations lacked coherence spikes. Cavity mismatch was investigated by adjusting the modelocker frequency and revealed a sensitive and asymmetric dependence in accord with Scavennec's numerical results [20]. Increasing the frequency caused

a slow increase in the pulse width and the appearance of coherence spikes in the autocorrelations. On the other hand, a decrease of just 30 Hz in 41 MHz caused the pulse to broaden abruptly to 50 ps. Reducing the output coupling to 5% produced a broad stable satellite pulse separated by 50 ps from the initial subpicosecond pulse. Tandem pumping of Rh-101 with the Rh-6G output did not produce shorter pulses than with direct Ar^+ pumping – a clear indication that pump duration is not the only factor limiting the pulse duration.

Using a very stable rf oscillator to produce 100 ps pump pulses, Jain and Ausschnitt [21] obtained pulse durations of 0.6–1 ps by increasing the filter bandwidth of the 3-mirror folded cavity. Alteration of the pump power necessitated adjustments to both the output coupling and the cavity length to maintain the best performance. The pulse shapes were sensitive to a mismatch of ca. 2 μ and the shortest pulses were obtained by shortening the cavity by 5 to 10 μ from the length giving maximum power. As had been observed by Frigo et al. [17], the synchronously pumped system allows the equilibrium pulse profile to be changed by tuning the cavity length since this affects the time of arrival of the dye pulse relative to the pump. Jain and Ausschnitt considered that the earlier arrival of the pulse when the cavity was shortened led to loss of power and consequently compresssion of the pulse. Some results were interpreted as bandwidth-limited pulses of single-sided exponential profiles. Further length compression was possible with increased bandwidth but with the introduction of significant background intensity level or a satellite pulse. In general, increasing the pump power and the output coupling together resulted in shorter pulses, although a satellite, typically 15–30 ps away from the main pulse was often present. The wavelength tuning range was reduced at high output couplings.

In a second paper (Ausschnitt and Jain [22]), the authors presented experimental support for a simple analytical prediction of the steady state pulse in which the pulsewidth was proportional to the square root of [pump duration / cavity bandwidth]. 100 ps Ar^+ pulses pumped a Rh-6G system in which the cavity bandwidth was controlled by birefringent elements. Autocorrelation widths for different combinations of cavity loss, pump power and bandwidth showed a good linear plot against $\sqrt{[\text{pump duration} / \text{bandwidth}]}$ over a variation of a factor of 5 in the latter. Zero-background autocorrelations were published for three bandwidths, showing cusp-shaped profiles. The auto-correlation width of 1.5 ps using only one filter element was attributed to a 0.75 ps single-sided

exponential pulse. The width could be reduced slightly by using a low finesse etalon, but operation below 0.75 ps was hampered by satellite pulses. Although the results appeared to agree closely with the model, it is significant that the cavity length was adjusted as the bandwidth was varied. The model assumed matched cavities and this was achieved experimentally by "adjusting the length of the dye cavity such that the shortest pulse is obtained". The birefringent plates had thicknesses in the ratio 1:4:16, the thinnest being 0.35 mm, and their removal would have substantially changed the cavity length. (Results to be presented later suggest that, although the shortest pulses may sometimes be obtained close to match with a detuning sensitivity approximately equal to the reciprocal bandwidth, the location of the "best" cavity length may be confused by satellites and substructure. The length adjustment neccessitated by the removal of a filter plate is not small compared to this tolerance, thus swamping fine mismatch effects, and the agreement with the model may be fortuitous).

Further experimental verification was claimed when the effect of cavity mismatch on the system in [22] was investigated in detail (Au chnitt et al. [23]). Zero-background autocorrelations for a total mismatch range of 130 μ showed the qualitative change clearly: the single, broad profile at long cavities, with a coherence spike for large detuning, narrowed towards match and was joined by a satellite. The final collapse to a broad, weakly modulated profile took place over a range of less than 10 μ. The authors noted that the controllable separation of the main and satellite pulses might have experimental uses. Plots of autocorrelation width and second harmonic power against mismatch showed, as usual, that the maximum of the former occurred at a shorter cavity length and that the variation was more sensitive when the bandwidth was increased. The approximate analytical model, extended to accomodate finite mismatch, seemed to fit the data quite well over the mismatch range for good modelocking.

Ryan et al. [24] published a comparison of synchronous and hybrid mode-locking of Rh-6G. Pulses as short as 1 ps were obtained from a typical prism-tuned, synchronously pumped system. Once again, these durations were only obtained when the cavity length was maintained to within 2 μ. The output was tunable from 560 to 630 nm with average conversion efficiencies of up to 8%. The variation of both average fundamental and 2nd harmonic power with cavity mismatch were measured over a cavity mismatch range of several hundred μ. The variation of the latter was much more sensitive and peaked at a slightly shorter

cavity length. Streak camera and autocorrelation measurements showed that well-modelocked pulses were only obtained for cavity lengths in the range from that for maximum 2^{nd} harmonic power to 10 μ shorter. Outside this range the autocorrelations showed the 3:2:1 contrast indicating substructure within a broad pulse envelope.

Streak camera measurements (for pump pulses of 150 instead of 90 ps) showed that, for cavity lengths away from optimum, dye pulses of 10 to 100 ps overall duration with a substructure width of 3 to 10 ps were produced. A further length tuning complication was seen in the laser spectrum. For long cavities, a reduction in the cavity length caused the centre of the lasing spectrum to move to shorter wavelengths, suggesting a connection with the time dependence of the Rh-6G gain after the arrival of the pump. Further shortening of the cavity caused the spectrum to jump back to longer wavelengths and the appearance of structure. The lateral movement of the beam profile across the cavity suggested that the system was increasing its effective length by altering the axis relative to the tuning prism.

The incorporation of saturable absorber (DODCI in a thin cell in contact with the 100% mirror) lead to the production of almost bandwidth-limited sub-picosecond pulses. The average efficiency of this hybrid system, although reduced to 2%, was still considerably greater than that (0.3%) of a purely passively modelocked system. Absorber concentrations as low as 1.5×10^{-6} M (compared with Rh-6G of 6×10^{-4} M) were sufficient to remove the wings of the autocorrelation profile. Modelocking became more stable and increasing the concentration to 1.2×10^{-5} M produced bandwidth-limited subpicosecond pulses. Although the absorber reduced the total cavity length range over which lasing was obtained, the range for optimum pulse generation was increased from 5 to 10 μ. The length sensitivity decreased with increasing absorber concentration and concentrations above 1.4×10^{-5} M always yielded stable subpicosecond pulses. The conversion efficiency was reduced to 2% but the peak pulse powers were comparable.

An elegant alternative to the use of Lyot filters or prisms for intracavity tuning was used by Bethea and Levine [25]. Broad and narrow-band electro-optic tuners were used in a conventional 3-mirror cavity pumped by 90 ps Ar^+ pulses. With the narrow-band element alone, transform-limited pulses of 3 to 7 ps duration were obtained by adjusting the cavity mismatch by a few μ. Background-free autocorrelations showed no coherence spike. The output could be tuned from

560 to 620 nm at an average laser efficiency of 23%. With the broad-band tuner the pulse width could be reduced to 1.3 ps with a consequent reduction of the mismatch tolerance to as little as 1 μ. This technique was extended by Blit et al. [26] who achieved simultaneous operation at two wavelengths 10 nm apart by applying a synchronous rf voltage to the EO tuner. The phase of the modulator was adjusted so that the two pulses, in a cavity twice the length of the pump, passed through the modulator at opposite extremes of the frequency sweep.

The influence of pump pulse duration on the quality of the dye pulse was seen by Sundström and Gillbro [27]. 1.5 ps pulses from a typical Ar^+/Rh-6G system were used to probe the pump pulses using nonlinear upconversion. The pump itself was found to be sensitive to small cavity mismatches relative to the modelocker frequency: the optimum duration (65 ps at 0.6–1 W output power) increased to 75 ps for a detuning of 50 μ and to 195 ps for 2 mm. The latter significant increase was reflected in an increase in the dye pulse duration by a factor of 2 to 3 and also resulted in the formation of a broad satellite pulse, especially at high pump powers. The location, duration and energy of the satellite depended sensitively on the pump power and cavity length. The satellite could be suppressed by adding DODCI to the rhodamine "without decreasing the energy of the pulse too much". Under optimum conditions, a minimum pulse width of 1.1 ps was obtained with an output power of ca. 100 mW at approximately 10% efficiency. These pulses lacked significant autocorrelation shoulders and satellites (over the 35 ps range of the correlation). The decrease of the pulse duration with pump power was attributed to the combined effects of increasing gain modulation and the reduction in pump pulse length at increased pump laser power.

In the normal procedure for taking autocorrelation measurements, the interferometer length is adjusted by a stepping motor and the full profile can be mapped out in a few seconds. Sala et al. reported a faster method [28] in which the interferometer path length was varied at 30 Hz by an audio loud-speaker, giving a continuous background-free measurement of a standard Rh-6G system. The results showed the effect of cavity mismatch particularly clearly. When the laser was operated with a broad-band (200 GHz) tuning wedge, the cusp-shaped autocorrelation at match had collapsed completely when the cavity was shortened by 5 μ and had broadened significantly, acquiring a coherence spike, at a detuning of +5 μ. The envelope continued to broaden as the mismatch was increased to 25 μ. The abrupt collapse for negative detunings remained when a

narrow-band (40 GHz) etalon was added to the cavity, but the correlation profiles for positive mismatches, though broadening in relation to the mismatch, lacked coherence spikes. These results were presented in the context of a detailed formulation of different types of autocorrelations for various analytic pulse shapes, but typical conclusions were reached about the pulse shapes in the the experiment. The cusped profile was attributed to a single-sided exponential pulse while the smooth profile (which also showed fine interference fringes) obtained at match with the fine tuning etalon was thought to correspond closely to a $sech^2$ pulse.

2.4 CW Ion Laser Pumping of Other Dyes

CW synchronous pumping has been successfully operated with several dyes lasing in the infrared, typically pumped by an acousto-optically modelocked Kr^+ laser. Although investigations have not been as extensive as those using Rh-6G, the details of the performance are clearly similar and confirm the general importance of critical matching of the master and slave oscillators.

In the first report Kuhl et al. [29] used oxazine, DOTC and HITC to obtain tunable pulses down to 25 ps at wavelengths ranging from to 685 to 900 nm. A 3-mirror cavity with output coupling of only 2% was tuned by birefringent filters and pumped by Kr^+ pulses of less than 200 ps duration. The average modelocked output varied considerably over the full tuning range of each dye, but output efficiencies as high as 420 mW for 1.4 W input power could be obtained (in this case pumping was substantially above the threshold power of 50 mW). The output spectral width using a 2-element filter was twice that under CW operation but narrowed considerably with a 3-element filter. Detailed autocorrelation measurements of the pulses from oxazine-1-perchlorate (tuned to the maximum of the gain profile) frequently consisted of a coherence spike with a width of a few picoseconds on a base typically tens of picoseconds wide. The substructure remained approximately at the filter bandwidth limit and the peak to background contrast was always 3:1. With a 3-element filter there was no pronounced sub-structure shoulder, however, and the cusped autocorrelation with 3:1 contrast was taken to indicate good modelocking. It was found that the shortest pulses were obtained for a cavity length about 0.2 mm longer than that giving maximum output power (in agreement with Goldberg and Moore [9] and with Scavennec's predictions [20] but at variance with Chan et al. [14] and Frigo et al. [17]).

Subpicosecond operation of an oxazine-750 system was obtained by Fehrenbach

et al. [30] using saturable absorption effects to improve the operation. Kr^+ pulses of 120–150 ps duration pumped a 200 μ dye jet in a 1% output cavity. With matched pump and dye cavities the shortest pulse duration obtained was ca. 18 ps when pumped at 3.5 times threshold. The autocorrelation had a sharp coherence spike with 3:2:1 contrast. Spectral width was correlated with inverse pulse width and it was found that etalon–related periodic structure in the spectrum was removed by adding further Lyot filter elements, giving bandwidth–limited pulses of the same duration. Halving the dye cavity length produced a significant pulse shortening together with an elevation of the threshold pump power. This was thought to show that the dye acted as saturable absorber on alternate, unpumped, transits. Subpicosecond pulses were achieved by adding a saturable absorber to the amplifier solution. Pulse durations of 0.8 to 4 ps (assuming gaussian profiles) could be achieved over the large tuning range of 750 to 835 nm. The pulse duration became insensitive to cavity mismatches within 10 μ and the autocorrelation lacked the characteristic shoulder.

Aoyagi et al. [31] also significantly improved a Kr^+–pumped OX–750 system using the saturable absorber HITC to reduce the best pulse duration (background–free autocorrelation) from 2.8 ps to 0.6 ps. With adjustments to the cavity this duration could be maintained from 750 to 780 nm. In contrast to Fehrenbach et al. [30], the pulse quality was still sensitive to cavity mismatches of ca. 1 μ with both pulsewidth and 2^{nd} harmonic power varying more rapidly for cavities on the short side of optimum. Once again, the length for minimum pulse width was a few μ shorter than that for maximum SHG. The optimum absorber concentration was only 1% of that of the oxazine: raising it by more than 50% reduced the output power and degraded the stability.

Further improvement of the oxazine system came in a detailed investigation of oxazine–1–perchlorate by Kuhl et al. [32]. Pulses down to 0.35 ps were produced by 100 ps pump pulses using tuner bandwidths larger than 50 nm. The dye cavity length was adjustable to within 0.5 μ and 10% pulse broadening was seen for cavity adjustments of 3 μ. The shortest pulses were again obtained for cavities slightly shorter than the maximum SHG length – in this case from 5 to 50 μ shorter depending on the pump power and filter bandwidth. The latter could be varied substantially using birefringent plates or a wedged interference filter. Background–free autocorrelations of "fully modelocked" pulses showed widths dependent on the bandwidth. Peaks or modulations in the pulse spectra were found to indicate the presence of multiple pulses and pulse substructure

(under which conditions the autocorrelation had a broad shoulder). The spectrum obtained when the laser was tuned by a single plate filter showed periodic structure which was associated with "Fabry–Perot effects of the birefringent filter". Curiously, a broad spectrum without substructure was only obtained at a few isolated wavelengths across the lasing range. The shortest pulses were obtained when the finesse of the single plate filter was degraded (by using adjacent orders) giving a smooth spectrum more than 10nm wide. The problem of secondary spectral maxima could be avoided by using a wedged etalon. The pulses obtained with the narrow band filters were tunable between 690 and 770nm, with ranges dependent on both pump power and output coupling. The 3–plate and wedge filters yielded, at low pump power, pulses with a time–bandwidth product of 0.5 (close to the limit for a gaussian) which increased significantly at higher pump powers – perhaps due to frequency sweeping. The single spectral peak of the wedged etalon allowed the production of picosecond pulses over a broad range of pump powers (with the duration decreasing with increasing pump power) without extensive readjustment of the cavity.

The production of satellite pulses through recovery of the gain before the end of the pump pulse was seen clearly. Small deviations from the optimum length caused pulse broadening, but with increasing mismatch a weak satellite appeared 30 to 40ps from the main pulse. With further detuning the satellite increased in strength and moved closer to the main pulse, to be followed by more satellites. Eventually all the satellites merged to form a broad pulse producing an autocorrelation with a sharp spike. Small amounts of saturable absorber could be used to suppress satellites but it was thought that this could also have been achieved by adjusting the pump power and output coupling. Reduction of the pulse duration by reducing the pump duration was attempted by using tandem pumping of OX–750 with the OX–1–perchlorate output. Although single pulses of approximately 1 ps duration were produced, this was not shorter than the best directly pumped results because of the reduced pump power: the main advantage was the absence of satellites. Tandem pumping was also used by Minami and Era [33] to obtain good modelocking from oxazine–1. Pumping with a standard Rh–6G system (160 mW at 610 nm) yielded 20 mW at 740 nm from the oxazine laser using 6% output coupling and a 1–plate birefringent filter. Zero–background autocorrelations without shoulders were significantly better fitted by a single–sided exponential profile than a gaussian, giving a pulse duration of 0.7 ps. A spectral width of 0.6 nm gave a time–bandwidth product of 0.23 (compared with

0.11 for a single-sided exponential). Varying the cavity length showed the typical rapid and asymmetric change in the pulse width and second harmonic power over the 10μ range for good modelocking.

Synchronous pumping was extended further into the infrared by Leduc [34] with Kr^+ pumping of several carbocyanines up to 1095 nm. The emphasis was on extending the tuning range and reducing threshold, and detailed pulse optimisation was not reported, although it was noted that the average power was not affected by length detuning of 0.5 mm.

Marason [35] found a substantial tuning range for the dye DCM pumped by Ar^+. Optimum output coupling varied from 20 to 40% as the wavelength was tuned from 605 to 725 nm. Autocorrelations indicated pulse durations of a few picoseconds. Cavity dumping the output at 1% of the round trip rate raised the average power by up to a factor of 10 but significantly increased the pulse duration. de Vries et al. had briefly reported modelocking of sodium fluorescein in the wavelength range 530 to 570 nm using Ar^+ pumping [16] while Eckstein et al. [36] produced tunable pulses in the deep blue by pumping stilbene 3 with an argon laser modelocked in the ultraviolet. The low loss (4% output) cavity was tuned by a 4-element birefringent wedge. Adjusting the cavity length to better than 1μ gave smooth autocorrelations without coherence spikes. With pump pulses shorter than 130 ps, dye pulse widths of 1.2 ps (assuming gaussian profiles) or 0.84 ps (single-sided exponential) were produced. Raising the pump power by using all the lines of the Kr^+ laser increased the pump duration to 300 ps and quadrupled the dye pulse width. DCM was also used by Jain [37] to produce efficient modelocking of the dye LD700 in the red and near infrared. The DCM was synchronously pumped by an argon laser, benefitting from the generally superior performance of Ar^+ compared to Kr^+, and the LD700 excited by energy transfer from the DCM.

Practical aspects of the pump and dye cavity configurations were investigated by Ferguson [38], resulting in much improved performance from blue dyes. The demand for high power from the ion laser leads to pump cavity lengths of 1-2 m. Extending the dye cavity to match this can result in stability problems caused by the increased base length or in increased loss with an intracavity delay line (a significant problem with inefficient dyes). By operating Ar^+ and Kr^+ lasers at the third harmonic of the cavity round trip rate, not only were the dye cavity problems reduced but the pump powers were considerably increased because of the reduction of spontaneous emission losses. The output

from stilbene 3 was increased from 7 mW to about 50 mW with the modified pump (Ar^+ at 364 nm) while that from coumarin 102 (Kr^+ pumping at 413 nm) was increased from 7 mW to 150 mW at the centre of the tuning range. The pulse duration was similar in both cases – background-free autocorrelations having widths of ca. 8 ps, limited by the 2-plate birefringent filter. The increase in mode spacing was expected to have advantages for mode stabilisation and in spectroscopic applications.

2.5 Detailed Investigations of Pulse Structure – (A)

AUTOCORRELATION

A reasonably consistent picture of the 2^{nd} harmonic autocorrelation behaviour has emerged from more recent experiments. The profile frequently consists of a bell-shaped envelope 10 ps or more in width surmounted by a spike, often sharply defined, of width ~1 ps. Only when the cavity is critically tuned can the correlation pedestal be made to contract into the spike, leaving a smooth, sharp autocorrelation. This may often be achieved only with the addition of a saturable absorber and sometimes, especially at high pump powers, not at all. The coherence spike is considered to indicate the presence of fast sub-structure under a pulse envelope of which the bell shape is the autocorrelation. The simpler background-free autocorrelation technique, now widely used, can lead to uncertainty in the results, but the substructure picture seems to be confirmed by the observation of "correct" 3:2:1 contrast ratios in non-zero background results. It is assumed that under poor modelocking the pulse remains as a noise burst (Pike and Herscher [39]) which can be "cleaned up" to give a short, structure-free envelope under optimum conditions. The details of the physical process leading to this are still not clear.

A few recent publications have addressed in detail the problem of fluctuations and noise structure in synchronous pumping. Striking support for a noise-burst model came from cross-correlation studies of a standard Rh-6G system by McDonald et al. [40]. The pulses were correlated not only with themselves but with near neighbours in the train by extending one arm of the autocorrelator by integral multiples of the laser round trip time. The normal background-free autocorrelations yielded typical results: for long cavities the traces had shoulders which could be eliminated by shortening the cavity. Further shortening introduced satellites which progressively sharpened, strengthened and moved

closer to the weakening central peak of the correlation profile. When the laser was operated with insufficient loss, the satellites appeared at lengths longer than that producing the best pulse. Optimum autocorrelation widths of 5.7 ps were obtained with 55% output coupling and 10% efficiency from 1.2 W pump power. These profiles remained optimum even when the correlation was delayed by 6 round trips.

It was expected that the form of the substructure in the detuned case would not be maintained for more than a few transits and that cross-correlations of increasingly separated neighbours would show rapidly diminishing coherence spikes. Surprisingly, this was not observed: the spike persisted with little distortion across several neighbours but was displaced relative to the pulse envelope by an amount closely corresponding to the accumulated cavity mismatch - either positive or negative (fig. 2.3). The gain was therefore reshaping the envelope to preserve synchronism with the pump while the substructure was locked to the transit time of the dye cavity. The displacement of the spike from the centre of the profile was measured for 1^{st} to 6^{th} neighbours and for different mismatches, leading to an absolute determination of the matched cavity length (which corresponded to the cavity setting giving giving the narrowest correlations). It was noted that, when the pulse envelope is significantly longer than the inverse noise bandwidth, the background-free autocorrelation can be expressed simply as the sum of the separate autocorrelations of the substructure and the envelope - the approximation is already reasonably accurate when only a factor of two separates the timescales. The contribution of the noise is easily distinguished when the envelope is broadened by significant mismatch, but the two become very difficult to separate if the envelope duration approaches that of the fluctuations. The correlations of "well-modelocked" pulses frequently appear to have exponential wings. Although single-sided exponential pulses give this result, McDonald et al. observed that the sum of two error functions with widths in the ratio 2:1 could closely approximate to the form over two decades. This picture of a gaussian or skewed gaussian envelope of width 2 to 2.5 times the width of the gaussian noise correlation seemed more realistic, and could lead to a doubling of the estimated pulse width compared with the noise-free, single-sided exponential model. Although the experimental resolution reported in [40] was significantly lower than in many others - the cavity mismatch was only reproducible to 10 μ and the 500 μ detuning range was large - the clear observation of consistent "phase" shifts of the

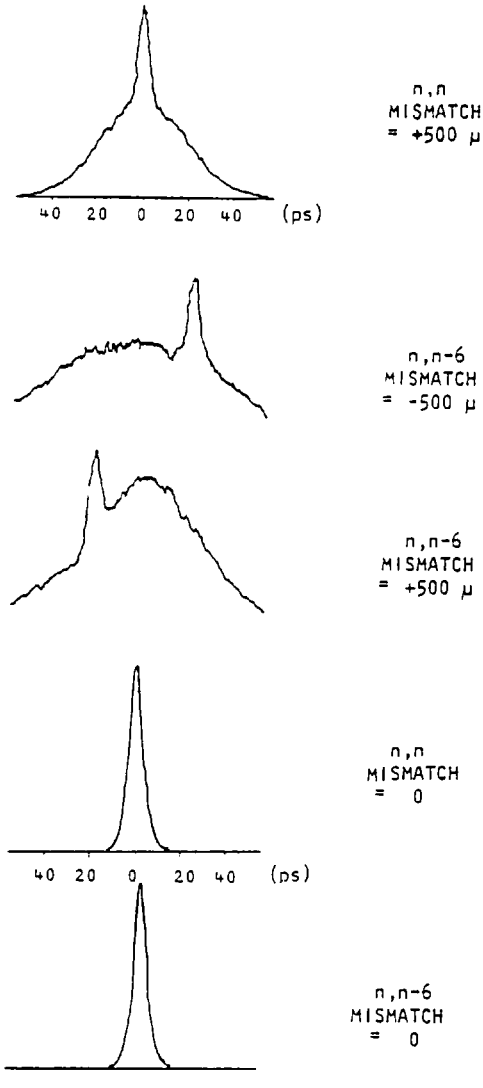


FIG. 2.3 : Cross- and Autocorrelations
(from McDonald et al. [40])

correlation spike shows that random substructure must be present when the cavity is detuned, and means that "well-modelocked" autocorrelation profiles must be treated with caution.

In a second publication [41] McDonald, Rossel and Fleming examined the noise structure in more detail. Simultaneous autocorrelation (zero background) and spectral measurements were taken for various cavity lengths, output couplings and filter bandwidths. If the functional form of both the envelope and the noise statistics was assumed, numerical curve fitting allowed the two widths to be separated, even when they were comparable. The noise was assumed to be gaussian while the pulse envelope correlation was fitted with gaussian, lorentzian and exponential profiles. The width of the spectrum was obtained from a gaussian fit, and it was found that the position of the spectral maximum was independent of cavity length but that the width of the spectrum was a strong function of the mismatch. The width was roughly constant at large negative detunings, rose quickly over a range of 100μ around match and then levelled out again for large positive mismatches. Using a 3-plate birefringent filter (BRF) the variation was sharper with 70% output coupling than with 55%. The variation using a wedged etalon was qualitatively very similar but over a much wider range. The spectra with the BRF were well fitted by a gaussian but that from the wedged etalon was less so and was unstable: this did not indicate, however, that an observed spectrum was always the average of individual fluctuating spectra. The gaussian fit to the coherence spike for the BRF was very good and led to a time-bandwidth product close to the limit for gaussian noise even when the noise and envelope correlations could not be visually separated. The dependence of the timescale of the noise on mismatch had an inverse relation to the spectral width, showing a swift drop as the mismatch was changed from negative to positive values. While the timescale of the noise was closely correlated to the spectral width, the duration of the pulse envelope was not. The widths showed the typical variation with mismatch. For very large negative mismatch they were broad and slowly varying. Towards "match" the width dropped rapidly, reaching a minimum at that position, and then increased steadily for positive detuning. The variations differed in degree with output coupling and type of filter but were qualitatively very similar in each case. The time-bandwidth product for the pulse envelope was, in contrast to that for the substructure, a strong function of the mismatch, with a minimum value corresponding to a gaussian pulse 2.5 times wider than the transform limit. As

in [40], the mismatch range used was several hundred μ. Even the most rapid variation in the widths took place over tens of μ around zero mismatch – a range much greater than the tolerance seen in other, more finely tuned, systems.

Detailed comparison of the various widths cast doubt on the validity of the assumption made in a number of earlier reports: that the excellent fit by near-optimum autocorrelations to the form exp(-|x|) indicated that the pulses themselves were bandwidth-limited single-sided exponentials. McDonald et al. concluded that this was not applicable to their results. Firstly because the spectra were significantly better fitted by a gaussian than by the required lorentzian profile and, secondly, because single-sided exponentials would have required a time-bandwidth product almost an order of magnitude smaller than that observed. In consequence, it was felt that other authors had underestimated their pulse widths by about a factor of three. Other causes of spectral broadening, such as chirp or variation in the position of the spectrum centre, were discounted because of the closeness of the substructure to the transform limit. The apparent exponential form arose from the combination of envelope and substructure correlations both of roughly gaussian shape and, at cavity match, similar widths. van Stryland [42] had recently pointed out that almost any shape of autocorrelation could be obtained by the summation of a distribution of gaussian functions of different widths – a reasonable possibility in view of the very large number of pulses ($\sim 10^7$) sampled to give each autocorrelation point. The analysis in [42] did not take random substructure into account and required a fairly large distribution of widths to produce the required shape. McDonald et al., however, only needed a "modest" distribtion of pulse durations to explain the deviation of their two-function fits from the observed data, and noted that a distribution of pure exponential or lorentzian functions was unable to reproduce the profiles for mismatched cavities. By using third order autocorrelations derived from the optical Kerr effect they also concluded that any skewing of the gaussian pulse envelopes was small.

2.6 Detailed Investigation of Pulse Structure – (B)

STREAK CAMERAS

Although second harmonic correlation offers high resolution (as well as certain practical advantages) the correlation profiles are neccessarily ambiguous and even the elaborate extensions described in the preceding section

can only give very limited information about fluctuating structure in the output. In a revealing letter, Shapiro et al. [43] returned to single shot streak camera measurements, comparing them directly to autocorrelation results. A standard Rh-6G laser with a 3-mirror cavity, spatial filter, tuning wedge and 30% output coupler, was pumped by 160 ps Ar^+ pulses. The cavity length could be adjusted to within 1 μ and the long term stability was such that autocorrelation and streak measurements were considered to be effectively simultaneous. The background-free autocorrelations showed typical variation with cavity mismatch. For long cavities a bell-shaped envelope was surmounted by a coherence spike. Shortening the cavity reduced the width of the bell until, at the length taken as matched, a "well-modelocked" cusped profile was formed. For shorter cavities the base contracted still further, eventually loosing power and becoming unstable.

The picture revealed by the streak camera was significantly different. For long cavities the pulse appeared as a single spike which broadened with mismatch. At the "matched" length the autocorrelations for operation close to and well above threshold were almost indistinguishable. The streak camera, however, showed a single pulse in the former case but usually two or more intense pulses in the latter. Multiple pulse production increased as the cavity was shortened further, with both the amplitudes and positions of the subpulses varying in time. The multiple pulses were clearly resolved by the camera (resolution 6 ps) and for short cavities the pattern extended over much of the duration of the pump pulse. Although the autocorrelations somtimes showed a satellite pulse, the multiple pulses were frequently not visible, and, while the profiles for significantly shortened cavities were weak and unstable, there was little to indicate the size of the fluctuations seen in the streak pictures. It was concluded that secondary correlations were easily lost and that, contrary to the normal view, the laser should be operated with a cavity several μ longer than match, particularly if pumped well above threshold. The desirable position coincided closely with that giving maximum second harmonic production.

The possibility of fluctuating structure which is not detectable by autocorrelation places results by May et al. [44] in a different light. A continuously operated synchronous streak camera ("Synchroscan") was used in conjunction with autocorrelations to determine the best operating conditions. A low loss (1% output) cavity was pumped by short (60 ps) Ar^+ pulses giving Rh-6G pulses of 1-2 ps in duration. In a passively modelocked system the camera

was capable of 1 ps resolution when triggered by the dye pulses themselves, but in this application the camera was triggered by pump radiation transmitted by the dye stream. Fluctuations in the energy of the pump pulses, with consequent jitter in the triggering threshold, degraded the resolution. It was thought that the resolution was further lowered by long term movement of the dye pulse relative to the pump profile, giving an overall figure of 9 ps for pulses with autocorrelation widths of 1.3 ps. Taking the matched position as that giving the minimum autocorrelation width (which also corresponded to the maximum SHG), the autocorrelation broadened slightly for negative mismatches of 1 to 2 μ: beyond -4μ the rapid reduction in the second harmonic power prevented accurate measurement. The behaviour with detuning was typically asymmetric and the autocorrelations for positive mismatches broadened steadily, reaching 12.4 ps at $+8\mu$ with 3:2:1 contrast. The greater sensitivity of the streak camera allowed measurement over a wider mismatch range, showing the more rapid broadening for negative mismatches. The measurements also revealed a weak, close (ca. 20 ps separation) satellite pulse at -2 and -4μ which was not visible in the autocorrelations. In contrast to the fluctuations seen in the single shot streaks of Shapiro et al. [43], this structure must have been reasonably stable to show up in the long time average of the synchroscan recording. On the other hand, the fluctuating structure revealed as a coherence spike in the autocorrelations was not resolved by the streak camera which showed smooth, broad profiles. In spite of the fact that the streak profiles were much broader than the widths deduced from the autocorrelations, the single 9 ps spike at zero mismatch was the narrowest profile measured and the profiles broadened perceptibly, and asymmetrically, for detunings of only 2μ in each direction. It was therefore felt that the synchroscan camera was capable of locating the best operating conditions. Cross-correlations of the pulse with its 6^{th} nearest neighbour, as in McDonald et al. [40], showed that at "zero" mismatch the cavity was in fact longer by 2μ at most – a value equal to the accuracy of the measurement.

2.7 Active stabilisation

The typical synchronously pumped system is particularly sensitive to noise, both intrinsic and external, across a very wide range of frequencies. At one extreme, fluctuations in the signal are related to the very large emission bandwidth of the dye. The process of "modelocking" the laser amounts to

enhancing and maintaining a single large spike out of the continuous background of spontaneous emission noise. Simple synchronous pumping does not appear to be particularly effective for this, often producing noise burst output in which the substructure may be changing rapidly – as shown by the frequent appearance of correlation spikes. At the other end of the frequency range, the use of the laser as a spectroscopic tool can require stable operation for hours or days. The mismatch tolerance of the system has been consistently reported as ~ 1 in 10^6. Maintainance of this accuracy places tight stability requirements on system components with widely differing response times. These have bandwidths which range from MHz for the rf electronics of the pump laser through Ar^+ plasma, dye stream and atmospheric oscillations to thermal response times of many seconds for the cavity mounting. Even with strenuous efforts at simple passive stabilisation the performance is considerably short of the theoretical limit. The performance can be improved by active stabilisation using feedback derived from the output pulse to adjust the operating parameters. The technique has been applied successfully to single frequency dye lasers and two different methods have been described for synchronously pumped systems.

A feasibility study by Frigo et al. [45] used the fact that the position of the dye pulse in local time relative to the pump pulse is a sensitive function of the cavity mismatch (with values of [shift in local time/mismatch] of 100 to 1000). By frequency mixing the output with a modified sample of the pump radiation they were able to generate a usable differential signal (which could have been used for piezo-electric length correction) that was clearly sensitive to small thermal perturbations in the laser mounting.

In a more elaborate study Rotman et al. [46] obtained a noise reduction of 10 dB at frequencies up to 10 KHz using both analog and digital feedback. Two dye lasers were pumped by the same 100 ps Ar^+ pulses producing pulse durations down to 0.7 ps (assuming single-sided exponential profiles) with efficiencies up to 20%. The length of the first laser was maintained passively by a quartz rod while the second was actively stabilised. The shortest pulses were produced by the latter by running it without a tuning element and at moderately high output coupling (30%). It was assumed that the noise was due to fluctuations in the dye pulse width (arising from variation in both the pump pulse and the dye cavity) and the feedback therefore required a measure of this. A much faster measure than full autocorrelation was derived from the total second harmonic produced by the output which, for constant pulse shape, is proportional to

(fundamental power)^2/(pulsewidth). Unlike the dye laser, the argon laser was hardly affected by a change of 1 in 10^6 in the modelocker frequency and the pump:dye mismatch could therefore be adjusted directly from the power measurements through the pump rf oscillator frequency. Although the bandwidth of the 2nd harmonic detection and rf control was ~MHz, the overall response was limited to 10kHz by the acousto-optic prism. The effect of the feedback stabilisation was demonstrated by low frequency spectral measurements of the time dependence of the fundamental and harmonic power. This showed a noise attenuation of up to 10dB at all frequencies up to 10KHz. There was, however, an increase in the noise above this frequency which was attributed to nonlinear effects, probably in the Ar^+ plasma. The spectra also clearly showed the effect of weak sidebands in one of the rf oscillators used.

Compensation at lower frequencies and of larger range was obtained by digitally processed feedback to the length of the dye cavity. A computer was programmed to find the optimum pulse width by measuring the autocorrelation at zero displacement and in the wings (allowing discrimination between badly formed and low power pulses). The autocorrelator was then fixed at the position of maximum overlap and the dye cavity length was adjusted by the computer in steps of 0.5μ. Although the response time was limited by both the computer system and the cavity length adjustment mechanism, the method was particularly successful in eliminating long term drift: an autocorrelation with a shoulder and of width 2.2ps measured over 1 hour was reduced with feedback to one without a shoulder and 0.7ps wide.

Feedback control need not be confined to the dye pulse or to the dye laser itself. Sizer et al. [47] used interferometric feedback to compensate for variation in the jet stream thickness (v.i. §2.11). The importance of pump laser stability was investigated by Klann et al. [48]. The dye pulse quality is sensitive to fluctuations in the pump and the modelocking of the pump is in turn affected by the acousto-optic modulator - in particular, to the depth of modulation. Good modelocking of the gas laser requires that the rf signal be matched not only to the cavity length but to an acoustic resonance of the modelocker. Temperature variations caused by the high rf power (ca. 1W) lead to significant changes in these resonant frequencies. Measurements of the incident and reflected rf signal allowed detection of the variation in phase about an acoustic resonance and hence the generation of a feedback correction to the rf power (not the frequency) to control the temperature change. This allowed

the modulator to be kept on resonance while running at high power for long periods. The slight variation in the rf power (typically 0.1 dB) had no direct effect on the quality of the modelocking. The feedback loop tolerated significant frequency variation and the rf could therefore be tuned to the cavity mode spacing without loosing acoustic resonance. The deep modulation resulted in much improved modelocking. Fluctuations on a timescale of about 1 μs in the output of the Ar^+ laser at low modulator power disappeared when the drive power was doubled. This improvement was reflected in the autocorrelation from a synchronously pumped Rh-6G laser. The slight shoulder and low background of the autocorrelation, which could not be suppressed by cavity adjustment alone, were absent when the pump was stabilised.

2.8 Unidirectional Ring Systems

An excited amplifier can, in principle, support pulses which pass simultaneously through the jet stream travelling in opposite directions. While a number of authors have reported that "only one pulse circulated in the cavity" the mutual competition for the gain when this is not the case may well be detrimental to the performance. The initiation of travelling wave operation in the conventional Fabry-Perot cavity presumably relies on initial instabilities resulting in preferential amplification of one pulse and on residual asymmetries between the two directions of operation. In particular, the gain seen by the two pulses depends on the position of the dye jet relative to the output coupler: if the jet is close to a 100% mirror then one pulse returns quickly to the jet allowing extraction of residual gain while the second pulse returns later when the residual gain may have relaxed significantly. On the other hand, the first pulse has been depleted by the output loss when it makes its first pass through the freshly pumped amplifier while the second has just been boosted by a secondary pass. A second asymmetry arises because the dye pulse which copropagates with the pump in the jet (assuming that it does so simultaneously) sees slightly greater gain than the counterpropagating pulse. This effect is normally very small because the pump pulse is much longer than both the signal pulse and the jet transit time. The pulses may also be sensitive to the precise nature of the focussing of both beams in the dye stream. Notwithstanding the possibility of asymmetries, effective travelling wave operation requires that the secondary pulse be substantially suppressed and this may not occur spontaneously when substantial single pass gain leads to strong ASE.

Blit and Tang [49] were concerned with the poor modelocking obtained with the high Q-values necessary for cavity dumping - an observation at variance with existing theories - and saw the presence of counterpropagating pulses as the cause. They also attributed the appearance of satellite pulses to the different arrival times of the two pulses at the output mirror. Accordingly, they sought a reliable way to suppress one of the pulses and turned to a ring system where discrimination is made easier by the different senses of rotation. With output couplings of 4% and 1%, spontaneous unidirectional operation was possible with careful alignment of the cavity, both with and without a birefringent tuner. The power ratio of the two beams was as high as 50:1 and the two pulses often had wavelengths separated by about 15 nm. The incorporation of a Faraday rotation "diode" to suppress the secondary direction gave travelling wave operation over a wide range of conditions and led to a substantial improvement in the zero-background autocorrelation - reducing a width of 130 ps by more than a factor of ten in the case of the 1% output coupling. Both of the published autocorrelation traces had coherence spikes with contrast ratios of less than 2:1 and the laser was adjusted in each case for maximum SHG. With both the diode and a 2-element tuner the laser was very close to threshold with the 1% output mirror, and it was observed that the pulse width decreased with decreasing output transmission (the model presented later shows that this is characteristic of operation near threshold). (Blit and Tang may have chosen the right system for the wrong reason: there are good experimental and theoretical grounds for attributing satellites to the recovery of the gain during a single pump event while counterpropagation effects definitely appear to be advantageous in hybrid modelocking (Fork et al. [50]) and perhaps also in conventional synchronous rings (May et al. [51])).

Better results were reported by Mitchell and Proffitt [52] using a "standard ring laser optical diode...which prevented all oscillation in the backward direction". Pulses as short as 0.9 ps, tunable over 60 nm, were produced by a Rh-6G system of half-synchronous length (giving a round trip rate of 152 MHz). The average power was 200 mW for 1.3 W pump power and 16% output coupling. Mismatch tolerances were not quoted. In both CW and cavity-dumped modes of operation the travelling wave performance was superior to the standing wave system: subpicosecond pulses were only obtained from a standing wave system at much reduced power and high output coupling. (All the lasers were tuned by a 2-plate birefringent filter).

Faraday isolators suffer from substantial loss and dispersion at the wavelengths of interest and their use requires a birefringent half-wave plate which complicates the tuning. To circumvent this, Halbout et al. [53] used instead a synchronously driven modulator - a KDP electro-optic amplitude modulator which acted as both tuning element and optical gate - which substantially improved the performance. Ar^+ pulses of 73 ps (gaussian) duration from a very stable oscillator ($1:10^7$) pumped a 4-mirror ring with the EOM roughly a quarter of the total cavity length from the dye stream. The best results were obtained at low pumping power, 12% output and with the EOM also acting to narrow the bandwidth. The non-zero background autocorrelation had 3:2:1 contrast without shoulders and the width of 0.7 ps together with the spectral width of 0.9 nm were taken to indicate single-sided exponential pulses close to the transform limit. The output could be tuned from 580 to 610 nm and the autocorrelation developed shoulders for a length change of less than 0.5 μ. At higher pump powers, when the pump pulse was appreciably longer, good modelocking was only possible with the insertion of a thin (7 μ) pellicle. This both raised the output to 30% and narrowed the bandwidth. Although the pulse duration was slightly increased, the mismatch tolerance was also increased to more than 1 μ.

2.9 Hybrid Modelocking

The beneficial effects of small amounts of saturable absorber have already been noted. It has been consistently observed that concentrations of only 1% of that of the amplifier dye lead to noticeably more stable output and reduce the minimum attainable pulse duration to about 0.5 ps. A specific investigation of a hybrid rhodamine 6G/DODCI system came from Ishida et al [54], using a 4-mirror cavity with a 200 μ jet stream, 3% output coupling and a broadband wedged etalon. The system produced pulse durations down to 0.13 ps in pure passive modelocking with a Rh6G concentration of 2×10^{-3} M. With pure synchronous pumping, however, using 150-200 ps pump pulses of the same average power, the shortest duration was 0.8 ps with a mismatch tolerance of 1-2 μ. Although autocorrelation shoulders were then absent, the pulse width could not be maintained for more than about half an hour without cavity adjustment. Addition of only 4×10^{-6} M DODCI reduced the pulse width to about one third and largely eliminated the autocorrelation wings. The pulse width reduced with increasing absorber concentration, reaching a minimum of 0.3 ps at 1×10^{-5} M. The tuning range was 594 to 605 nm and a time-bandwidth product of 0.35 was taken to

indicate near bandwidth-limited $sech^2$ profiles. Under these conditions, the pumping was close to threshold (1.5 W against 1.2 W) and at higher absorber concentrations the pump power was insufficient for stable modelocking. The behaviour of the hybrid system was qualitatively similar to that under pure synchronous pumping but the mismatch tolerance was much greater. The extrema of the second harmonic power and pulse width were located at successively shorter cavity lengths than that for the maximum fundamental power. The broad and asymmetric distribution of the last changed most rapidly over a 10μ range which overlapped with the peak of the SHG and the minimum of the pulse width. Good, stable modelocking was obtained over a 20μ range – an order of magnitude improvement – although the FWHM broadened to 0.5–1 ps within 5μ. Surprisingly, removal of the broadband tuning element allowed the maintainance of "very stable and good modelocking" with pulse durations of 1–1.4 ps over the large mismatch range of ±1.5 mm.

A similar investigation of a hybrid oxazine system was reported in [31] by Aoyagi et al., giving more details than the first report by Fehrenbach [30]. With the saturable absorber HITC, stable tunable subpicosecond pulses were obtained from OX-725 (6×10^{-4} M) pumped by 150 ps Kr^+ pulses. The minimum autocorrelation width of 4.2 ps without absorber was steadily reduced to 0.9 ps at an absorber concentration of 7×10^{-6} M. At concentrations above 10^{-5} M the output power decreased and the stability worsened. Both of the autocorrelations published – for concentrations of 0 and 7×10^{-6} M – lacked significant shoulders. In contrast to the behaviour of Rh6G/DODCI systems, it was found that the pulsewidth was still very sensitive to cavity mismatch and, as usual, that the minimum width was measured at a length a few μ shorter than that for maximum SHG. The minimum pulsewidth was maintained as the laser was tuned from 750 nm to 780 nm by a 2-element birefringent filter: the worsening of the stability at long wavelengths was attributed to the increase in the threshold.

A study of the gain evolution came from Yamashita and Sato [55] for a Rh-6G/DODCI system. Ar^+ pulses of 150 ps duration and 1.5 W average power pumped a jet of 1×10^{-3} M Rh-6G with the DODCI (8×10^{-6} M) flowing in a separate stream. The minimum pulse width, measured by autocorrelation of the 1st kind, was 0.4 ps using 10% output with a birefringent tuner. Under the conditions used for the "gain spectroscopy", with a pump power of more than twice the threshold value, the minimum pulsewidth was 0.8 ps at an average

output power of 50 mW. The gain of the rhodamine was measured directly by probing it with a fraction of the output pulse which was subjected to a variable delay to allow the time evolution to be mapped out. Evolutions for cavity detunings from +40 μ to −16.5 μ (relative to the length for maximum SHG) were published, together with the corresponding autocorrelations. The main qualitative feature confirmed earlier results: for large positive detunings, a broad pulse arrived late in the pump pulse, causing a sharp dip in the gain. The pulse compressed as the cavity was shortened and the dip advanced in local time, becoming less well defined. At a mismatch of −16.5 μ, the 3:2:1 contrast had disappeared and "satellite pulses occurred". The results are generally less clear than those of Frigo et al. [17] and contain several anomalies: the sharp dip in the gain towards the end of the pump pulse for large positive mismatches appears to be preceeded by a smaller one as much as 50 ps earlier (although this may be a detector artifact) and, while some of the probe results extend over more than 1 ns, no mention was made of the effect of the return pass through the amplifier.

The evolution of the gain in the absence of laser action was investigated by using half of the Ar^+ beam to pump a second cavity. Probing the gain in this with the output from the hybrid system showed the depression of the maximum level of the population inversion when the secondary system was allowed to lase. If the threshold level in the published figure is correct, then the net gain remained at or above unity during the passage of the pulse and only fell significantly below this as the inversion relaxed. The low pumping level meant that the arrival of the dye pulse was difficult to discern, however, and it is not clear whether the observation is valid.

2.10 Hybrid Rings and Colliding Pulses

The initial stimulus for using ring cavities seems to have been the hope of improved performance under unidirectional operation instead of competitive counterpropagation. This reasonable suggestion gained some support from the results of [49] and [53], but different results from other systems involving "colliding" pulses – i.e. where the counterpropagating pulses arrive simultaneously at the active medium – indicate that the full picture may be much more complicated. On a simple view, the mutual saturation of the gain may affect the stability, or even the duration, of the pulses to advantage. At a higher level, recent work on "colliding" pulse modelocking [56] suggests that

the standing waves set up by the collision may substantially affect the pulse compresssion, particularly for very short pulses. Furthermore, the mounting support for a "noise-burst" picture of synchronously pumped modelocking raises questions about the effect of counterpropagation on both fluctuations in the pulse and on the still obscure role of saturable absorbers.

Heritage and Isaacs [57], obtaining the shortest pulses yet from a synchronously pumped ring without absorber, attributed the improvement to enhanced gain depletion by pulse collision. The Rh-B system (130 μ jet without tuning element and 900 mW, 80 ps Ar^+ pumping) produced 20 mW in each beam and cross-correlations showed that the laser was operating bidirectionally with the pulses overlapping at the dye jet. The steep-sided autocorrelation appeared to lack the exponential wings of typical cusped profiles; the width of 0.8 ps was attributed to a 0.5 ps $sech^2$ pulse. The laser could also be tuned over a wide range with an intracavity etalon, yielding nearly transform-limited pulses.

May et al. [51] investigated simple and hybrid ring systems in which overlapping pulses were evident. A basic 4-mirror cavity (100 μ jet of 2×10^{-3} M Rh-6G, prism tuning and 5% output) produced counterpropagating beams of equal power. The total conversion efficiency was ca. 10% for pumping at 3.5 times threshold. Synchronous streak camera measurements showed that the pulses overlapped at the dye jet to within the camera resolution. The autocorrelation width of 0.7 ps was considerably shorter than the results obtained from a conventional cavity, but although the published trace had 3:1 contrast without shoulders, the time-bandwidth product of 0.88 indicated operation well above the transform limit. Continuous tuning over a wide range (562-630 nm) was possible and the reduced pulse duration and greater stability than in the conventional system were attributed to the enhanced depletion of the gain by the standing wave. With the cavity length doubled and output with via a pellicle only, the threshold power was raised from 200 mW to 230 mW but the pulse widths were unchanged. The pulsewidth decreased with increasing pump power, dropping from 1.8 ps at 100 mW above threshold to 0.7 ps at 440 mW above (a change which was large compared to the spread in the measurements).

This long cavity configuration was used for the hybrid system. The absorber (a mixture of 1×10^{-5} M DODCI and 1×10^{-5} M DQOCI with lifetimes of 16 ps and 1.15 ns respectively) flowed in a second jet stage, the position of which as adjusted so that the pulses overlapped at the jet. (It is to be assumed that the cavity then contained two pairs of counterpropagating pulses,

one pair passing through the amplifier at the moment that the other overlapped in the absorber). The pulse autocorrelation changed considerably as the jet was displaced through ±100 μ about the optimum position. Although a variation in the width of 1.4 ps to 0.5 ps to 1.3 ps was claimed, the main effect appears to have been a narrowing of the coherence spike towards optimum, and the results do not seem to be conclusive. The minimum duration obtained was about 0.3 ps but the published autocorrelation shows a significant shoulder and again the result is doubtful. The average pulse duration increased to 0.9 ps at a DODCI concentration of 6×10^{-5} M and to 1.3 ps at 1×10^{-3} M. Mixing the absorber with the amplifier dye instead of using a second jet, in order to avoid the problem of precise pulse overlap, yielded similar results although heating by the pump radiation was thought to have had an adverse effect.

The simple colliding pulse configuration was felt to give significant improvement in conversion efficiency and pulsewidth and stability but the timing requirements in the hybrid extension made it less useful. It is notable that, while the effects of detuning the absorber position by tens of microns were considered a disadvantage, no mention was made of the overall cavity mismatch tolerance. Furthermore, it is not clear how compatible and reproducible were the other operating parameters: the losses in the two cavities were different and the translation of the entire absorber stage with its mirrors may have led to a secondary change in the total cavity length.

2.11 Below 100 fs

The slow reduction in the pulse durations obtained from systems pumped by gas lasers seems to have come to a halt at approximately 0.3 ps. It is still not clear which of the main operating features – pump power, cavity mismatch, bandwidth, pump duration, satellite formation, stability, jet stream thickness and dispersion, absorber action and collision effects – is the limiting factor. The reason for the adoption of modelocked gas lasers in place of Q-switched solid-state lasers was the continuous operation of the former. Apart from the substantial advantage of this in many experimental situations, Q-switched envelopes are probably not long enough to allow the development of really short pulses. (It will be shown later that pulse formation is dominated by gain saturation and the standard models of modelocking evolution in systems such as gas lasers are inapplicable).

Although modelocked giant pulse pumping is still used and modifcations such as tandem pumping have been tried, ion laser pumping predominates in more recent work where minimum pulse duation is the goal. There is, however, one notable exception: in a series of papers, Sizer, Mourou et al. reported the development of a rhodamine 6G system pumped by frequency-doubled output from a CW Nd:YAG laser, ultimately obtaining a pulse duration of 70 fs from a hybrid system. The Nd:YAG pump was attractive because of the possibilty of high power amplification by using part of the YAG output to drive a synchronous dye amplifier chain. The first paper (Sizer et al. [58]) reported pulsewidths of less than 2 ps. As with rare gas lasers, the pulse quality of the Nd:YAG laser depended sensitively on the spectral purity of the rf drive of the acousto-optic modulator. Extracavity up-conversion ($Ba_2NaNb_5O_{15}$) was used, partly for bandwidth considerations but also to improve stability by reducing the number of cavity components. The length of the folded dye cavity was half that of the pump and the pulse therefore saw loss on alternate transits, giving rise to alternating pulse peak heights, but saturable absorption by the dye was assumed to reduce the pulse width on every other pass. 5% output coupling gave an output power of ca. 30 mW. No bandwidth limiting elements were incorporated and pulse durations of less than 2 ps were consistently obtained without excessive stabilisation. (The duration of both pump and dye pulses was measured by background-free autocorrelation). The jitter of the dye pulse was closely related to that of the pump, the latter being amplified by the frequency doubling and the former by operation of the dye laser close to threshold. Length detuning of 5 μ resulted in unstable dye output and broader pulses. Several advantages were seen in the use of the YAG pump: the pump pulse can be shorter than with an Ar^+ laser and is further shortened by frequency doubling to as little as 40 ps. The Nd laser also has certain other practical advantages over the gas laser.

In a second paper Sizer et al. [47] described the use of part of the pump radiation to seed a regenerative Nd:YAG amplifier, the frequency-doubled output of which was in turn used to pump a series of dye amplifers giving a total pulse amplification of more than 10^6. With the dye laser now on a low expansion mount, reproducible pulse durations of 0.5 ps were obtained from a 60 ps pump pulse. Although amplification of pump instabilities was again noted (there was a 1% peak-peak fluctuation in the pump power), the main limitation on the dye pulsewidth was thought to be dye cavity variations - in particular a 0.2 μ

fluctuation at 200 Hz in the thickness of the dye stream. Interferometric feedback to the piezo-electric length control (using fringes from the jet itself) significantly reduced the total length fluctuation but did not produce shorter pulses. The addition of a small amount of the saturable absorber cresyl violet produced pulses shorter than 0.4 ps (s-s exp.) and reduced satellite pulse formation.

The pulse duration was further compressed in a hybrid system using DQOCI (Sizer et al. [59], Mourou & Sizer [60]). A conventional 4-mirror folded cavity of the same length as the pump laser (both of which were stabilised by invar slabs) contained a single 200 μ jet stream and a 2 μ pellicle. The dye mixture contained 5×10^{-4} M Rh-6G and 3×10^{-5} M DQOCI. The position of the jet was not important and no mention was made of counter-propagating pulses. The minimum pulse duration was 70 fs ($sech^2$) at 615 nm when the laser was tuned for maximum output power (30 mW from 300 mW pumping). The pellicle did not restrict the laser bandwidth and allowed tuning from 590 to 615 nm with an increase in pulse width. No satellite pulses or coherence spikes were observed. The pulse width was measured by zero-background autocorrelation and the width of the spectrum - more than 10 nm - suggested either chirp or a failure to measure the real pulse width because of phase matching and geometrical problems in the autocorrelator. The KDP crystal used in this was 1 mm thick and it was thought that the use of a 100 μ crystal and small beam convergence could have improved the resolution. The behaviour of the pulses in dispersive media indicated that there was frequency sweeping, the chirp being positive at the frequency corresponding to minimum pulsewidth, and there was the possibility that "grating pair" compression could yield transform-limited pulses of 30 fs. The laser exhibited maximum stability and power at minimum pulse width "reflecting the dramatic effect of the saturable absorber".

Although the dye concentrations were specified, the threshold pump power output coupling and mismatch behaviour were not. The use of DQOCI, with an absorption band closely matching the Rh-6G emission band, gave a large intensity discrimination and tuning range. Time delay fluorimetry had shown that the 1/e fluorescence time of the dye is not more than 3 ps. When DQOCI was replaced by DODCI [? - the published paper is unclear], with a longer relaxation time, the pulse duration increased to 200 fs. (It is likely that the true figure for the lifetime of DQOCI in the experiment is much longer. Streak camera fluorescence measurements by Taylor et al. [61] show a lifetime as low as 15 ps for DQOCI in

pure methanol rising to ca. 400 ps in 90% glycerol and a value of ca. 100 ps in ethylene glycol, but it is nevertheless much shorter than the value for DODCI, ~1 ns, measured by Sibbett et al. [62].) The duration of the pump pulses was also not given. Although the duration of the frequency-doubled pulses was probably rather less than most ion laser pulses, the power used was not high.

2.12 Cavity Dumping

The peak power available from CW synchronously pumped systems is limited to about 1 kW and this restricts their applications in nonlinear optics. The power can be increased substantially by external synchronous amplification but this requires elaborate extra equipment. A simpler approach is to raise the intra-cavity power by increasing the pump power while decreasing the output coupling. The energy is then extracted by periodic cavity dumping, using, for example, an acousto-optic deflector. One of the earliest Ar^+ systems was actually dumped in this way (Harris et al. [13]). The technique is not now used when minimisation of the pulse duration is sought, because, as a number of authors have remarked, the production of single short pulses requires a low cavity Q. When the output coupling is low, the recovery of the gain after the passage of the main pulse almost inevitably leads to the formation of secondary pulses, particularly if the pump pulse is long (say, 200 ps). Nevertheless, cavity dumping has been reported not just for standing wave systems but in more elaborate cavity configurations which appear to produce shorter, more stable output.

Although an efficient cavity dumper will give the pulse a fresh start after, typically, each 100 round trips, autocorrelations show that the pulse is still very sensitive to the cavity mismatch. Lengthening the cavity causes broadening of the pulse and the appearance of substructure while short cavities lead to satellite production, now exacerbated by the larger ratio of pump power to cavity loss. Nevertheless, good pulses of a few ps duration have been produced by careful balancing of all the system parameters, including, once again, the addition of saturable absorbers.

Apart from the early report by Harris et al., detailed investigations of the cavity dumped performance of standing wave systems did not appear until around 1981 although such devices had become commercially available. The Ar^+/Rh-6G system reported by Sundström and Gilbro [27] gave, without cavity dumping, optimised output of 1.1 ps pulses at 60-150 mW average power from pumping at

550–900 mW. The pulses showed no background or satellites. Cavity dumping with an extinction ratio of 100:1 gave a 30-fold increase in pulse energy, yielding a maximum average power of 30 mW at 600 nm at a dumping rate of 800 kHz. Long cavity lengths gave pulses of 15 to 20 ps showing coherence spikes while reducing the cavity length caused the pulse to shorten to 2 ps but introduced a satellite containing as much as 50% of the energy. The satellite was removed by tuning to longer wavelengths with a wedged filter (bandwidth 0.3 nm) and reducing the pump power. The pulse quality was affected by the dumping rate, rapid dumping leading to operation closer to the undumped performance: at 4 MHz the pulse had reduced autocorrelation shoulders without a satellite. (This suggests that the dumping was inefficient. At 4 MHz the pulse has only a few tens of transits to recover before being switched out again: if the dumping is efficient the recovery begins from a small seed pulse. If the absolute value of the net gain (as opposed to the ratio of gain to loss) is large then the compressive evolution of the pulse will certainly be rapid, but this does not mean that noise fluctuations can be fully removed in this transient regime). The satellite could also be suppressed, with little effect on the output energy, by adding saturable absorbers, but only for low pump powers and restricted tuning ranges.

These observations on mismatch and wavelength are closely paralled by those of Wirth et al. [63] using a system of Ar^+ (500 mW), Rh-6G, 2-element Lyot filter with 70% cavity dumping at 4.2 MHz. TPF autocorrelations showed "bandwidth-limit noise" for long cavities or a good pulse of a few ps followed by a satellite. The pulse was sensitive to length changes of a few μ. Addition of the absorber malachite green, which had been used successfully for passive modelocking, had no effect but DODCI reduced the pulse duration (with a corresponding increase in bandwidth) without significantly affecting the output power or the effects of cavity mismatch. The satellite reappeared at shorter wavelengths, even with high absorber concentrations, which was seen as evidence for red-shifted photoisomerisation.

Johnson [64] had earlier adjusted the losses by displacing the dye jet from the beam waist by ca. 1 mm, thereby improving pulses of 15 ps and 2 kW peak power to 6 ps and 15 kW. Although this will affect the gain saturation by changing the beam area, the full explanation may involve the overlap of pump and dye beam profiles.

Cavity dumping has also been reported for unidirectional ring lasers. Blit and Tang [49] claimed nearly transform-limited pulses of 5ps and peak powers up to 7kW when their system was dumped at 1% of the round trip rate, although the dumping was only 2% efficient. Satellite formation was not mentioned but it was noted that the system was not optimised - without the "optical diode" the pulse duration increased to 100ps. In contrast, Mitchell and Proffitt [52] found that satellite formation was as much a problem in a high-Q unidirectional system as in travelling wave operation. Cavity dumping the half-synchronous ring (Rh-6G,Ar^+,76 MHz) raised the power 5-fold while doubling the pulse width, giving up to 5kW peak power and 2ps FWHM. Although satellites were still produced, the performance of the cavity dumped ring was generally superior to that of the standing wave system.

2.13 Other Synchronously Pumped Experiments

Giant pulse Neodymium laser pumping does offer some advantages and experimental reports have continued to appear. Although the pump envelope is not long enough to produce really short dye pulses, the short duration and high power of the pump pulses, particularly from glass lasers, means that the formation of the dye pulse is very rapid and reasonably short pulses of high power can easily be produced. Investigations of dye pulse parameters from Q-switched Nd:YAG pumping have been presented by Bezrodnyi and Tikhonov [65] and Lokhnygin et al. [66]. In [65], polymethine dyes were pumped by the fundamental while the 2^{nd} harmonic was used to pump Rh-6G, cresyl violet and nile blue, spanning the range 550-730 nm, with pump and dye pulse autocorrelation widths of 10 and 25ps respectively. Competition from ASE was found to be a problem. Output power resonances for cavity mismatches around lengths of 1,1/2,1/3 & 1/4 times the pump length were shown for a rhodamine system. The mismatch tolerance was very much greater than for continuously pumped systems, the power curves having halfwidths of ca. 15ps. The increase in cavity length ratio was accompanied by a rapid decrease in the lasing line width from 1.5nm to 0.05nm.

Lokhnygin et al. used acousto-optically modelocked Nd:YAG pulses (250-300ps in an envelope of 200-500 ns) to pump Rh-6G in a 60 cm resonator. "Appreciable" excess power meant that the optimum output coupling was 40%. Partially modelocked pulses of 25-30ps were produced with a single Fabry-Perot etalon in the cavity. The addition of a second etalon removed the auto-correlation spike without increasing the pulse width and reduced the spectral

width from 1 to .05nm. Typical variations of average power and pulsewidth with mismatch were seen, the former varying slowly and asymmetrically over 2mm, the latter much more rapidly.

The high power of the pump makes possible the generation of pulses in the UV by using the 3rd harmonic of the pump or even the 2nd harmonic of the dye output. Azuma et al. [67] used the former method to pump BBQ and bis MSB, obtaining pulses which were tunable from 380 to 410 nm and from 410 to 430 nm respectively with peak powers of several MW, pulse widths of about 25ps and a time–bandwidth product of about 2.5. The output power showed the typical asymmetric variation with mismatch, halving for a detuning of +2mm.

The Nd pulse train can also be used to pump a series of dye amplifiers, the rapid pumping allowing efficient storage by reducing fluorescence and ASE losses. Wokaun et al. [68], using a Rh–6G oscillator and a chain of three amplifiers pumped by a single frequency–doubled pulse from the Nd train, saw polarisation sensitivity in both the oscillator and the amplifiers. The pulse width doubled and the energy halved when the pump polarisation was orthogonal to that imposed by the oscillator tuning grating. The amplifier gain was much more sensitive to the delay of the probing pulse than would have been expected from the 4 ns lifetime of Rh–6G. The gain showed a 50 ps risetime due to the pump followed by decay in 100ps to about 1/2 of the maximum and then further, slower relaxation. The initial fall was consistent with the measured orientational relaxation time of 100–200ps for Rh–6G in low viscosity solvents.

The use of argon lasers for synchronous pumping has not been completely confined to actively modelocked systems. Vinogradova et al. [69] reported the production of 2–3ps pulses from a Rh–6G laser pumped by an argon laser which was passively modelocked by a high pressure argon cell. The cavity length for minumum pulsewidth corresponded to that for maximum SHG but was 30μ longer than that for maximum average power. The pulse duration increased rapidly as the modelocking of the pump laser was degraded. Kobayashi et al. [70] simplified the pump laser by using external acousto–optic modulation of a CW argon laser. The much slower gain modulation resulted in pulses of 30–50 ps. At high pump powers a large satellite pulse could be seen with a detector resolution greater than 200 ps. This could be quenched by DODCI (the tuning range for the suppression being restricted by the absorber) but the pulse jitter relative to the modulation then increased and the operation was viewed as passive modelocking with the formation of secondary pulses gated by the modulation.

1 Glenn,W.H., Brienza,M.J., de Maria,A.J. - Appl. Phys. Lett., **12**,54 (1968)

2 Soffer,B.H., Linn,J,W, - J. Appl. Phys., **39**, 5859 (1968)

3 New,G.H.C. - I.E.E.E. J. Quant. Electron. QE-**10**, 115 (1974)

4 New,G.H.C., Rea,D.H. - J. Appl. Phys., **47**, 3107 (1976)

5 New,G.H.C., Orkney,K.E., Nock,M.J.W. - Opt. and Quant. Electron., **8**, 425, (1976)

6 Bradley,D.J., Durrant,A.J.F. - Phys. Lett., **27A**, 73 (1968)

7 Derkachyova,L.D., Krymova,A.I., Malyshev,V.I., Markin,A.S. - Opt. and Spectrosc., **26**, 572 (1969)

8 Royt,T.R., Faust,W.L., Goldberg,L.S., Lee,C.H. - Appl. Phys. Lett., **25**, 514, (1974)

9 Goldberg,L.S., Moore,C.A. - Appl. Phys. Lett., **27**, 217 (1975)

10 Dienes,A. - Opto-Electron. **6**, 99 (1974)

11 Ippen,E.P., Shank,C.V., Dienes,A. - Appl. Phys. Lett., **21**, 348 (1972)

12 Chan,C.K., Sari,S.O. - Appl. Phys. Lett., **25**, 403 (1974)

13 Harris,J.M., Chrisman,R.W., Lyttle,F.E. - Appl. Phys. Lett., **26**,16 (1975)

14 Chan,C.K., Sari,S.O., Foster,R.E. - J. Appl. Phys., **47**, 1139 (1976)

15 Kogelnik,H.W., Ippen,E.P., Dienes,A., Shank,C. - I.E.E.E. J. Quant. Electron. QE-**8**, 373 (1972)

16 de Vries,J., Bebelaar,D., Langelaar,J. - Opt. Commun., **18**, 24 (1976)

17 Frigo,N.J., Daly,T., Mahr,H. - I.E.E.E. J. Quant. Electron., QE-**13**, 101, (1977)

18 Heritage,J.P., Jain,R.K. - Appl. Phys. Lett., **32**, 101 (1978)

19 Ferguson,A.I., Eckstein,J.N., Hansch,T.W. - J. Appl. Phys., **49**, 5389, (1978)

20 Scavennec,A. - Opt. commun., **17**, 14 (1976)

21 Jain,R.K., Ausschnitt,C.P. - Opt. Lett., **2**, 117 (1978)

22 Ausschnitt,C.P., Jain,R.K. - Appl. Phys. Lett., **32**, 727 (1978)

23 Ausschnitt,C.P., Jain,R.K., Heritage,J.P. - I.E.E.E. J. Quant. Electron., QE-**15**, 912 (1979)

24 Ryan,J.P., Goldberg,L.S., Bradley,D.J. - Opt. Commun., **27**, 127 (1978)

25 Bethea,C.G., Levine,B.F. - I.E.E.E. J. Quant. Electron., QE-**15**, 547, (1979)

26 Blitt,S., Olsson,A., Tang,C.L. - Opt. Lett., **4**, 245 (1979)

27 Sundström,V., Gillbro,T. - Appl. Phys. Lett., **24**, 233 (1981)

28 Sala,K.L., Kenney-Wallace,G.A., Hall,G.E. - I.E.E.E. J. Quant. Electron., QE-**16**, 990 (1980)

29 Kuhl,J., Lambrich,R., von der Linde,D. - Appl. Phys. Lett., **31**, 657 (1977)

30 Fehrenbach,G.W., Gruntz,K.J., Ulbrich,R.G. - Appl. Phys. Lett., **33**, 160 (1978)

31 Aoyagi,Y., Segawa,Y., Namba,S. - Jpn. J. Appl. Phys., **20**, 1595 (1981)

32 Kuhl,J., Klingenberg,K., von der Linde,D. - Appl. Phys., **18**, 279 (1979)

33 Minami,F., Era,K. - Opt. Commun., **35**, 393 (1980)

34 Leduc,M. - OPt. Commun., **31**, 66 (1979)

35 Marason,E.G. - Opt. Commun., **37**, 56 (1981)

36 Eckstein,J.N., Ferguson,A.I., Hansch,T.W., Minard,C.A., Chan,C.K. - Opt. Commun., **27**, 466 (1978)

37 Jain,R.K. - Appl. Phys. Lett., **40**, 296 (1982)

38 Ferguson,A.I. - Opt. Commun., **38**, 387 (1981)

39 Pike,H.A., Hercher,M. - J. Appl. Phys., **41**, 4562 (1970)

40 McDonald,D.B., Waldeck,D., Fleming,G.R. - Opt. Commun., **34**, 127 (1980)

41 McDonald,D.B., Rossel,J.L., Fleming,G.R. - I.E.E.E. J. Quant. Electron, QE-**17**, 1134 (1981)

42 van Stryland,E.W. - Opt. Commun., **31**, 93 (1979)

43 Shapiro,S.L., Cavanagh,R.R., Stephenson,J.C. - Opt. Lett., **6**, 470 (1981)

44 May,P.G., Sibbett,W., Smith,K., Taylor,J.R., Willson,J.P. - Opt. Commun., **42**, 285 (1982)

45 Frigo,N., Hemenway,C., Mahr,H. - Appl. Phys. Lett., **37**, 981 (1980)

46 Rotman,S.R., Roxlo,C., Bebelaar,D., Yee,T.K., Salour,M.M. - Appl. Phys. B, **28**, 319 (1982)

47 Sizer,T., Kafka,J.D., Krisiloff,A.K., Mourou,G. - Opt. Commun., **39**, 259 (1981)

48 Klann,H., Kuhl,J., von der Linde,D. - Opt. Commun., **38**, 390 (1981)

49 Blit,S., Tang.C.L. - Appl. Phys. Lett., **36**, 16 (1980)

50 Fork,R.L., Greene,B.I., Shank,C.V. - Appl. Phys. Lett., **38**, 671 (1981)

51 May,P.G., Sibbett,W., Taylor,J.R. - Appl. Phys. B, **26**, 179 (1981)

52 Mitchell,G., Proffitt.W. - I.E.E.E. J. Quant. Electron., QE-**17**, (1981) (Technical Digest CLEO '81, Washington, 1981)

53 Halbout,J.-M., Olsson,A., Tang,C.L. - Appl. Phys. Lett., **39**, 463 (1981)

54 Ishida,Y., Yajima,T., Naganuma, K. - Jpn. J. Appl. Phys., **19**, L717 (1981)

55 Yamashita,M., Sato,T. - Appl. Opt., **21**, 2092 (1982)

56 Kuhlke,D., Rudolph,W., Wilhelmi,B. - Appl. Phys. Lett., **42**, 325 (1983)

57 Heritage,J.P., Isaacs,E.D. - I.E.E.E. J. Quant. Electron. QE-**17**, (1981) (Technical Digest CLEO '81, Washington, 1981)

58 Sizer,T., Mourou,G., Rice,R.R. - Opt. Commun., **37**, 207 (1981)

59 Sizer,T., Kafka,J.D., Gable,C., Mourou,G. - Appl. Phys. B, **28** (1982) (abstracts of XIIth Int. Quant. Electron. Conf., Munich, 1982)

60 Mourou,G.A., Sizer.T. - Opt. Commun. **41**, 47 (1982)

61 Taylor,J.R., Adams,M.C., Sibbett,W. - Appl. Phys., **21** (1980)

62 Sibbett,W., Taylor,J.R., Welford,D. - I.E.E.E. J. Quant. Electron., QE-**17**, 500 (1981)

63 Wirth,M.J., Sanders.M.J., Koskelo, A.C. - Appl. Phys. Lett., **38**, 295 (1981)

64 Johnson, R.H. - I.E.E.E. J. Quant. Electron., (1979) (technical digest, IEEE/ESO Conf. on Laser Engineering & Applns)

65 Bezrodnyi,V.I., Tikhonov,E.A. - Sov. J. Quant. Electron., **10**, (1980)

66 Lokhnygin,V.D., Onishchukov,G.I., Fomichev,A.A. - Sov. J. Quant. Electron., **11**, 1230 (1981)

67 Azuma,K., Nakagawa,O., Segama,Y., Aoyagi,Y., Namba,S. - Jpn. J. Appl. Phys., **18**, (1979)

68 Wokaun,A., Liao,P.F., Freeman,R.R., Storz,R.H. - Opt. Lett., **7**, 13 (1982)

69 Vingradova,A.A., Krindach,D.P., Nazarov,B.I., Tsapenko,A.M. - Sov. J. Quant. Electron. **10**, (1980)

70 Kobayashi,T., Hosokawa,T., Sueta,T. - Opt. Commun., **27**, 431 (1978)

3

EXISTING THEORETICAL TREATMENTS OF SYNCHRONOUS PUMPING

3.1 Introduction

The literature presenting specific theoretical models of synchronously pumped modelocking is not extensive. The central feature of interest is the ability of the system to generate pulses of much shorter duration than the pump and the extreme sensitivity of the signal quality to the cavity length detuning. Most treatments of the problem involve simple models with these characteristic times as important parameters. Almost all of the published papers describe the gain evolution by rate equations and, if at all, model the effects of the finite cavity bandwidth by approximations to a lorentzian line profile. A single, fairly recent, Russian paper starts with equations for the signal electric field and medium polarisation, although approximations are needed to derive the final results. None of the existing treatments handles, although one or two mention, the effects of spontaneous emission: we shall show later that this can play a significant role in shaping the steady state pulse.

The first published description was that of Yasa and Teschke [1] who followed numerically the evolution of an initial burst of noise spikes in a matched cavity using rate equations without a filter. The burst evolved towards a steady state profile which was in equilibrium with the pumping rate once the gain exceeded threshold (and consequently of similar duration as the pump). The model was apparently directed at picosecond pumping from modelocked solid state lasers and is incapable of predicting the subpicosecond pulses obtained from a finely tuned Ar^+ pumped system. (Nevertheless, this "equilibrium solution" will later be shown to be the transitional phase as the cavity mismtch is changed from positive to negative values.)

In 1976 Scavennec [2] presented the results of computer evolutions of a lorentzian start pulse in a mismatched cavity. Although the model did not contain a filter and a problem associated with the far wings of the pulse was neglected, the general features of the results are significantly closer to our final model than those of most subsequent attempts using approximate analytic methods. Most importantly, the work showed a qualitative difference between the solutions obtained for long and those for short cavities. For positive cavity

mismatches, a large single pulse with slight asymmetry was produced. Reduction of the detuning towards zero compressed, enhanced and advanced pulse, allowing the formation of a late satellite. As the detuning passed through zero, the pulse degraded rapidly into a single broad pulse centred on the pump profile.

Scavennec noted correctly that the model was unable to predict the location of the stationary pulse for long cavities, which depends on spontaneous emission. An approximate treatment, based on the work of Basov et al., of the case where the signal was delayed until pumping was complete, led to values for the characteristic times of the exponential wings of the pulse. Exact results for this case will be presented later.

The next stage in the search for a simple yet sufficient model introduced the effects of finite intracavity bandwidth through the operator expansions of Haus [3],[4],[5] and the self-reproducing profile technique of Kuizenga and Siegman [6]. The approach assumes that the cavity bandwidth is due to a passive linear element with a lorentzian spectral profile and describes the gain evolution with simple rate equations. All of these treatments, in some way, derive the parameters of the steady state pulse by considering the balance between compresssive and expansive forces acting at the centre of the pulse. There does not seem to be an obvious a priori reason why this should be sufficient to determine the pulse parameters, even approximately, in view of the nonlinear nature of the gain saturation. Nevertheless, several authors have claimed reasonable agreement between the approximate theories and experimentally observed parametric dependencies.

Frigo et al. [7], following an elaborate experimental investigation of the relative timing of pump and signal pulses, analysed the steady state pulse starting with the "cavity admittance" model of Haus. In this, the coupled modes are represented by equivalent electrical circuits with complex admittances dependent on the net gain at the mode frequency. The gain modulation is thought of as deriving from a fictitious loss imposed on a peak possible gain. The explicit form of this loss, which in reality is governed by an integro-differential equation, must be subjected to substantial approximation. The mode equation is Fourier-transformed to obtain approximate differential representations of the modifications to the pulse during a round trip. These are then substituted into the self-reproducing equation, leading to a "Schrödinger" equation for the pulse envelope. Experimental measurements of the fluorsecence of the inversion were used to obtain approximate forms for the fictitious loss

in different regions of local time leading to analytic solutions for the pulse in these regions.

Ausschnitt and Jain [8], Ausschnitt et al. [9] and Kim et al. [10] applied the self-reproducing profile method first introduced by Kuizenga and Siegman [6] in the study of active modelocking of homogeneously broadened systems. This consists of assuming a "reasonable" analytic form for the signal pulse and subjecting it to operators describing the action of the elements of the cavity during a round trip. The self-consistency condition is then used to determine the free parameters of the solution. In this case the solution is assumed to be gaussian and second order expansions of the filter, gain and shift operations suffice to determine the width, energy and location of the pulse.

In [9] the self-reproducing condition on the pulse amplitude V(t) is derived as

$$\left[g(t) - L + \delta T\frac{d}{dt} + \frac{1}{\omega_c^2}\frac{d^2}{dt^2}\right] V(t) \quad = \quad 0 \qquad (3.1)$$

where g is the round trip gain, L is the linear loss, δT is the cavity mismatch and ω_c is the intracavity bandwidth. The gain function is expanded about the pulse peak and an approximate value for the integrated gain up to the arrival of the pulse leads to simultaneous equations for the pulse parameters. When the pump and slave cavities are matched - i.e. when $\delta T = 0$ - the simple solutions

$$\tau_{dye} \propto \sqrt{\tau_{pump}/\omega_c} \qquad (3.2)$$

$$I_{peak} \propto 1/\tau_{pump} \qquad (3.3)$$

are obtained. The $\sqrt{\ }$ dependence of the signal duration on the bandwidth is closely related to the result of Kuizenga and Siegman: experimental results were presented in [8] which seemed to confirm it.

Kim et al. [10] followed similar lines but found that the pulse duration depended on $[1 / \omega_c]^{2/3}$ and on the 1/3 power of the "gain modulation strength". In the next section we present a detailed reformulation of their calculation, reaching slightly different conclusions. A very similar operator expansion approach has been applied by Ram and Reddy [11] and by Reddy [12]. In the latter, a synchronous loss modulator was included with a claimed reduction of the length sensitivity.

We defer until ch.7 mention of more recent and potentially more accurate treatments by Herrmann and Mottschmann [13],[14], Nekhaenko [15] and Yasa [16].

3.2 The Closed Form Gaussian Solution

This section presents a detailed reformulation of the method outlined in Kim et al. [10] with certain modifications. The derivation of moderately simple relationships between the main input and output parameters (the pump power, cavity mismatch, signal duration etc.) can only be obtained after numerous appoximations have been made. Even then, the method used here requires the solution of a complicated transcendental equation. Although the basic approach is simple, it appears to be difficult to derive a final result which is both "transparent" and sufficiently accurate. Furthermore, we shall show later that the assumption made at the outset about the form of the solution conceals a significant feature of the physics and suggests that the self-reproducing method may lead to substantial errors when applied to this type of system.

The standard simplifying assumptions will be made:

1) The laser is a ring cavity containing a thin amplifying medium and a linear loss.
2) The amplification coefficient is sufficiently well described by a 2-level rate equation and is driven by a gaussian pump pulse. Pump depletion and signal re-absorption are neglected.
3) All dispersive and bandwidth narrowing effects are attributed to an ideal passive filter with a lorentzian power spectrum.
4) The signal consists of a slow amplitude modulation of a chirp-free carrier wave. No phase effects are considered.

The rate equation governing the gain coefficient, A, is

$$\left[\frac{d}{dt} + \frac{1}{T_s} V^2(t)\right] A = \frac{P\Gamma}{t_p\sqrt{\pi}} \exp\{-(\frac{t-\Delta t}{t_p})^2\} \qquad (3.4)$$

where V is the signal amplitude (as a function of local time, t) normalised to the saturation flux of the amplifier, $1/T_s$. The strength of the pump pulse relative to the linear loss factor, Γ, is given by P such that

$$\int_{-\infty}^{\infty} \text{Pump}\ dt = P\Gamma \qquad (3.5)$$

We assume a gaussian form for the signal pulse, $V = \exp(-\gamma t^2)$ and seek solutions for γ, T_s and the delay between the peaks of the pump and signal pulses given by Δt.

The steady-state pulse satisfies the condition

$$\text{Filter}\left\{\text{Gain} \times V(t)\right\} = V(t+t_m) \tag{3.6}$$

where the cavity mismatch, t_m, is defined by

$$t_m = [L_{dye} - L_{pump}]/c \tag{3.7}$$

The rate equation becomes

$$\frac{dA}{dt} + \frac{e^{-2\gamma t^2}}{T_s} A = \frac{P\Gamma}{t_p\sqrt{\pi}} \exp\left[-\left(\frac{t-\Delta t}{t_p}\right)^2\right] \tag{3.8}$$

Using the integrating factor for (3.8),

$$\exp\left(\int \frac{1}{T_s} e^{-2\gamma t'^2} dt'\right) \tag{3.9}$$

and

$$\int_0^t \frac{1}{T_s} e^{-2\gamma t'^2} dt' = \frac{1}{2T_s}\sqrt{\frac{\pi}{2\gamma}}\, \text{erf}(\sqrt{2\gamma}t) \tag{3.10}$$

gives

$$\frac{d}{dt}\left[A \exp\left(\frac{1}{2T_s}\sqrt{\frac{\pi}{2\gamma}}\, \text{erf}(\sqrt{2\gamma}t)\right)\right] = \frac{P\Gamma}{t_p\sqrt{\pi}} \exp\left[-\left(\frac{t-\Delta t}{t_p}\right)^2\right] \exp\left[\frac{1}{2T_s}\sqrt{\frac{\pi}{2\gamma}}\, \text{erf}(\sqrt{2\gamma}t)\right] \tag{3.11}$$

Integrating, with $A(-\infty) = 0$, gives

$$A(t) = P\Gamma \exp\left\{-\frac{1}{2T_s}\sqrt{\frac{\pi}{2\gamma}}\, \text{erf}(\sqrt{2\gamma}t)\right\} \times \int_{-\infty}^{t} \frac{1}{t_p\sqrt{\pi}} \exp\left\{-\left(\frac{t-\Delta t}{t_p}\right)^2\right\} \exp\left\{\frac{1}{2T_s}\sqrt{\frac{\pi}{2\gamma}}\, \text{erf}(\sqrt{2\gamma}t)\right\} dt \tag{3.12}$$

The erf in the exponent under the integral sign is only appreciably greater than -1 for a period $\sim 1/\sqrt{\gamma}$ about t (i.e. close to the centre of the signal pulse). Assuming that the solution is significantly shorter than the pump, we approximate this second erf by -1, giving

$$A(t) \simeq \frac{P\Gamma}{2} \exp\left[-\frac{1}{2T_s}\sqrt{\frac{\pi}{2\gamma}}(1+\mathrm{erf}(\sqrt{2\gamma}t))\right]\left[1+\mathrm{erf}\left[\frac{t-\Delta t}{t_p}\right]\right] \quad (3.13)$$

We now expand the gain coefficient, A, in a Taylor series about $t=0$, using (3.13) to find the zeroth order term:

$$A(t) \simeq A(0) + \dot{A}(0)\, t + \ddot{A}(0)\, t^2/2 + \ldots \quad (3.14)$$

From (3.13),

$$A(0) \simeq \frac{P\Gamma}{2}\, \mathrm{erfc}\left(\frac{\Delta t}{t_p}\right) \exp\left[-\frac{1}{2T_s}\sqrt{\frac{\pi}{2\gamma}}\right] \quad (3.15)$$

while, from the rate equation (3.8),

$$\dot{A}(0) = -\frac{1}{T_s} A(0) + \frac{2P\Gamma}{\sqrt{\pi}t_p} \exp\left[-\left(\frac{\Delta t}{t_p}\right)^2 \right] \quad (3.16)$$

Differentiating gives

$$\ddot{A}(0) = -\frac{1}{T_s}\dot{A}(0) + \frac{2P\Gamma}{\sqrt{\pi}t_p} \exp\left[-\left(\frac{\Delta t}{t_p}\right)^2 \right] \quad (3.17)$$

$$= \frac{1}{T_s^2} A(0) - \frac{P\Gamma}{\sqrt{\pi}t_p T_s} \exp\left[-\left(\frac{\Delta t}{t_p}\right)\right] + \frac{2P\Gamma\Delta t}{\sqrt{\pi}t_p} \exp\left[-\left(\frac{\Delta t}{t_p}\right)^2\right] \quad (3.18)$$

The action of the gain is described by

$$V'(t) = e^{\frac{1}{2}\left[A + A(0)t + A(0)t^2/2\right] - \Gamma/2} \cdot V(t) \equiv g(t)\, V(t) \quad (3.19)$$

The filter is modelled by the convolution action of a damped linear device of response time T_f:

$$V(t) \otimes \mathcal{J}(t) \rightarrow \frac{1}{T_f} \int_{-\infty}^{t} V(t')\, e^{(t'-t)/T_f}\, dt' \quad (3.20)$$

Using the inverse filter operator gives the steady state condition

$$g(t)\ V(t) \quad = \quad \left[1 + T_f \frac{d}{dt}\right] V(t+t_m) \tag{3.21}$$

Substituting for g and V leads to

$$\begin{aligned}\left[A_o + A_1 t + \tfrac{1}{2}A_2 t^2 - \Gamma\right]/2 - \gamma t^2 \quad &= \\ - \gamma (t+t_m)^2 + \ln\left[1-2\gamma(t+t_m)T_f\right]&\end{aligned} \tag{3.22}$$

Expanding up to order t^2:

$$\ln\left[1-2\gamma(t+t_m)T_f\right] \simeq \ln(1-2\gamma t_m T_f) - \frac{2\gamma t T_f}{1-2\gamma t_m T_f} - \frac{2\gamma^2 t^2 T_f^2}{(1-2\gamma t_m T_f)^2} \tag{3.23}$$

Equating coefficients of t gives

$$\tfrac{1}{2}(A_o - \Gamma) \quad = \quad -\gamma t_m^2 + \ln(1 - 2\gamma t_m T_f) \tag{3.24a}$$

$$\tfrac{1}{2}(A_1) \quad = \quad - 2\gamma t_m - 2\gamma T_f \,/\, (1-2\gamma t_m T_f) \tag{3.24b}$$

$$\tfrac{1}{2}(A_2/2) \quad = \quad - 2\gamma^2 T_f^2 \,/\, (1-2\gamma t_m T_f)^2 \tag{3.24c}$$

and, substituting for A leads to the

$$\frac{P\Gamma}{4} \operatorname{erfc}\left(\frac{\Delta t}{t_p}\right) \exp\left[\frac{-1}{2T_s}\sqrt{\frac{\pi}{2\gamma}}\right] = -\gamma t_m^2 + \ln(1-2\gamma t_m T_f) + \frac{\Gamma}{2} \tag{3.25a}$$

$$\begin{aligned}\frac{1}{2}\left[\frac{P\Gamma}{2} \operatorname{erfc}\left(\frac{\Delta t}{t_p}\right) \exp\left\{\frac{-1}{2T_s}\sqrt{\frac{\pi}{2\gamma}}\right\} - \frac{P\Gamma}{\sqrt{\pi}\,t_p} \exp\left\{-\left(\frac{\Delta t}{t_p}\right)^2\right\}\right] &= \\ 2\gamma t_m + \frac{2\gamma T_f}{(1-2\gamma t_m T_f)}&\end{aligned} \tag{3.25b}$$

$$\begin{aligned}\frac{1}{2}\left[\frac{P\Gamma}{4T_s^2}\operatorname{erfc}\left(\frac{\Delta t}{t_p}\right) \exp\left\{\frac{-1}{2T_s}\sqrt{\frac{\pi}{2\gamma}}\right\} - \frac{P\Gamma}{\sqrt{\pi}\,t_p^2}\left(\frac{t_p}{T_s} - 2\frac{\Delta t}{t_p}\right) \exp\left\{-\left(\frac{\Delta t}{t_p}\right)^2\right\}\right] &= \\ \frac{4\gamma^2 T_f^2}{(1-2\gamma t_m T_f)^2}&\end{aligned} \tag{3.25c}$$

These equations, after further simplification, are solved numerically.

Plots of the pulse parameters, normalised to the pump scale time, t_p, are shown in fig. 3.1.

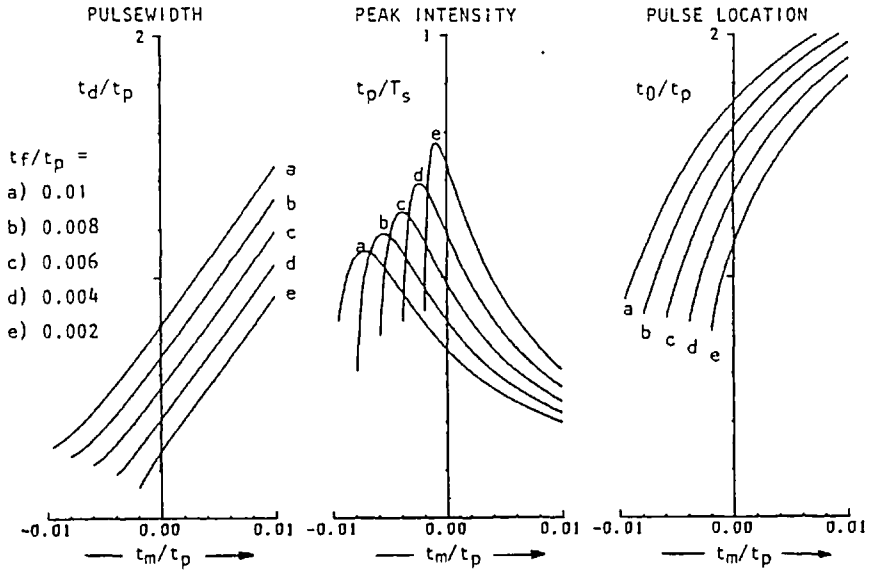


FIG. 3.1 : Gaussian solution parameters

Chapter 3 : References

1 Yasa,Z.A., Teschke,O. - Opt. Commun., **15**, 169, (1975)

2 Scavennec,A. - Opt. Commun., **17**, 14 (1976)

3 Haus,H.A. - J. Appl. Phys., **46**, 3049 (1975)

4 " - I.E.E.E. J. Quant. Electron., QE-**11**, 323 (1975)

5 " - ibid **736** (1975)

6 Kuizenga,D.J., Siegman,A.E. - I.E.E.E. J. Quant. Electron., QE-**6**, 709 (1970)

7 Frigo,N.J., Daly,T., Mahr,H. - I.E.E.E. J. Quant. Electron., QE-**13**, 101 (1977)

8 Ausschnitt,C.P., Jain,R.K. - Appl. Phys. Lett., **32**, 727 (1978)

9 Ausschnitt,C.P., Jain,R.K., Heritage,J.P. - I.E.E.E. J. Quant. Electron., QE-**15**, 912 (1979)

10 Kim,D.M., Kuhl,J., Lambrich,R., von der Linde,D. - Opt. Commun., **27**, 123, (1978)

11 Ram,J., Reddy,K.P.J. - Opt. Commun., **33**, 323 (1980)

12 Reddy,K.P.K. - Opt. Commun., **37**, 77 (1981)

13 Herrmann.J., Mottschmann,U. - Opt. Commun., **40**, 379 (1982)

14 . . - Appl. Phys.B, **27**, 27 (1982)

15 Nekhaenko,V.A. - Sov. J. Quant. Electron., **11**, 446 (1981)

16 Yasa,Z.A. - Appl. Phys.B, **30**, 135 (1983)

4

DIRECT STEPPING CALCULATION OF STEADY STATE PULSE PROFILES

4.1 Introduction

The closed form solution attempted in the last chapter is not only complicated in spite of the approximations, but is unrealistically constrained. This chapter presents a simple technique which allows the direct prediction of steady state pulse profiles under certain circumstances. Although the method requires numerical evaluation, it is simple yet essentially exact within the rate equation approximation, and makes few of the further simplifications of most other published treatments. In general the method requires the iteration of a first or second order difference equation for points on the pulse profile coupled to a rate equation for the gain. For certain parameter values the behaviour of the equations closely resembles the evolution of a giant pulse in a Q-switched laser with a long energy storage time.

The analysis emphasises the importance of the injection of noise into the cavity by spontaneous emission (although it is treated here in a grossly simplified fashion) and demonstrates that the time variation of the pumping rate has less effect on the pulse duration than has been suggested previously. The method predicts experimentally observed details of the pulse structure which are not generally seen in simple "analytical" treatments and, in subsequent chapters, will be extended to include further processes which make analytic solution impossible.

The incorporation of a Fabry-Perot etalon allows the action of a specific bandwidth-limiting device to be modelled simply yet exactly (while the interaction of the signal with the gain is still described by a rate equation). The inclusion of the filter does not change the essence of the prediction equation in the quasi-"giant pulse" regime of operation: in this case the filter simply expands the time-scale of the pulse. Without the filter, a significant change in the form of the pulse is predicted as the cavity length mismatch passes through zero. The introduction of the filter moves this transition point towards negative mismatches, allowing the "giant pulse" regime to persist for

slightly short cavities. Unless the negative detuning is small, however, the direct prediction technique breaks down: the failure arises partly from the mathematical formulation of the problem but also, more fundamentally, from uncertainty in the knowledge of the boundary values required for a solution. These problems will be discussed in subsequent chapters.

4.2 The Foundation Of The Stepping Model

The normal simplifying assumtions will be made for much of the analysis:

1) The interaction of the signal pulse with the gain medium can be described by a 4-level rate equation. The signal pulse will be described by an intensity envelope or, when the action of a filter is discussed, by an amplitude profile given simply by the square root of the intensity.
2) The effect of spontaneous emission into the cavity can be described by adding a small intensity to the signal. In the formulation of the steady state prediction equations no account will (or perhaps can) be taken of fluctuations on any time-scale.
3) The laser is a ring cavity with a thin gain medium and an isolated linear loss. Initially, the only nonlinear process considered will be the saturated gain seen by the pulse as it passes through the amplifier.
4) The pumping consists of a continuous train of jitter-free gaussian pulses. The round trip time of the ring cavity is very close to the pump pulse spacing and only one signal pulse circulates in the cavity. The absorption of the pump pulse by the gain medium is described by a rate equation in which saturation is neglected.
5) We consider only uniform, plane, signal and pump waves. All geometrical and diffraction effects will be ignored.
6) The dye laser cavity is long enough for any inversion remaining after the passage of the laser pulse to have relaxed before the next pump pulse.

We seek a steady state solution giving a well-contained signal pulse, hopefully shorter than the pump pulse duration and certainly shorter than the cavity round trip time (although there is no certainty that it will actually exist). The nature of the gain evolution is such that the population inversion can never fall to zero and consequently that there is continuous spontaneous emission into the cavity. Under good modelocked operation the pulse is indeed well defined and shorter than T_{ring} by a factor of more than 10^3. The laser output is very sensitive to small length detunings and it seems likely that these will be

centred on a cavity length close to exact match. Apart from a time shift which is compensated for by the mismatch, the pulse reproduces itself on each passage through the amplifier. The detuning range, and therefore probably the detuning itself, is normally found to be small compared to the duration of the signal pulse, indicating that the relative reshaping of the envelope on each transit is small. The pulse therefore cannot reform from noise on each transit. Unless the cavities are exactly matched, however, the pulse can be pictured as moving slowly across the noise background which fills the rest of the cavity. Throughout most of a cavity circuit the gain seen by the signal must remain below unity to keep this background at a low level. The gain is brought rapidly above threshold by the pump pulse and we expect the dye pulse to arrive at the amplifier close to this moment in the circuit. The pulse energy is unchanged after passing through the gain and loss, so, in the absence of dispersive effects,

$$\int F(t)\, g(t)\, dt \quad = \quad \int F(t)\, dt \qquad (4.1)$$

where $F(t)$ is the pulse intensity as a function of local time, t, and g is the net gain at t for one cavity circuit. Integration is over the immediate vicinity of the pulse (ignoring the energy contained in the noise background). Since F and g are always >0 it follows that either $g=1$ always or $g>1$ for part of the pulse and $g<1$ for the remainder. The first case (or at least a very close approach to it) forms the transition between the two modes of operation as the cavity mismatch passes through zero. (The solution where $g=1$ always is that in Yasa and Teschke [1]).

When the cavity mismatch, t_m, is not zero, the gain must deviate from unity if the reshaping of the pulse is to be caused by gain modulation alone. When the dye cavity is long (i.e. $t_m > 0$) the pulse must be advanced by the gain which must therefore be greater than 1 on the leading edge of the pulse. The signal will remain at a low level until the gain has exceeded threshold. The pulse will begin to deplete the gain once it reaches the level of the saturation flux and g will drop below unity in the tail of the pulse, advancing the tail in local time and holding down the noise level once the pulse has passed. For $t_m < 0$, net loss is required over the whole of the front of the pulse and net loss on the trailing half: it is not immediately obvious that a stable balance can then be achieved. Although the numerical evolution studies

to be presented later show that this can be obtained, the problematic balancing act that it seems to require lies at the heart of the failure of the stepping approach for $t_m < 0$. We therefore begin by considering the case of $t_m > 0$.

The basic stepping algorithm hinges on the fact that the self-reproducing condition for a pulse in a mismatched cavity equates the flux at one point in local time to that at another separated by a delay or advance equal to the mismatch time (fig.4.1). The two values are related through the operator which describes the effect of all the cavity processes (apart from the shift) at that particular moment in local time. Given sufficient knowledge of this operator, together with a boundary value, the complete pulse profile can, in principle, be mapped out along a mesh of time points separated by t_m. Providing that the pulse itself is considerably longer than t_m, this will give an accurate "map" of the pulse. The success or failure of the method is largely determined by the sign of the mismatch: for positive values of t_m, information is "stepped" through the pulse in the same direction as the integration of the saturated gain. More importantly, the fact that the pulse only arrives at the amplifier after the gain has exceeded threshold allows a reasonable estimate to be made of the initial values for both the signal and the gain evolutions.

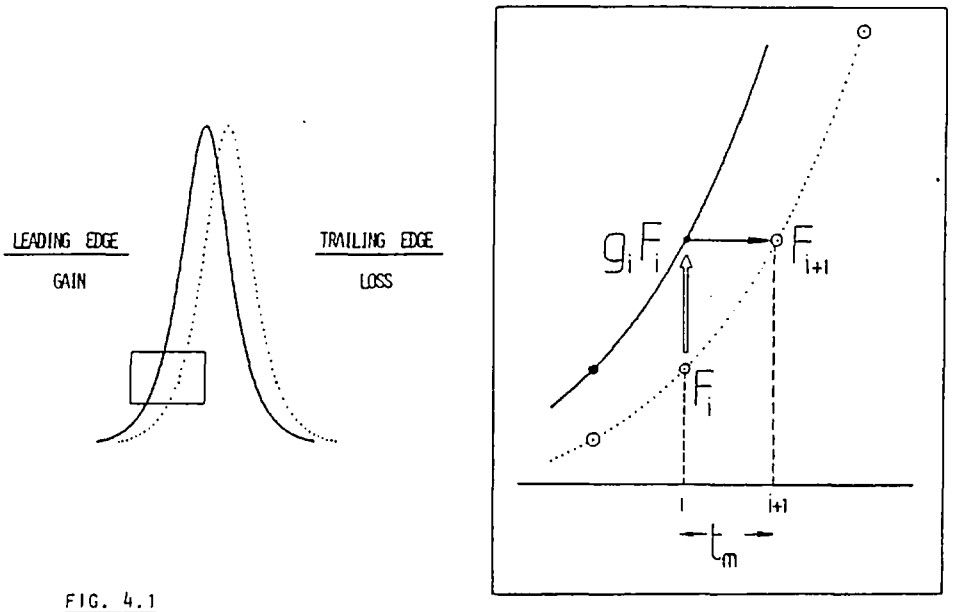


FIG. 4.1

4.3 The Stepping Model For Positive Cavity Detunings

The self-reproducing condition on the pulse is

$$O[F(t)] = F(t+t_m) \tag{4.2}$$

where O represents the action of the cavity elements on the intensity F during one round trip. Taking these as just the gain and loss gives

$$F(t)\ \exp(A(t)-\Gamma) = F(t+t_m) \tag{4.3}$$

Expressing the intensity as a mesh of values F_i separated in time by t_m gives

$$F_{i+1} = F_i\ \exp(A_i - \Gamma) \tag{4.4}$$

This, together with the rate equation

$$\dot{A} = \text{Pump} - F\ (e^A - 1) \tag{4.5}$$

is the basic stepping algorithm. Providing that the step size is small enough to allow accurate integration of the gain it only remains to find initial values for F and A. As a first step we assume that the noise level is so low that the time evolution of the gain up to threshold takes place without significant depletion. In case we find that the solution is of the same duration as the pump pulse, we use a moderate value of t_m - say (pump duration)/1000 - and in the absence of detailed knowledge of the noise level we choose an initial value of F which is simply small compared to the normalised saturation flux - say $F_0=10^{-4}$.

The gaussian pump pulse is again given by

$$\text{Pump} = \frac{P\Gamma}{t_p\sqrt{\pi}}\ \exp(-[t/t_p]^2) \tag{4.6}$$

where the factor P gives the pumping strength relative to the linear loss coefficient Γ. Throughout what follows local time is normalised to the scale time of the gaussian pump, t_p. The threshold time (in the absence of a depleting signal) is the solution, θ, of

$$\int_{-\infty}^{\theta} \frac{P\Gamma}{\sqrt{\pi}} \exp(-t^2)\, dt \quad = \quad \Gamma \tag{4.7}$$

$$\theta \quad = \quad \mathrm{erf}^{-1}\left(\frac{2}{P} - 1\right) \tag{4.8}$$

Fig. 4.2 shows the pulse profile obtained by starting the evolution of F at threshold ($\theta = 0.684$) with an initial F value of 10^{-4} for weak pumping (P=1.2) and $\Gamma = 0.2$. The method is apparently an immediate success, generating a single symmetrical pulse which is substantially narrower than the pump itself. The gain remains below threshold once the peak of the pulse has passed.

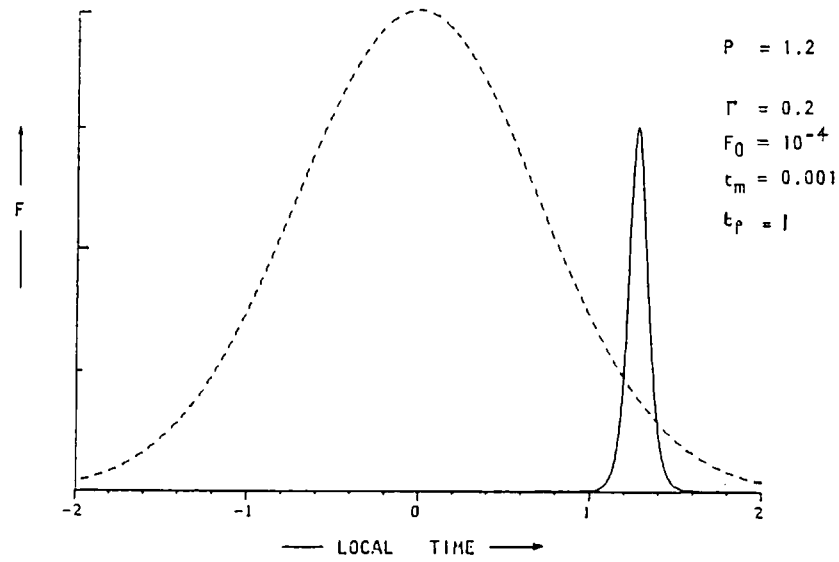


FIG. 4.2 : Basic stepping profile

Before investigating the effects of varying the input parameters we introduce an empirical noise "injection" term which allows the signal to find its own level during the early stages of the evolution instead of fixing it through a single boundary value at threshold. Apart from the fact that we no longer have to solve the threshold equation, this allows to some extent for gain depletion as the signal grows just before threshold. The modified stepping algorithm is

$$F_{i+1} = F_i\, g_i + N \qquad (4.9)$$

The noise term will normally be kept at a small constant value. A term proportional to the inversion might be a little more realistic but under most, if not all, circumstances, the noise level must be changed by an order of magnitude to have a significant effect on the profile: the value of A changes by much less than this during the passage of the pulse. When the net gain is below unity, the stepping equation (4.9) converges rapidly for any small seed value. We therefore begin the iterations some time before threshold and start the process with F=N (or even zero). Providing that N is small, the injection term has little effect for $t_m > 10^{-4}$. Fig.4.3 shows the pulse generated by the modified algorithm for the same parameters as fig.4.2 (P=1.2, Γ=0.2, $t_m=10^{-3}$) together with an injection term rather smaller than the initial value used in the first profile, $N=10^{-5}$. Although somewhat advanced and attenuated, the new profile is qualitatively very similar. The difference immediately demonstrates an important point which has been ignored in a number of previous treatments; that the steady state profile depends on the level of spontaneous emission.

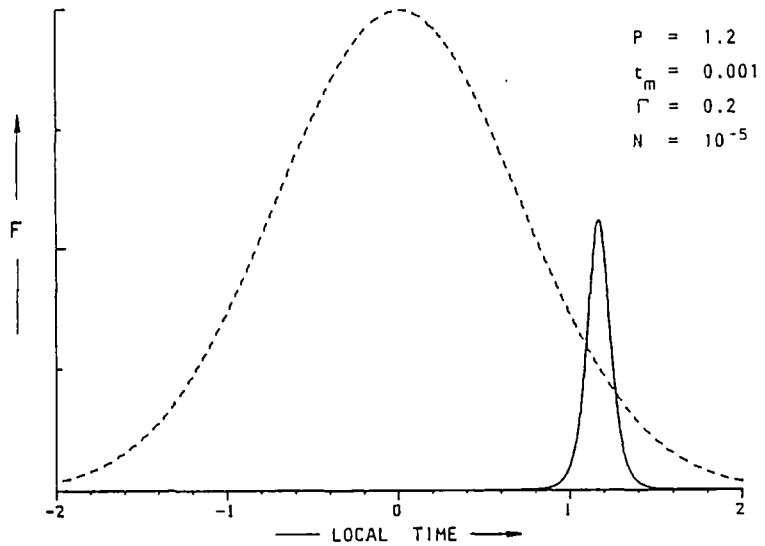


FIG. 4.3: Addition of noise term

4.4 Dependence Of The Solutions On The Principal Parameters

We now investigate briefly the effect of varying P, t_m and N. It is found experimentally that good, single pulsed modelocking is only obtained at low pumping levels. Autocorrelation measurements show that raising the pump power often leads to the appearance of satellite pulses. This has been attributed by a number of authors to the recovery of the gain before the end of the pump pulse and the effect is immediately apparent from the stepping solutions. Fig.4.4 shows pulse profiles for different, low pumping levels (expressed relative to the loss by P).

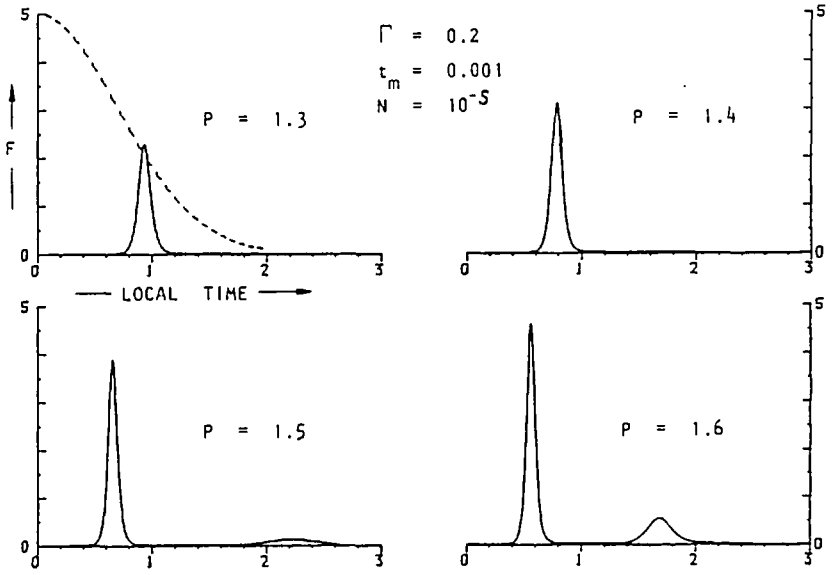


FIG. 4.4: Increasing pump power

The increase in the pumping brings the pulse forwards in local time, compressing it swiftly. In terms of the stepping algorithm, the signal rises steadily out of the noise after the gain has passed threshold. Once the intensity is significantly above the noise we can view the rise as an exponential curve with a coefficient which increases slowly as more gain is delivered. The rise limits when the pulse begins to deplete the gain. At higher pump powers, this process takes place much faster but the low start continues to hold dowm the signal in its early stages. Consequently, there is

more gain available at the point where depletion sets in, and sharper and sharper pulses are formed as P is increased. As the rise becomes faster so does the fall in the tail of the pulse. The evolution overshoots because depletion of the gain takes place much faster than the pumping, and the tail of the pulse drops rapidly until it reaches the background noise level. If, however, the pulse arrives early enough, the remaining pump energy may be sufficient to raise the gain above threshold once more. As it does so the stepping iteration generates another pulse. There is no limit in this model to the number of pulses in the train. Fig.4.5 shows what happens as P is raised further. The onset of multipulsing is swift and a train of increasingly sharp, well-separated pulses is formed. The energy of each pulse does not appear to be fixed and the number and distribution of the subpulses depend on all the input parameters.

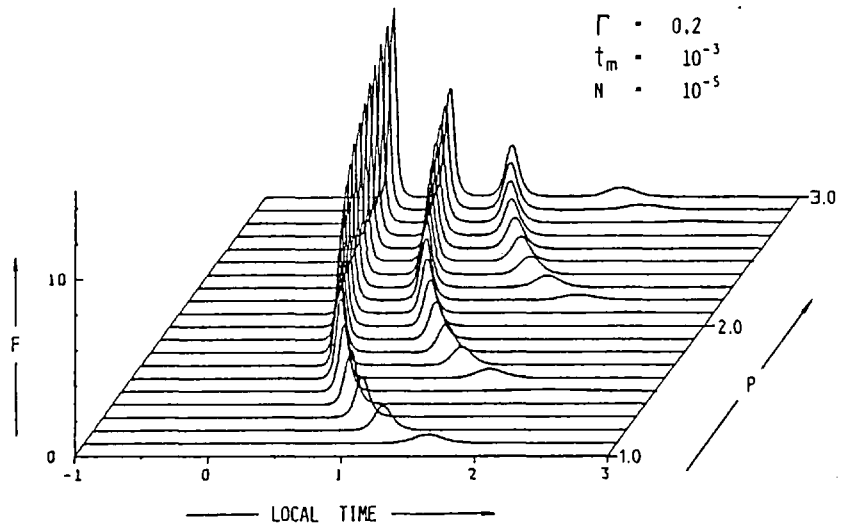


FIG. 4.5

It is evident that this overall picture of the steady state balance differs significantly from that in the gaussian model where approximations are made to the conditions for dynamic balance around the centre of the pulse. The stepping algorithm is a nonlinear oscillation, generating the pulse profile by a "hunting" process with well-damped overshoots - behaviour which is closely

analogous to the evolution of a giant pulse in a laser where the energy storage lifetime is much longer than the cavity transit time (Wagner and Lengyel [2]). Because of this connection between the scale time t_m of the stationary state and the lifetime of a giant pulse, we view eqn.(4.9) in evolutionary terms and refer to it as the "stepping model" of the pulse.

This overshooting – that is failure to reach dynamic equilibrium with the pumping rate – is characteristic of the model when $t_m > 0$. The timescale is controlled by t_m but N plays an important role as t_m is reduced to zero. For very small values of t_m the solution can be viewed as a perturbed version of that given by Yasa and Teschke [1], in which the pulse is in full equilibrium with the gain once threshold has been reached. For negative values of t_m the solution moves away from equilibrium in a qualitatively different manner. Later sections will show, by altering the relative parameter sizes and adding saturable absorbers, other examples of familiar "macroscopic" laser behaviour which have "microscopic" analogues in these steady-state profiles.

The gas laser pulses used experimentally are typically between 80 and 250 ps (FWHM) in duration, and we shall for convenience assume that t_p is 100 ps. The value of t_m used above was chosen to allow a reasonably fine mesh of points across the pump pulse without requiring an excessively large number of iterations to complete the map of the signal pulse. With t_p equal to 100 ps, this is equivalent to a cavity detuning of approximately 15 μ. Although some experimental reports indicate detuning tolerances as small as 1 μ, it is within the range of many experimental measurements and is a reasonable value to start with. Fig.4.6 shows the dependence on the mismatch at a noise level low enough to give sharply defined pulses. When the pulse arrives late in the pumping the duration is scaled by t_m but satellite formation begins as the pulse advances under the pump.

Even at low pumping levels the stepping model can generate profiles which are appreciably shorter than the pump pulse, but the results shown so far suggest that satellites are likely to be present if picosecond or subpicosecond pulses are to be obtained. The generation of isolated ultrashort pulses evidently requires a balance of all the parameters (including dispersive effects which we which we shall introduce shortly through a linear filter). Because the signal pulses are usually much shorter than the pump, it seems likely that the variation of the gain due to pumping during the passage of the pulse peak is of secondary importance. The dominant process here is the depletion of the gain by

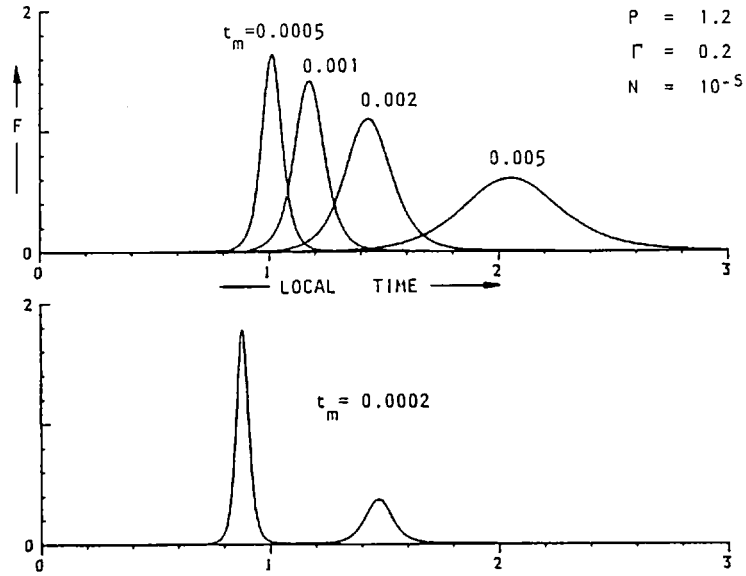


FIG. 4.6: Reduction of mismatch

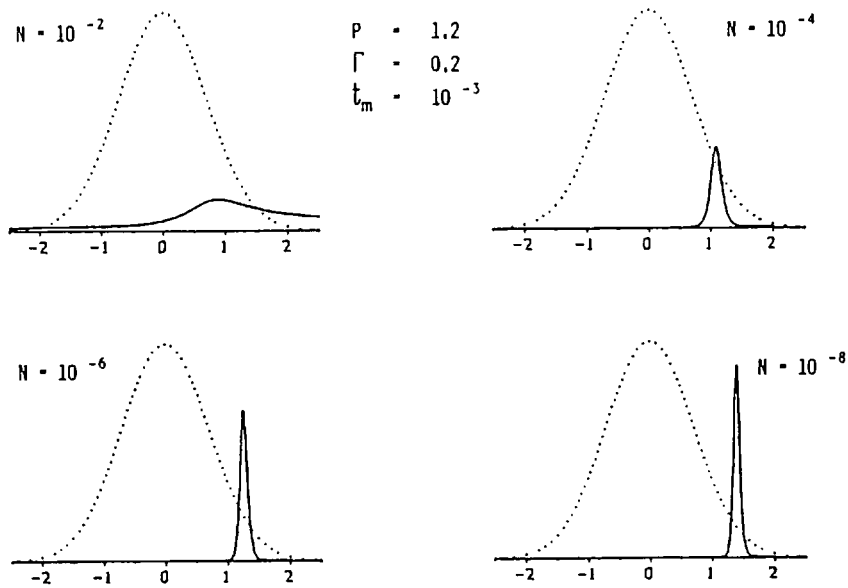


FIG. 4.7: Effect of the noise level

the pulse itself. Indeed, for moderate values of t_m and P and low values of N, the signal arrives after most of the gain has been delivered. Under these circumstances the behaviour of the stepping model is very close to giant pulse evolution. The pulse wings will be exponential in form although the characteristic time of the leading edge need not be the same as that of the tail.

The effect of altering the noise level under weak pumping is shown in fig.4.7. For small values of N the pulse appears well after the "ideal" threshold time (that derived assuming no gain depletion in the early stages). As N is reduced the pulse arrives later and compresses as the Q-switched overshoot becomes stronger. Compression will continue until N is small enough to delay the signal until the pumping is complete, beyond which value the pulse will simply be delayed. For small t_m and energetic pumping this may require a value of N far below a realistic noise power.

Fig.4.8 shows a log plot of three of the solutions: for the low noise level the pulse has exponential wings over several decades. In this case the pulse is also symmetrical, indicating that $|G-\Gamma|$ has the same value in the each wing of the pulse. In general this need not be so: the net loss is limited to $e^{-\Gamma}$ in the tail whereas the gain is not constrained on the leading edge. In practice, however, the maximum attainable value of the gain on the leading edge is limited by the extremely rapid rise of the pulse itself. The elegant symmetry of the pulses can persist up to high pumping levels when satellite formation allows the gain seen by each subpulse to be relatively small. Figs.4.9 show the effect of reducing the value of N on the gain evolution during the latter half of the pump pulse. The symmetrical swing of the gain, as it passes through Γ at the centre of the pulse is clearly shown, particularly in the latter case. This is generally so for weak pumping and positive t_m; the value of A in the tail of the pulse consequently becomes closer to Γ as P is reduced. The exponential wings are therefore slower and the pulse extracts a smaller fraction of the total gain.

One fundamental point that the results so far indicate is that steady state pulses of finite duration are predicted in a system where the gain satisfies a simple rate equation. This is in sharp contrast to the rate equation analysis of passive modelocking by saturable absorbers where pulse compression can continue indefinitely, and shows that the compression mechanism in synchronously pumped modelocking is intrinsically less strong. (The role of

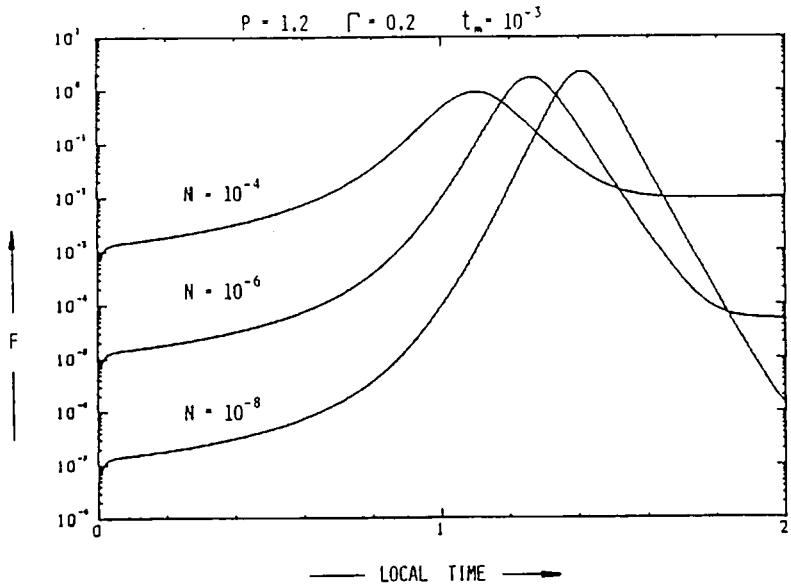

P = 1.2 Γ = 0.2 $t_m = 10^{-3}$
N = 10^{-4}
N = 10^{-6}
N = 10^{-8}
F
LOCAL TIME

FIG. 4.8

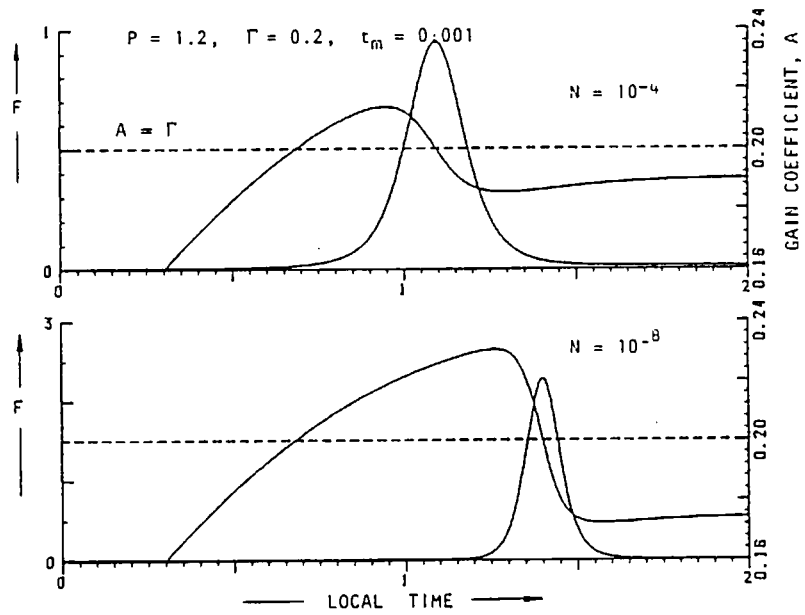

P = 1.2, Γ = 0.2, t_m = 0.001
N = 10^{-4}
A = Γ
N = 10^{-8}
F
GAIN COEFFICIENT, A
LOCAL TIME

FIG. 4.9

noise injection and of a bandwidth-limiting filter in passive modelocking will be considered later). The predictions of the stepping model are accurately confirmed by numerical simulations of the evolution of the pulse from a low noise start (the results of which will be presented later) and agree in some respects with those obtained by Scavennec [3] and Herrmann & Mottschmann [4]. When the duration of the signal pulses is greater than, say, 10 ps (and therefore well above the homogeneous lifetime of the amplifier), the solutions should have some validity – even if they only predict the envelope of a noise burst.

The time scale of the pulse is largely governed by t_m and the value of the net gain. We must now consider what happens as t_m is reduced to zero. If the stepping algorithm without N is used, the number of satellite pulses increases indefinitely while their duration decreases. In the presence of noise injection, however, the formation of satellites becomes increasingly damped as repeated small noise additions between the pulses cause significant filling of the trough. In reality, of course, the finite cavity bandwidth will play a dominant role in limiting the subpulse durations.

Fig.4.10 shows this process of noise damping as t_m is reduced from 10^{-3} to 10^{-5}. In (f) the pulse is already quite close to the long "equilibrium" solution for $t_m = 0$. The values of N used here are not particularly small but the effect ultimately occurs for all values of N, although there may be many more spikes in the signal before damping sets in. The oscillation in the last frame of fig.4.10 is relatively slow when damping has become significant. A perturbation analysis shows that the oscillation frequency varies as $\sqrt{t_m}$ and the slow time-scales involved suggest that the effect may have some validity even though an unrealistic noise model has been used.

4.5 Matched Cavities and the Etalon Filter

The intensity stepping model has produced encouraging results for $t_m > 0$. When the cavity mismatch is zero there is no intrinsic step and the picture is not so clear. If noise injection is neglected, the equilibrium solution of [1] is obtained. A similar result is obtained when the noise term is included: the self-reproducing condition for $t_m = 0$ gives

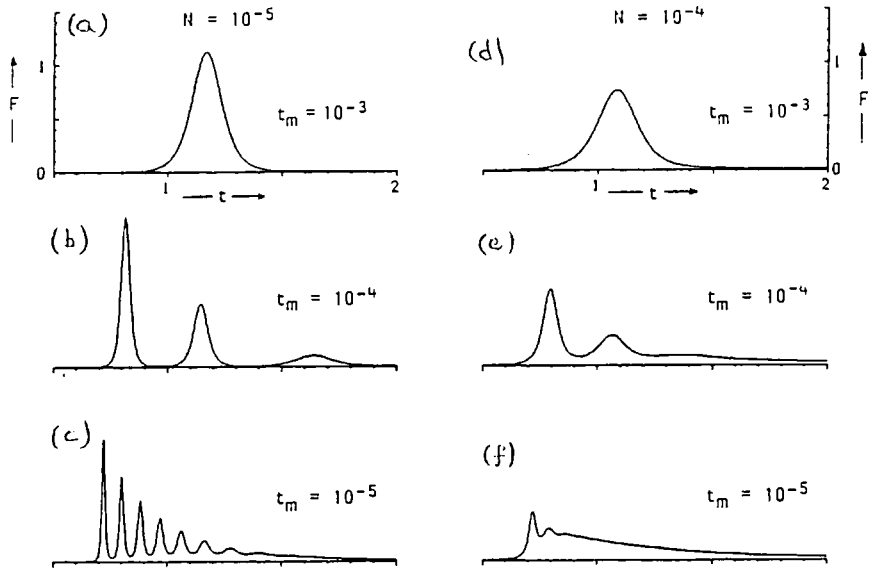


FIG. 4.10

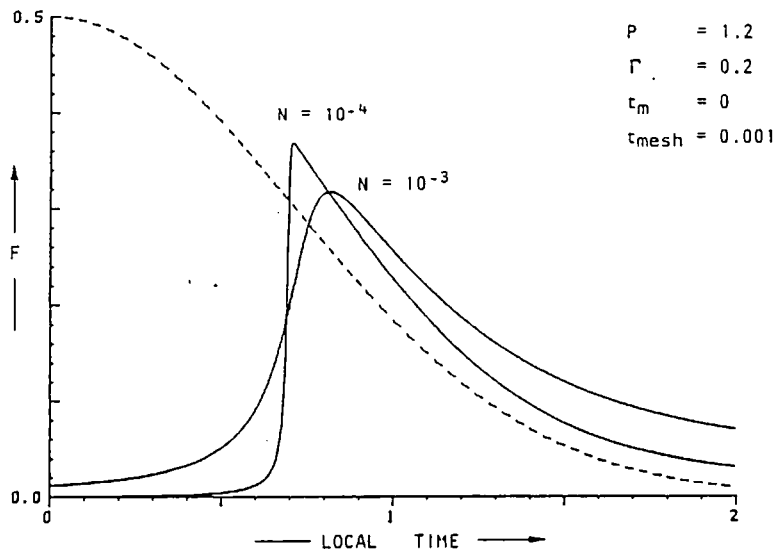


FIG. 4.11

$$F_i = \frac{N}{(1 - g_i)} \qquad (4.10)$$

yielding fig. 4.11 for $N=10^{-3}$ & 10^{-4}. Although this removes the physically unacceptable rising edge of the solution in [1], a number of experimental reports suggest that the shortest pulses are obtained when the mismatch is close to zero and this "smoothed" version of the equilibrium solution therefore seems unacceptable. The degree of deviation is determined entirely by the noise term, and the solution retains the unacceptable rising edge when N is small. To overcome this problem we now introduce a bandwidth-limiting device which can be modelled very simply. Not only does this prevent the formation of fast rising edges but it leads to a stepping equation for $t_m=0$ which is closely related to that for $t_m>0$.

The response of a linear system to a signal of amplitude V(t) is given by the convolution

$$V^{out} = V^{in} \otimes \mathcal{J}(t) \qquad (4.11)$$

where $\mathcal{J}(t)$ is the impulse response of the system. This is particularly simple for an ideal Fabry-Perot etalon consisting of two thin, plane, parallel mirrors with partial reflectivities which are independent of wavelength. The transmission impulse response is an exponentially decaying "comb" of δ-functions (fig. 4.12) separated by the double transit time of the etalon, t_e, with the form

$$\mathcal{J}(t) = (1-R)\,[\delta(t - nt_e)]\,\mathcal{R}^n, \quad n = 0,1,2\ldots \qquad (4.12)$$

where R is the intensity reflectivity of one mirror. There are no phase factors if the etalon is used in transmission and on resonance with a chirp-free wave. (The pulse will be treated as a slowly varying envelope on a monochromatic carrier). The reflectivity is related to the bandwidth through

$$R = \exp(-t_e/T_f) \qquad (4.13)$$

where T_f is the filter response time.

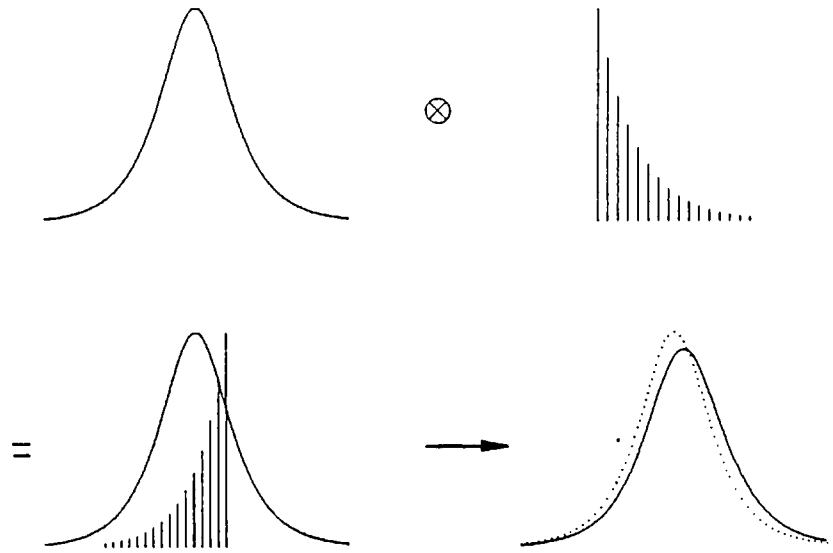


FIG. 4.12: The filter convolution

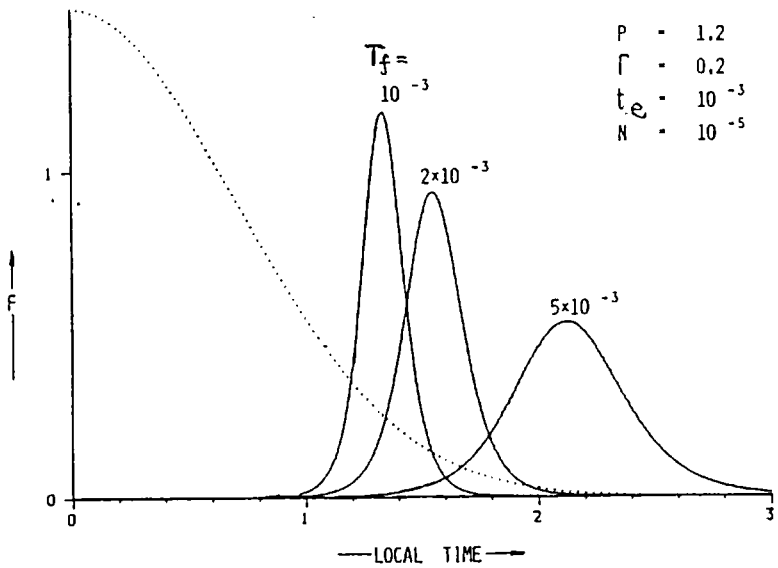


FIG. 4.13: Effect of filter bandwidth

There are two reasons for choosing such a filter. Firstly, it corresponds, to a greater or lesser extent, to real devices used to limit the lasing bandwidth and bears some relation to the effect of homogeneous broadening in the laser medium itself. Secondly, the particular form of the impulse function leads to a numerical convolution which is not only both fast and exact but which can be "undone" easily. There are similar advantages in using the convolution integral corresponding to the response of a damped simple harmonic oscillator.

When t_e is much less than T_f (i.e. when the filter has good free spectral range), the filter spectrum consists of well-separated lorentzian bandpasses with a width determined by T_f. Providing that the bandwidth of the signal is small compared to the free spectral range of the filter, it might be hoped that the action of the filter will be largely determined by T_f and that variations in t_e will have little effect. When the etalon round trip time is set equal to the signal sampling interval the convolution can be written as the simple summation

$$V_i^{out} = (1-R)\sum_{j=-\infty}^{i} V_j^{in} R^{i-j} = S_i \qquad (4.14)$$

Combining this with the corresponding expression for V_{i+1} gives

$$V_{i+1}^{out} = [R(1-R)\sum_{j=-\infty}^{i} V_j^{in} R^{i-j}] + (1-R)V_{i+1}^{in} \qquad (4.15)$$

that is

$$V_{i+1}^{out} = R\,S_i + (1-R)\,V_{i+1}^{in} \qquad (4.16)$$

$$= R\,V_i^{out} + (1-R)\,V_{i+1}^{in} \qquad (4.17)$$

This relation between discrete signal values allows us to derive a stepping algorithm for matched cavities. Furthermore, the filter operation can be incorporated into the stepping relations for $t_m \neq 0$ by setting $t_e = t_m$. This means that the free spectral range of the filter changes as t_m is varied, although the response time T_f is fixed. (Although it might be thought that this would be of secondary importance if the bandwidth of the signal is much less than $1/T_f$, it will be shown later that the solutions are, in fact, quite sensitive to the etalon finesse).

In the following derivation of the complete amplitude stepping equations, the pulse amplitude will be given by the square root of the intensity envelope. For the moment we neglect the noise term and consider only that part of the pulse above the noise level. Taking the cavity operations in the order GAIN - FILTER - SHIFT, the steady state equation for the amplitude is now

$$\mathcal{F}\,[Vg]_t \;=\; V(t+t_m) \tag{4.18}$$

where $\mathcal{F}$ is the filter operator and g, now the net amplitude gain factor, is given by

$$g \;=\; \exp(\,[A-\Gamma\,]/2\,) \tag{4.19}$$

We represent the convolution sum on Vg up to the i_{th} mesh point by

$$[Vg]_i \;=\; (1-R)\sum_{j=-\infty}^{j=i} V_j\, g_j\, R^{i-j} \;=\; \sigma_i \tag{4.20}$$

and derive the following new stepping relations:

a) $t_m>0$

The self-reproducing condition gives

$$\sigma_{i-1} \;=\; V_i \;,\; \sigma_i \;=\; V_{i+1}$$

$$R\,\sigma_{i-1} + (1-R)\,V_i\,g_i \;=\; V_{i+1}$$

$$V_{i+1} \;=\; V_i\,[\,R + (1-R)\,g_i\,] \tag{4.21}$$

b) $t_m=0$

$$\sigma_i \;=\; V_i \;,\; \sigma_{i+1} \;=\; V_{i+1}$$

$$R\sigma_i + (1-R)\,V_{i+1}\,g_{i+1} \;=\; V_{i+1}$$

$$V_{i+1} \;=\; V_i\,\frac{R}{1-(1-R)\,g_{i+1}} \tag{4.22}$$

c) $t_m < 0$

$$\sigma_{i+1} = V_i \, , \; \sigma_i = V_{i-1}$$

$$R\sigma_i + (1-R)\, V_{i+1}\, g_{i+1} = V_i$$

$$V_{i+1} = \frac{V_i - RV_{i-1}}{(1-R)\, g_{i+1}} \qquad (4.23)$$

The filter has the expected effect for $t_m > 0$. As is the case without the filter, the profile decays before threshold unless it is maintained by noise injection. The signal begins to rise as the gain exceeds threshold, but the effective "gain coefficient" given by $[R+(1-R)g]$ is now always closer to unity, thus slowing down the rise and fall of the pulse. As the filter bandwidth is increased, $T_f \to 0$, $R \to 1$ and the equation reduces to the simple intensity relation (as T_f becomes smaller than t_m the filter ceases to operate effectively).

The equation for $t_m = 0$ is similar to that for positive t_m but the effective gain coefficient is different in form and sets an upper limit on the acceptable value for g. The higher order equation for negative t_m is quite different and is difficult to handle. A surprising feature of all three equations is that stationary points of the solutions still occur when $g = 1$.

4.6 Stepping Profiles with the Filter

The stepping formulae for $t_m \geq 0$ are qualitatively very similar to the basic intensity stepping algorithm and it seems likely that the filter will broaden the pulse when t_m is positive and delay the arrival of the pulse until after threshold when $t_m = 0$. There is now a problem about the boundary value, however. The algorithm gives information about the (chirp-free) signal amplitude but the pulse before threshold has so far been treated by a simplified noise power. The first way to deal with the problem is to proceed as we did with the original stepping model – by choosing an initial value at threshold and iterating the algorithm as it stands.

We begin with $t_m = 0$. The mesh step is now a free variable so to start with we select values which are similar to those used before, setting $t_e = T_f = 10^{-3}$ and choosing an initial amplitude equal to the square root

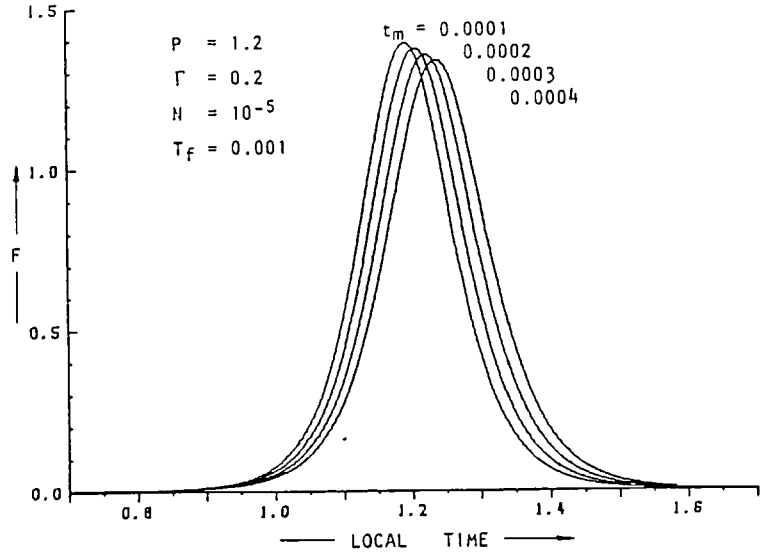

1.5
1.0
0.5
0.0
F
P = 1.2
Γ = 0.2
N = 10⁻⁵
T_f = 0.001
t_m = 0.0001
0.0002
0.0003
0.0004
0.8
1.0
1.2
1.4
1.6
LOCAL TIME

FIG. 4.14

of the former initial flux value. Once more, as fig.4.13 shows, the results are encouraging. The filter prevents the formation of the fast rising edge of the Y+T solution, delaying the arrival of the pulse until significant gain has been delivered, and allows the profile to "overshoot" exactly as it did for $t_m > 0$. The filter response time is playing the same role as the mismatch time. Fig.4.14 shows the effect of increasing positive mismatch using eqn.(4.21).

4.7 Noise and the Filter

The leading edge of the pulse under the conditions modelled so far, with net gain on the leading edge, represents a continuous transition through a laser threshold. The spectral content will change in a complicated way between the far leading edge and the peak of the pulse and the bandwidth of the system will affect this. With the inclusion of a bandwidth limiting process, the spontaneous emission, while still providing the foundation of the pulse, can no longer be modelled simply. The diffusion of noise structure through the pulse means that there is no steady state: at best the stepping model can predict the time average of the fluctuating profile. It might be possible to include a local-time dependent loss function to account for the change in spectral width down the pulse, but it is unlikely to be simple and the noise must still be taken into account between deeply modulated satellites.

We proceed by making a substantial approximation: that the noise is still added to the signal intensity while the filter acts on the square root of the intensity. With the operations in the order GAIN-LOSS-NOISE-FILTER-SHIFT, simple stepping equations can still be obtained. The self-reproducing condition is

$$[\ \mathcal{F}\sqrt{(Fg + N)}\ ]_t = V(t+t_m) \qquad (4.24)$$

and g is again the gain factor for the intensity

giving

$$t_m > 0: \quad V_{i+1} = V_i\ [R + (1-R)\sqrt{g_i + N/F_i}\ ] \qquad (4.25)$$

$$t_m = 0: \quad V_{i+1} = V_i \times \frac{R}{1 - (1-R)\sqrt{g_{i+1} + N/F_{i+1}}} \qquad (4.26)$$

$$\&\ (F_{i+1} \simeq F_i)$$

These equations will normally be used and the same approximation will be used for the numerical evolutions presented later.

Chapter 4 : References

1 Yasa,Z.A., Teschke, O. – Opt. Commun., **15**, 169, (1975)

2 Wagner,W.G., Lengyel,B.A. – J. Appl. Phys., **34**, 2040 (1963)

3 Scavennec,A. – Opt. Commun., **17**, 14 (1976)

4 Herrmann,J., Mottschmann,U. – Opt. Commun., **40**, 379 (1982)

5

NEGATIVE MISMATCH : NUMERICAL EVOLUTIONS

5.1 Failure of Direct Stepping

The simplest expression of the self-reproducing requirement suggests that the reversal of the sign of t_m may affect the search for a steady state solution. Since $O[V]_i = V_{i-1}$, the action of the cavity at the i^{th} point in local time now determines a signal value which is ahead not behind. While the filter stepping algorithms for $t_m > 0$ and $t_m = 0$ are similar, that for $t_m < 0$ is of higher order. Nevertheless, the inclusion of the filter ensures that the pulse remains well defined as positive mismatch is reduced to zero. The response time T_f plays a similar role to t_m and the pulse still arrives after the gain has exceeded threshold. A small negative value mismatch may simply further compress and advance the pulse without changing it qualitatively.

The attempt to evolve the stepping equation

$$V_{i+1} = \frac{V_i - RV_{i-1}}{(1-R)\, g_{i+1}} \qquad (5.1)$$

directly (starting at threshold but now using two initial values) fails however. The iteration diverges rapidly and sensible evolution of even the first hundred terms occurs only for a critically defined ratio of the initial values. The instability of the iteration can be demonstrated as follows:

The difference equation is

$$(1-R)\, g_{i+1}\, V_{i+1} - V_i + R\, V_{i-1} = 0 \qquad (5.2)$$

and let

$$V_i = \prod_{k=0}^{i} e_k$$

giving

$$(1-R)\, g_{i+1}\, e_{i+1}\, e_i \;-\; e_i \;+\; R \;=\; 0 \qquad (5.3)$$

We assume that we can choose some e_0 to give the required V_0 at the boundary and seek the e_k. Since the iteration starts far out on the leading edge of the pulse, the e_k should be slightly greater than 1 (and probably slowly increasing).

Let $\quad e_i = a_i e_{i-1} = a_i e \quad$ giving

$$(1-R)\, a_{i+1}\, g_{i+1}\, e^2 \;-\; e \;+\; R \;=\; 0 \qquad (5.4)$$

with solution

$$e \;=\; \frac{1 \;\pm\; \sqrt{(1 \;-\; 4R(1-R)a_{i+1}g_{i+1})}}{2(1-R)a_{i+1}g_{i+1}} \qquad (5.5)$$

with the lower of the roots giving the factor just >1 required for a slowly rising edge.

For real roots, we require

$$R(1-R) \;\leqslant\; 1 \;/\; (\; 4\; a_{i+1}\; g_{i+1}\;) \qquad (5.6)$$

Now, $\quad e_{i+1} \;=\; \dfrac{1 \;-\; R \;/\; e_i}{(1-R)\; g_{i+1}} \quad$ (from (5.3))

and, if g_{i+1} is fixed or varies only slowly, successive iterations of the series converge rapidly (fig.5.1) to the upper root of

$$X \;=\; \frac{1 \;-\; R \;/\; X}{(1-R)\; g_{i+1}}$$

The fact that as the mismatch becomes increasingly negative, the direction of the "information flow" down the pulse begins to reverse, suggests trying the iteration backwards. The difference equation is now

$$(1-R)\; g_{i-1}\; V_{i-1} \;-\; V_i \;+\; R\, V_{i+1} \;=\; 0 \qquad (5.7)$$

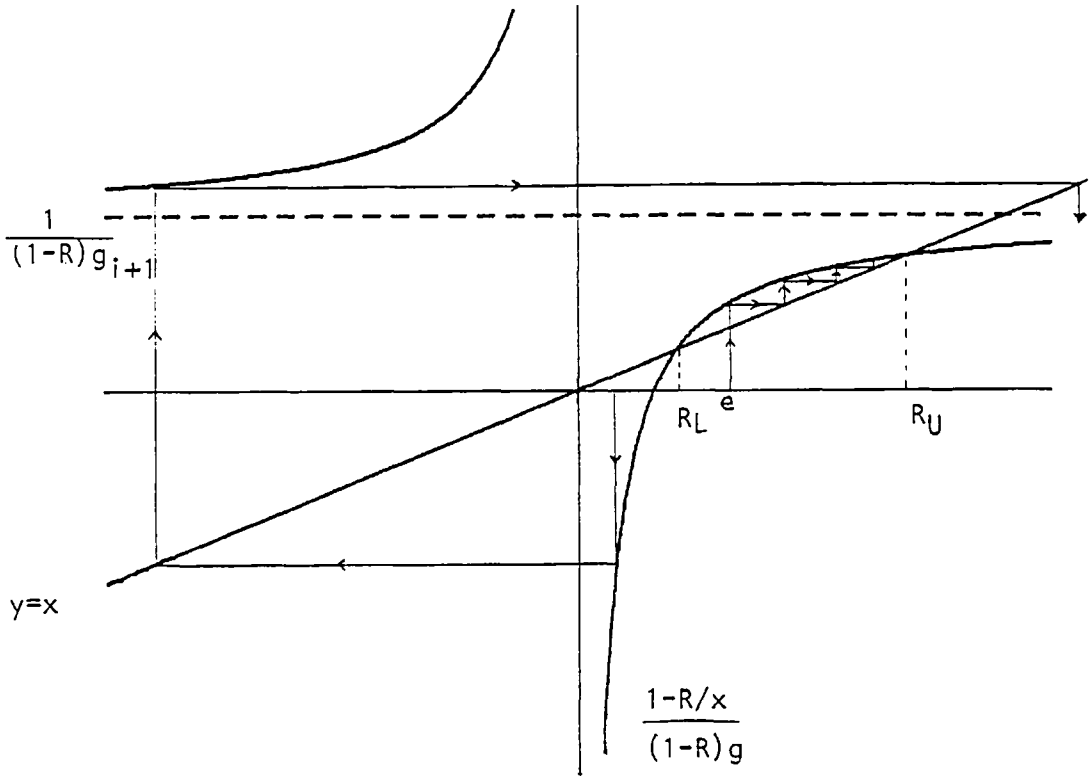


FIG. 5.1 : Divergence of t_m -ve stepping

Repeated iteration of $X_{i+1} = [1-R/X_i]/(1-R)g_i$ converges rapidly to the upper root of $X = [1-R/X]/(1-R)g$ for all initial values. The root required for a slowly varying profile, $R_L \simeq 1$, is unstable.

giving

$$e = \frac{1 \pm \sqrt{1-4R(1-R)g/a}}{2R}$$

and the upper root is now the one close to unity. Working from the tail of the pulse, the iteration rises while $g<1$ and falls once the gain is greater than unity. However, the signal values must also decrease again on the leading edge of the true pulse and the fact that the boundary values are in the tail of the pulse makes a simple solution unlikely.

The sudden failure of forwards stepping and the hampering of backwards stepping by solution dependent boundary values point to a qualitative change in the pulse as the mismatch changes sign. When the mismatch is positive, the delay in the arrival of the pulse plays a major role in its formation. The direction of the stepping is the same as the dynamical evolution and the coupled equations can be evolved in a stable way. When t_m is significantly less than zero, the flow of information – the stepping direction – reverses. In contrast to the case of positive mismatch where the pulse can slide later and later as t_m is increased, it must now be centred on the pump pulse: the signal cannot extract energy before it has been delivered. A self-reproducing profile must be attenuated on the leading edge when $t_m<0$ and the retardation by the filter must exceed the effect of the gain if the pulse arrives after the threshold point. The retardation by the filter cannot exceed T_f, however, and with further reduction of the cavity length the pulse must arrive before threshold. A well-contained pulse presumably also requires loss on the trailing edge and the pulse must therefore be balanced over the peak of the gain profile. The pulse is now able to modify the position of threshold and the anchor point of the stepping approach has been lost. It seems reasonable to ask whether the balance of the pulse over the gain is actually stable. First, is there a discontinuous transition from one regime to the other at some negative value of t_m? Second, since the tail of the pulse feels the effect of a perturbation on the front through the gain evolution while the perturbed tail is itself fed forwards, could there be instabilities or even self-exciting fluctuations?

5.2 Solution by Matrix Elimination

We now make one more attempt to solve eqn.(5.1). The equations for n values on the profile can be written:

$$\begin{bmatrix} 1/R & (1-1/R)g_2 & 0 & 0 \ldots 0 & 0 \\ -1 & 1/R & (1-1/R)g_3 & 0 \ldots 0 & 0 \\ 0 & -1 & 1/R & (1-1/R)g_4 \ldots 0 & 0 \\ 0 & 0 & -1 & 1/R \ldots 0 & 0 \\ . & . & . & . \ldots . & . \\ & & & -1 & 1/R \end{bmatrix} \begin{bmatrix} V_1 \\ V_2 \\ V_3 \\ V_4 \\ . \\ V_n \end{bmatrix} = \begin{bmatrix} V_0 \\ 0 \\ 0 \\ 0 \\ . \\ -(1-R)V_{n+1} g_{n+1} \end{bmatrix}$$

$$A \; V \; = \; Y \qquad (5.8)$$

The tri-diagonal matrix A can be decomposed into

$$\begin{bmatrix} B_1 & C_1 & 0 & 0 \ldots \\ A_2 & B_2 & C_2 & 0 \ldots \\ 0 & A_3 & B_3 & C_3 \ldots \\ . & . & . & . \\ & & A_n & B_n \end{bmatrix} = \begin{bmatrix} a_1 & & \\ A_2 & a_2 & \\ & A_3 & a_3 \\ . & . & . \\ & A_n & a_n \end{bmatrix} \times \begin{bmatrix} 1 & b_1 & \\ & 1 & b_2 \\ & & 1 \\ & & \ldots \\ & & 1 \end{bmatrix}$$

$$A \; = \; L \, U \qquad (5.9)$$

and let $$U \, V \; = \; Z \qquad (5.10)$$

$$\Rightarrow \; L \, Z \; = \; Y \qquad (5.11)$$

To "undo" the matrix we move first forwards and then backwards through the indices. From eqn.(5.11) we have

$$Z_1 = Y_1 / a_1$$

$$Z_i = \frac{Y_i - A_i Z_{i-1}}{a_i} \qquad i = 2 \ldots n$$

Using Z in (5.10) yields the solution

$$V_n = Z_n$$

$$V_{n-1} = Z_{n-1} - b_{n-1} V_n$$

$$V_{n-k} = Z_{n-k} - b_{n-k} V_{n-k+1} \qquad k = 1,2 \ldots n-1$$

The intermediate coefficients a_i, b_i are found by noting that

$$a_1 = B_1 \quad , \quad b_1 = c_1/a_1$$

$$a_i = B_i - A_i b_{i-1} \quad , \quad b_i = c_i/a_i \qquad i = 2,3 \ldots n-1$$

$$a_n = B_n - A_n b_{n-1}$$

and that $A_i = -1$ and $B_i = 1/R$

The formulation of the problem now contains boundary values at both ends of the solution which we may interpret as a reflection of the counter-flow of information through the pulse (swept backwards by the filter and pushed forwards by the mismatch). The solution is insensitive to the trailing edge boundary value over the parameter range for which a solution can actually be obtained and we shall simply choose "small" values at both boundaries.

The main problem is that the complete matrix of gain values is needed in advance. When the stepping algorithm moves forwards only the current gain value is needed and this is easily determined. Even if we step backwards the signal value is known and the rate equation can be evolved safely in reverse (although there is a substantial problem over the initial value). In the present method we resort to finding an approximation to the matrix and then attempting to iterate the solution. We assume that the profile for small negative t_m is similiar to that for $t_m=0$ and therefore use the stepping model for $t_m=0$ to generate the approximate gain profile. The etalon spacing is a free parameter

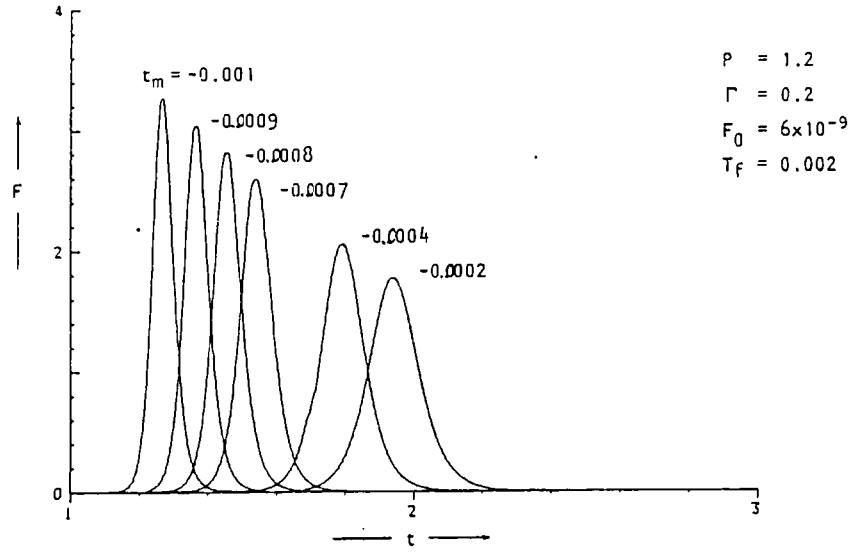

t_m = -0.001
-0.0009
-0.0008
-0.0007
-0.0004
-0.0002
P = 1.2
Γ = 0.2
F_0 = 6x10^{-9}
T_f = 0.002
F
t
0
1
2
3
4

FIG. 5.2

when $t_m = 0$ and it can be set equal to $|t_m|$, simplifying the computation. If a reasonable pulse profile can be fitted to the initial gain array in the matrix above, a new gain approximation can be generated by feeding the pulse back through the rate equation.

For small values of $|t_m/T_f|$, the method converges quickly, giving a pulse which is advanced and compressed with respect to that for zero mismatch. Fig. 5.2 shows profiles for values of $|t_m|$ up to approx. $T_f/2$. For small $|t_m/T_f|$ information is still being swept backwards by the filter, and the matrix solution is insensitive to the right hand boundary value.
As the magnitude of t_m is increased, convergence becomes increasingly slow, and as $R \rightarrow 1/2$ the process becomes very sensitive to numerical errors in the gain profile. This was controlled by reducing the feedback strength so that the $i+1^{th}$ gain profile was a weighted average of the i^{th} gain profile and that obtained by repassing the i^{th} signal profile through the rate equtation. Eventually it was necessary to use feedback strengths of less than 10%.

At higher pump levels the iterative method brings another problem. The pulse still acquires satellites, the shape and position of which depend sensitively on the depletion of the gain by structures earlier in local time. The solution for a secondary pulse does not begin to converge until convergence is complete for earlier parts of the pulse.

5.3 Numerical Evolutions

The matrix solutions suggest that the transition from positive to negative mismatches is continuous: the compression of the pulse as t_m is reduced increases the retarding effect of the filter while the advance of the pulse reduces the effect of the gain so that steady state is maintained by the small negative mismatch. However, profiles with net gain on the leading edge are only obtained when R is greater than the upper root of $R(1-R) = 1/4$ – i.e. "positive-type" solutions require $|t_m/T_f| < \ln 2$. The filter in the stepping algorithm degrades steadily as $|t_m| \rightarrow T_f$ but a similar limit to the range exists for the integral filter. From the steady state condition

$$V(t+\tau)\, g(t+\tau) = V(t) + T_f \dot{V}(t), \quad \tau = |t_m|$$

But $$V(t+\tau) = V(t) + \tau \dot{V} + \frac{\tau^2}{2} \ddot{V} \ldots$$

therefore $|t_m| < T_f$ for a solution with $g>1$ on the leading edge.

The other root in eqn.(5.5) corresponds to a falling pulse edge, that is to the "negative-type" solution where the leading edge is ahead of threshold. Are there two solutions for $|t_m|<T_f$?

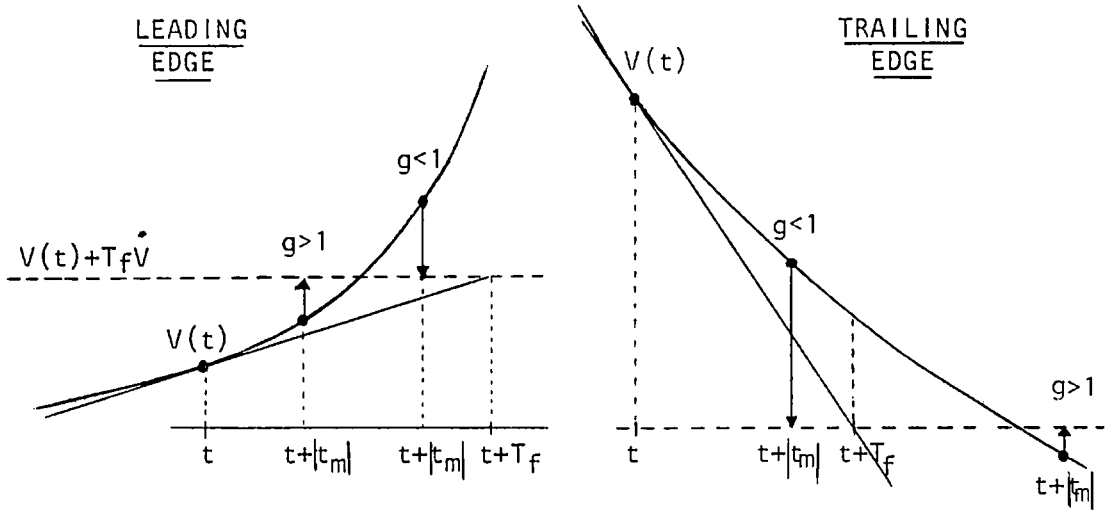


FIG. 5.3

Solutions of both types are possible on the leading edge (fig.5.3) but $|t_m|<T_f$ requires $g<1$ on the trailing edge. The second solution seems to be the optimum for passive modelocking but is presumably unstable for synchronous pumping. For $t_m < -T_f$, the only solution has $g<1$ on the leading edge and $g>1$ in the tail. Is the transition to this regime smooth and are the solutions stable? The numerical evolutions already published in [1] and [2] show evidence of the marked broadening seen in almost all experimental auto-correlations, but those experiments also show coherence spikes while Shapiro's streak camera study [3] showed large scale fluctuations. Are these just the result of fluctuations from the spontaneous emission or is the regime intrinsically unstable?

To investigate this we resort to numerical simulation of the pulse evolution from a weak, flat initial signal. The equations are the same as those in the full stepping model: unidirectional ring propagation allows the integrated rate equation to be used, a constant noise power is added to the signal intensity and the filter acts on the square root of the intensity. The cavity is initially assumed to be long compared to the amplifier lifetime. In the expectation that the pulse is confined to the vicinity of the pump in local time, only the flux in this region is considered. The pump is treated as the stationary reference frame and cavity mismatch is accounted for by shifting the

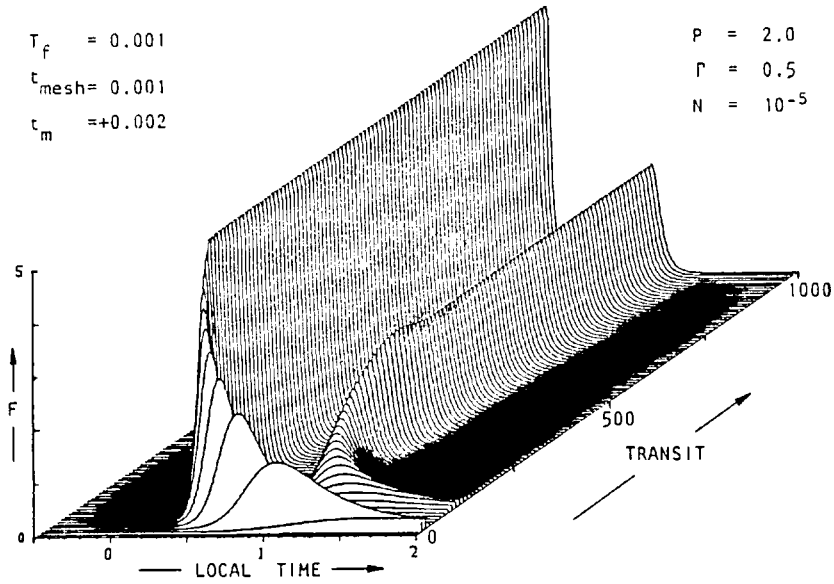


FIG. 5.4a: Evolution from a flat start

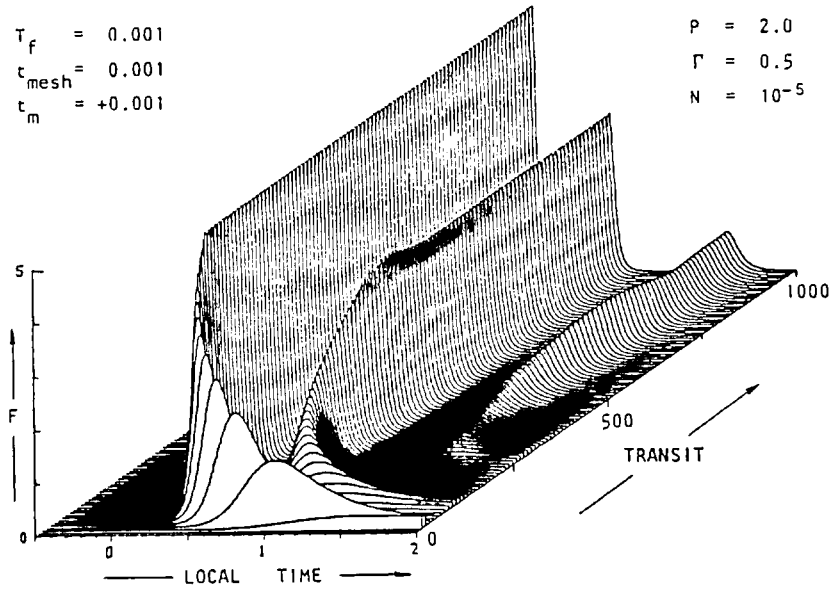


FIG. 5.4b

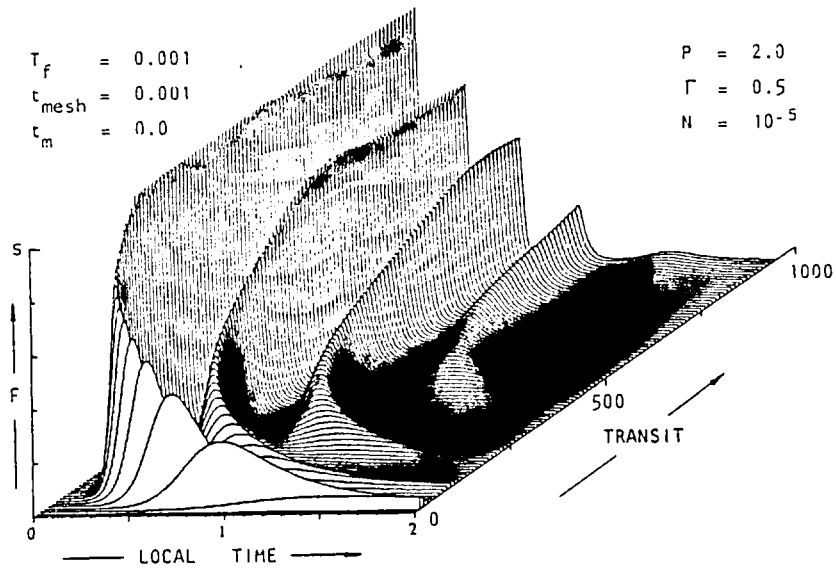


FIG. 5.4c

T_f = 0.001
t_{mesh} = 0.001
t_m = -0.001

P = 2.0
Γ = 0.5
N = 10^{-5}

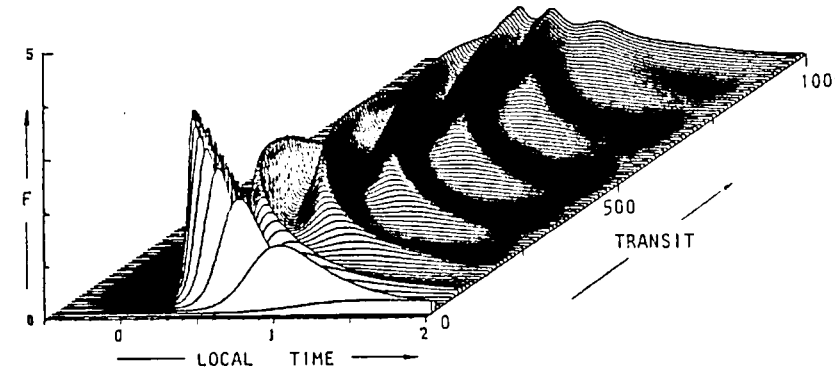


FIG. 5.4d

profile by 1 or more mesh steps on each transit. The constraint that $|t_m|$ be an integral multiple of the mesh step limits the mismatch to fairly large values even with several thousand mesh points. The movement of the profile means that new values must be fed in at one end: for $t_m > 0$, the new values are just the noise feed before threshold. Figs.5.4a–c show evolutions for P=2, Γ=0.5, $T_f = t_{mesh} = .001$ and successively reducing values of cavity mismatch. The picture is one of slow, damped convergence as successive satellites advance under the gain. These profiles were computed with 2500 mesh steps giving a minimum t_m value of .001 and a poor filter. Nevertheless, the evolution converges to the expected steady state even at t_m=0. Note that:

The final profiles are in excellent agreement with the stepping model

The rate of convergence depends on t_m

The latter point highlights a fundamental aspect of this rate equation treatment of synchronous pumping. When t_m is large and positive, the steady state profile can be viewed in local time as a single population overshoot – a giant pulse. As t_m is reduced with appropriate T_f and N the overshooting begins to repeat until a train of satellites is produced – the giant pulse becomes a relaxation oscillation. As the profile moves towards equilibrium with the pump the net gain reduces. Therefore, not only is information stepped more slowly through the pulse as t_m is reduced but the reshaping force per transit on the pulse also diminishes (the filter ensures that convergence is possible at t_m=0). The strong pumping used here both demonstrates that evolution is stable in the presence of satellites and accelerates the convergence.

Fig.5.4d shows what happens as the sign of the mismatch is changed. There is an immediate and substantial effect. The filter cannot hold the pulse in the positive-type regime and the energy spills forwards of threshold. The damping of the internal relaxation oscillations is now complete and information flows the other way. This broadening has been anticipated in a number of publications and agrees qualitatively with Scavennec's result [1], but detailed evolutions have not apparently been presented before. The rate of convergence again depends on the magnitude of t_m but the profile itself is much less sensitive to the value. The advance of the leading edge beyond threshold and the long tail show that the boundary constraints in the matrix solution were certainly in error. The long tail arises because the pulse comes into dynamic equilibrium with the pump: the gain in the tail is only just below threshold for small t_m. In reality, much, if not all, of the pulse may be A.S.E. In

T_f = 0.001
t_{mesh} = 0.001
t_m = -0.002

P = 2.0
Γ = 0.5
N = 10^{-5}

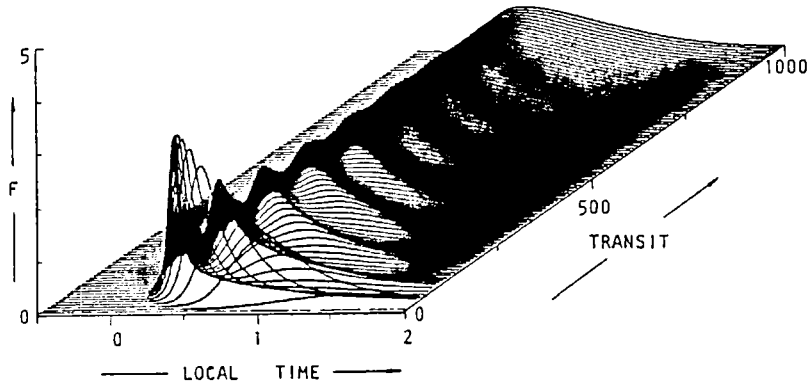


FIG. 5.4e

T_f = 0.001
t_{mesh} = 0.001
t_m = -0.003

P = 2.0
Γ = 0.5
N = 10^{-5}

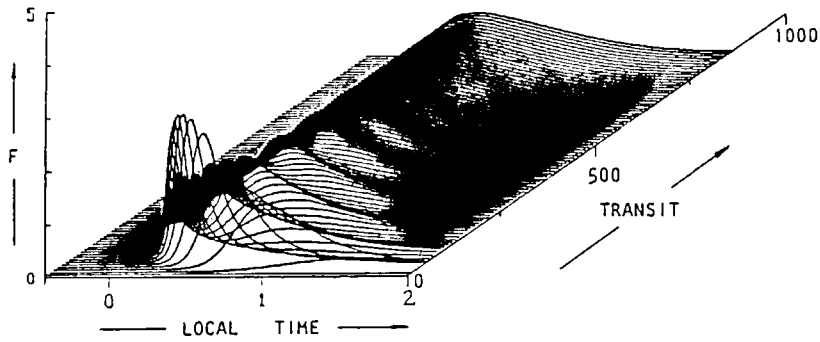


FIG. 5.4f

T_f = 0.001
t_{mesh} = 0.001
t_m = -0.01

P = 2.0
Γ = 0.5
N = 10^{-5}

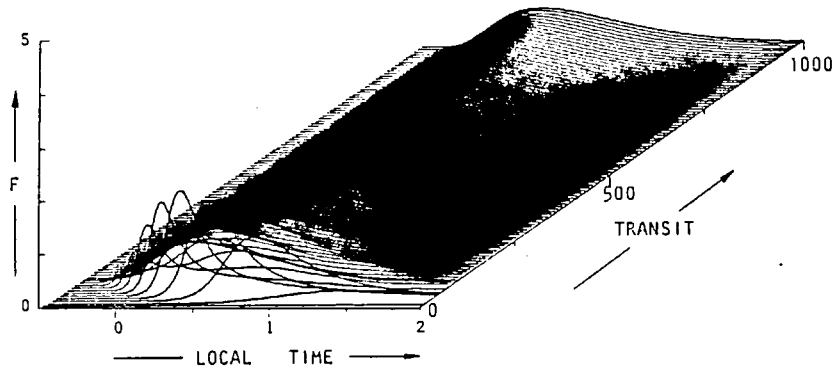


FIG. 5.4g

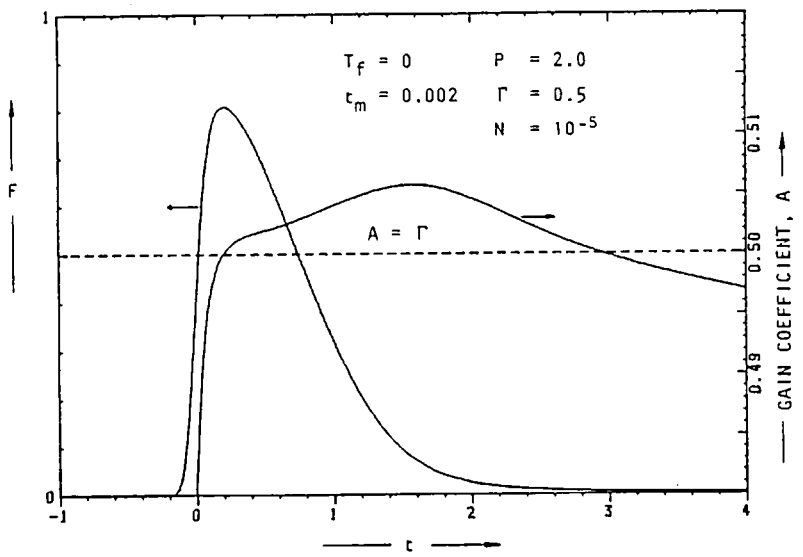


FIG. 5.5

principle, the significant intensity in the tail causes a problem for the simulation since values are now fed from the right. However the evolution seems to be very insensitive to this feed and, indeed, to the noise value itself. Profiles have been generated by feeding in either the same value as at the tail of the profile (allowing the feed to find its own level) or a small constant value, with very little difference.

In fig.5.4d t_m is already beyond the point where the stepping model must fail ($t_m = -T_f \times \ln 2$), but it is noticeable that the convergence is even slower than at $t_m = 0$ (and is not yet complete). At a point in the range $-T_f < t_m < -T_f/2$ the flow of information is stationary to first order. Fig.5.4d is only just beyond this and the evolution shows a large number of satellites (the number of which is controlled by the dispersion of the filter) and appears to evolve through all the positive-type solutions before reaching the smooth equilibrium. For mismatches significantly beyond the transition, the filter has little affect on the solution, but the speed of the convergence increases again as $|t_m|$ increases (figs.5.4e-g). The converged pulse and gain profiles in fig.5.5 show the close approach to the equilibrium solution.

The knowledge that steady states much longer than T_f exist, together with some information about the boundary conditions, suggests trying stepping backwards without a filter. The equation is simply

$$W_i = W_{i+1} / g_i \quad [-N]$$

(the algorithm is not stable if a noise term is subtracted). The iteration must be started in the tail of the pulse with a fairly small value W value and the gain just below threshold: outside a narrow range of initial A values, W diverges or A becomes negative. Nevertheless, the resulting profiles agree qualitatively with the numerical evolutions. The backwards filter algorithm appears to be unstable.

Chapter 5 : References

1 Savennec,A. - Opt. Commun., **17**, 14 (1976)

2 Herrmann,J., Motschmann,U. - Opt. Commun., **40**, 379 (1982)

3 Shapiro,S.L., Cavanagh,.R.R., Stephenson,J.C. - Opt. Lett., **6**, 470 (1981)

THE COMPLETE PICTURE

6.1 The transition from +ve to −ve mismatch

The collapse of the steady state profile as the mismatch takes negative values is summarised in fig.6.1 from the results in the previous chapter. For this value of t_{mesh} the smallest mismatch available was $-T_f$ and the details of the transition from positive to negative-type profiles are not apparent. The intermediate stages are visible in fig.6.2 where T_f has been increased by a factor of 5 (the profiles for $t_m > 0$ were generated by the stepping model). The "background-free" autocorrelations given by

$$G(\tau) = \int V^2(t)\, V^2(t-\tau)\, dt$$

are shown in fig.6.3. In spite of the improved f.s.r. of the filter, the collapse is still complete at $t_m = -T_f$ suggesting that good pulses are only produced in the region where the stepping algorithm works. The fact that the stepping model only handles the filter accurately when $|t_m|$ is significantly less than T_f is therefore not a serious problem: outside this range the pulse has collapsed for $t_m < 0$ and for $t_m > 0$ the scale length of the solution is dominated by t_m. Furthermore, noise fluctuations may actually restrict the mismatch range for good pulses to within $\pm T_f$. We therefore proceed with the stepping model with some confidence, noting that the restriction $|t_m| < T_f$ does not improve the accuracy of the imposed gaussian profile method.

6.2 Further Parameter Variations

The substantial improvement that results from reducing the noise level to delay the pulse until the gain is well above threshold was shown in ch.4. A similar effect can be achieved by reducing the pump duration: fig.6.4 shows the results of a reduction by a factor of ten, converting a satellite train into a single intense pulse. Although the faster gain delivery causes the leading edge of the pulse itself to rise faster, and satellites can still be formed, the improvement is again substantial. In the gaussian solution, the pump duration sets the time scale of the solution. With the fixed fluorescence boundary

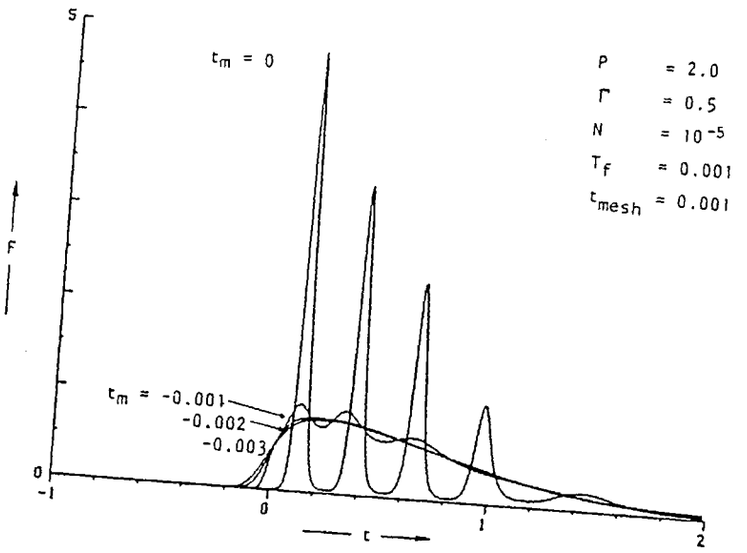

5
t_m = 0
P = 2.0
Γ = 0.5
N = 10^{-5}
T_f = 0.001
t_{mesh} = 0.001
F
t_m = -0.001
-0.002
-0.003
0
-1
0
1
2
t

FIG. 6.1

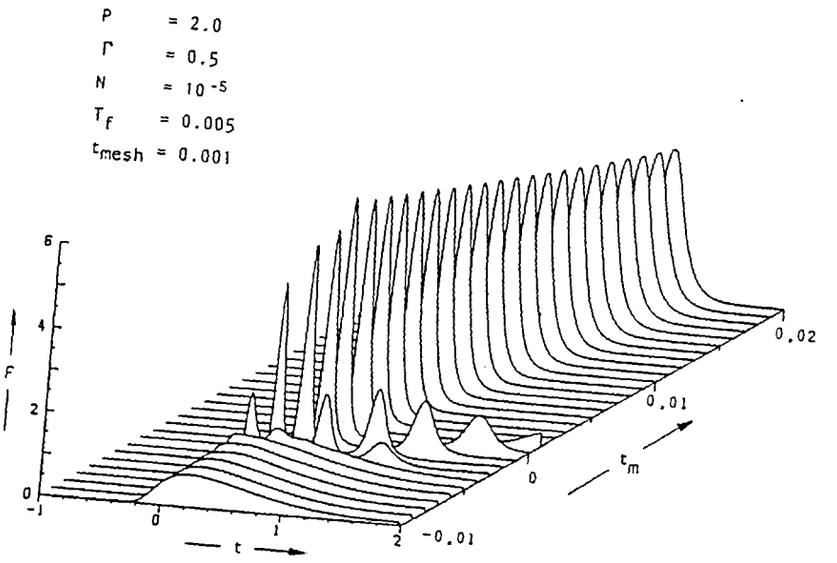

P = 2.0
Γ = 0.5
N = 10^{-5}
T_f = 0.005
t_{mesh} = 0.001
6
4
2
0
F
-1
0
1
2
t
-0.01
0
0.01
0.02
t_m

FIG. 6.2

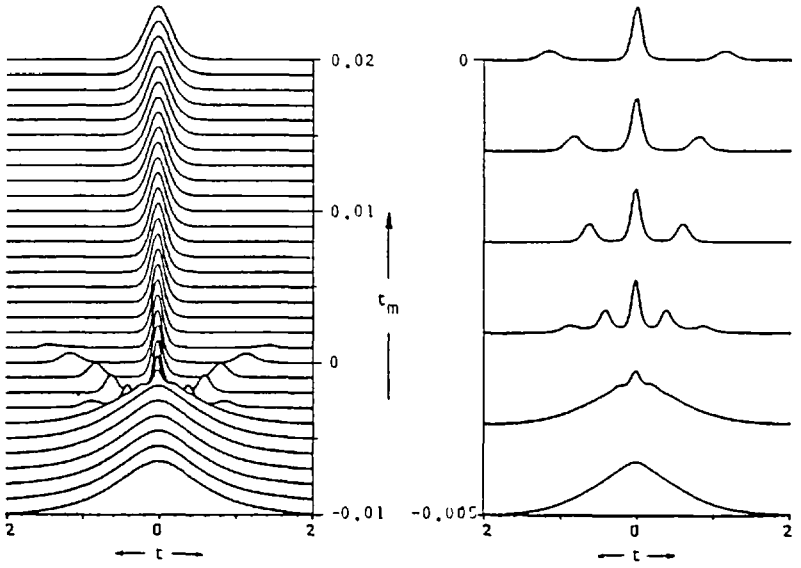


FIG. 6.3: Background-free autocorrelations

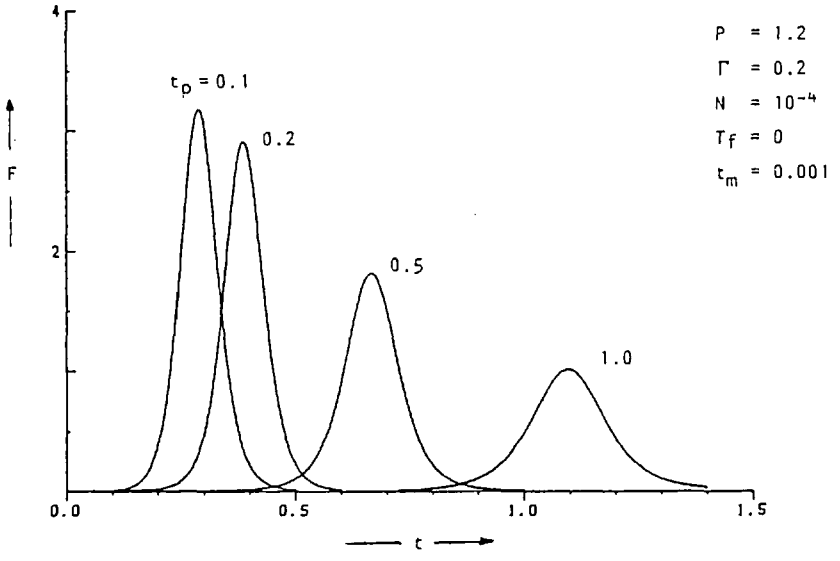


FIG. 6.4a : Reduction of pump pulse width

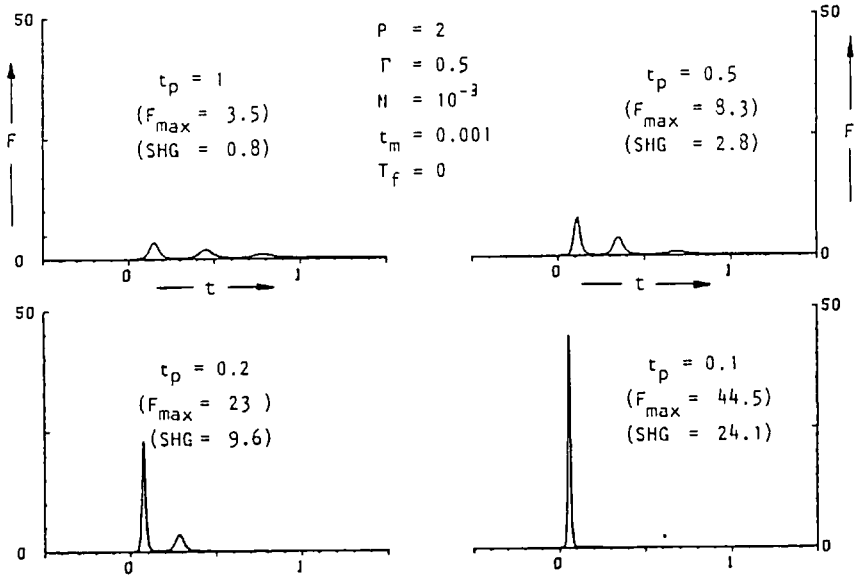
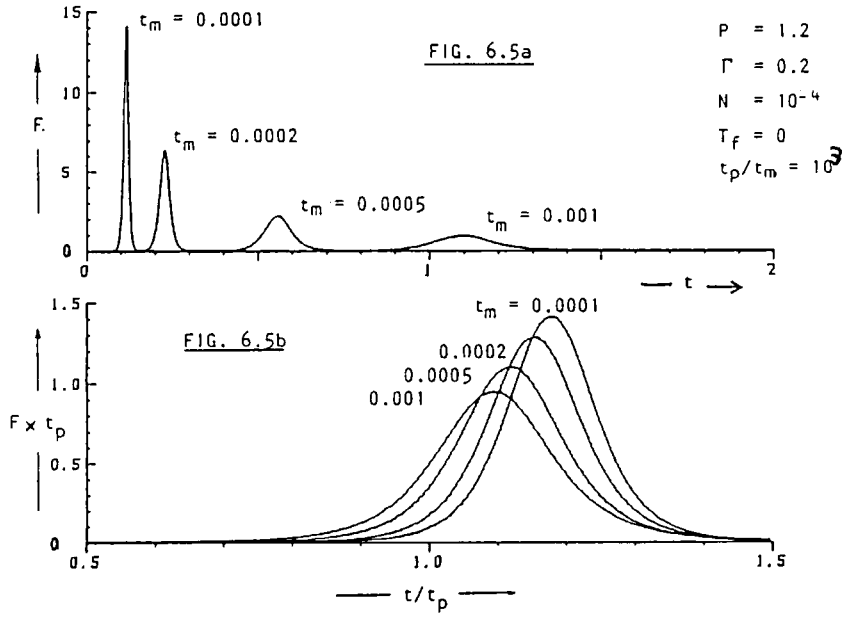

P = 2
Γ = 0.5
N = 10^-3
t_m = 0.001
T_f = 0
t_p = 1
(F_max = 3.5)
(SHG = 0.8)
t_p = 0.5
(F_max = 8.3)
(SHG = 2.8)
t_p = 0.2
(F_max = 23)
(SHG = 9.6)
t_p = 0.1
(F_max = 44.5)
(SHG = 24.1)
F
t
50
0
1

FIG. 6.4b


FIG. 6.5a
P = 1.2
Γ = 0.2
N = 10^-4
T_f = 0
t_p/t_m = 10^3
t_m = 0.0001
t_m = 0.0002
t_m = 0.0005
t_m = 0.001
F
t
15
10
5
0
1
2
FIG. 6.5b
t_m = 0.0001
0.0002
0.0005
0.001
F x t_p
t/t_p
1.5
1.0
0.5
0
0.5
1.0
1.5

condition this scaling no longer holds. Fig.6.5a shows the pulse compression as both t_m and t_p are reduced (with $T_f = 0$). The normalised plots in fig.6.5b show the breakdown of the scaling.

Figs.6.6a & b show the rapid formation of the pulse for two values of filter bandwidth as the pump is increased to the point where the satellite becomes significant. The dependence of the fundamental and second harmonic energies, peak height and pulsewidth are shown in figs.6.6c & d. The result of decreasing the bandwidth at fixed pump power is shown in figs.6.7a & b.

At a fixed noise power, reduction of the pulse duration by increasing the pump power leads quickly to satellite formation when the scale time (t_m+T_f) is short. Attempting to control this by reducing the bandwidth leads to skewed pulses at high pump powers (fig.6.8a). A long satellite burst decays roughly exponentially, the first pulse being the sharpest except under extreme circumstances, and this raises the possibilty that the autocorrelations of "single-sided exponential" pulses in fact come from a "single-sided" burst envelope (although this interpretation brings two problems: first, substructure of the satellites will lead to an anomalous spectral width and, second, the burst will presumably extend over much of the pump duration). Fig.6.8b shows that the satellite structure can be sufficiently periodic to show clearly in the autocorrelations. van Stryland [1] has remarked that a fairly narrow random distribution of gaussian pulses can have a substantial effect on the autocorrelation. It remains to be seen how this satellite burst picture is altered by random fluctuations.

A number of experimental publications remark that satellite formation can be reduced by increasing the output coupling. At a fixed pump power, this clearly delays threshold and, although the excess gain is reduced, the increased output coupling may mean that the extracavity pulse power actually increases (few, if any theoretical treatments appear to observe this). Fig.6.9b shows this effect to a small extent in comparison to the intracavity profiles of fig.6.9a.

6.3 A simple analytic solution

When the steady-state comprises a single pulse late in the pumping, the time variation of the pump can be neglected. When the mismatch is small compared to T_f a first order expansion of $V(t+t_m)$ allows simple expressions to be derived for the pulse parameters. With the inverse filter $(1+T_f d/dt)$, the

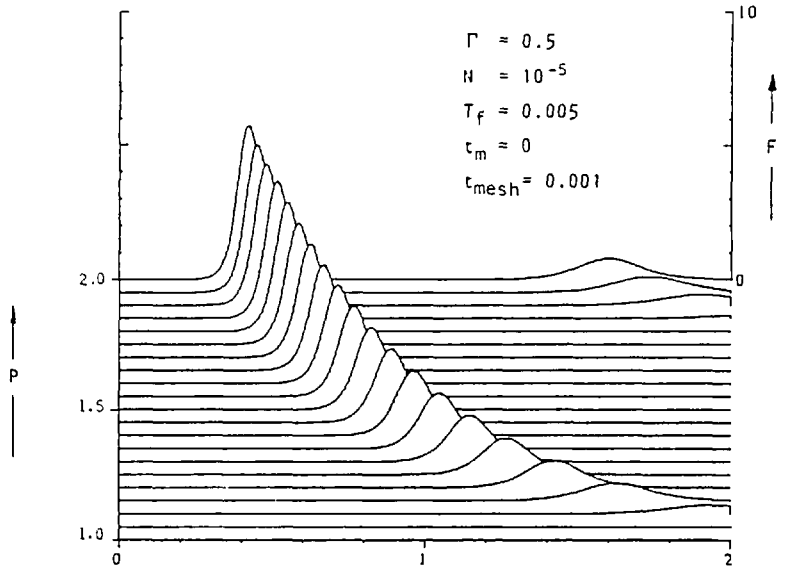


FIG. 6.6a

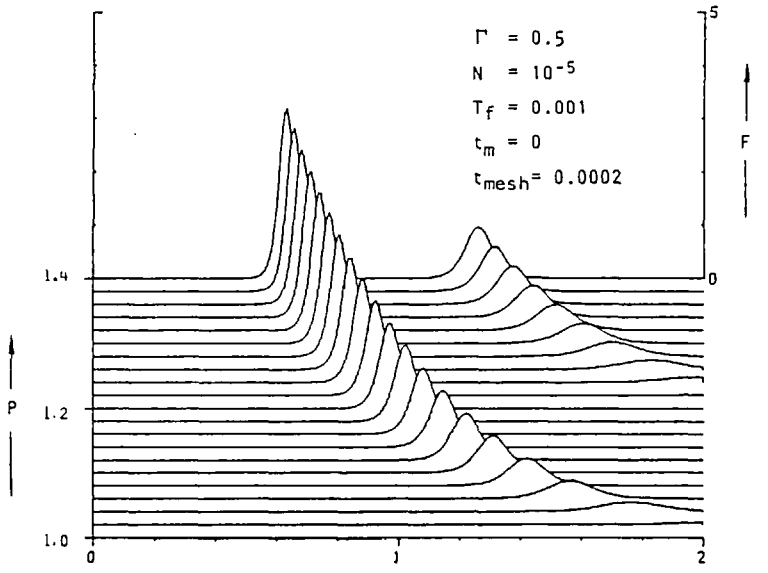
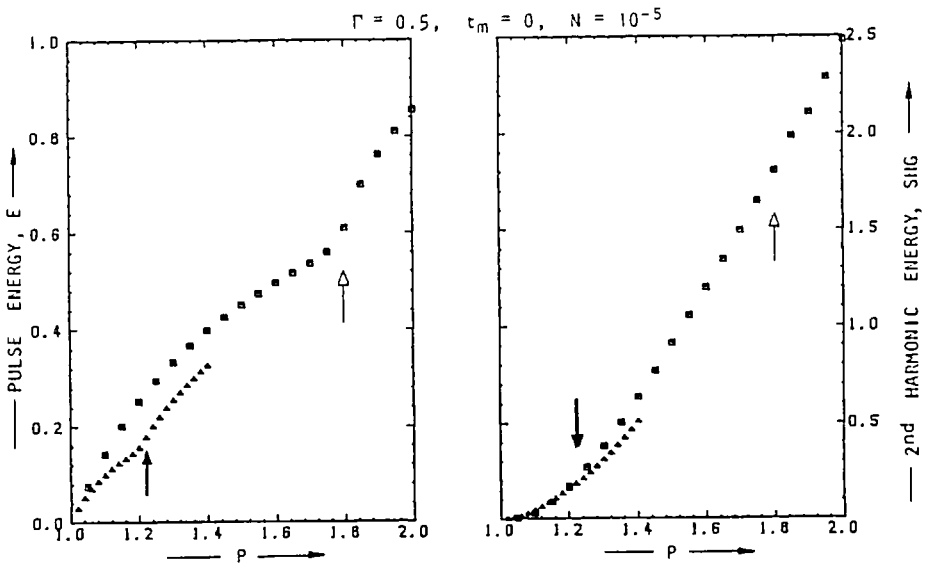


FIG. 6.6b



(arrows indicate the onset of satellite formation)

FIG. 6.6c

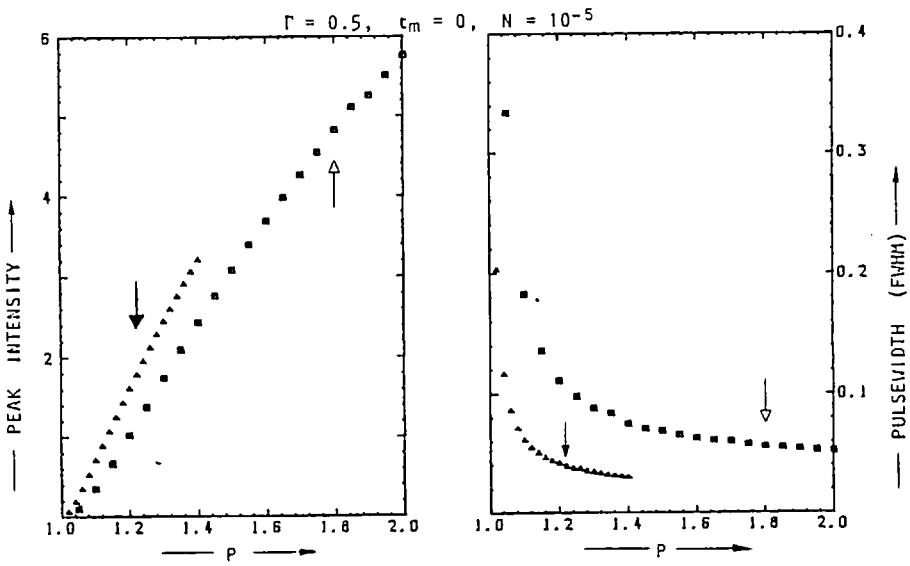


FIG. 6.6d

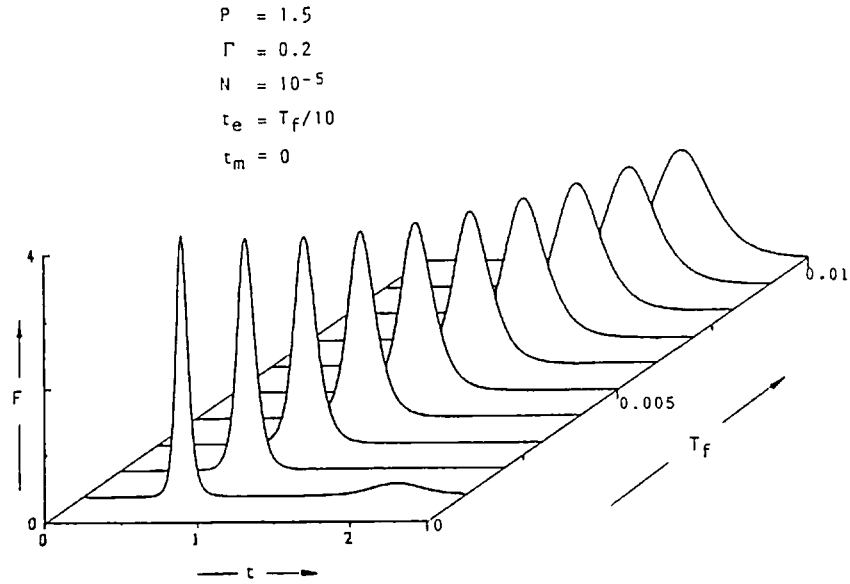


FIG. 6.7a

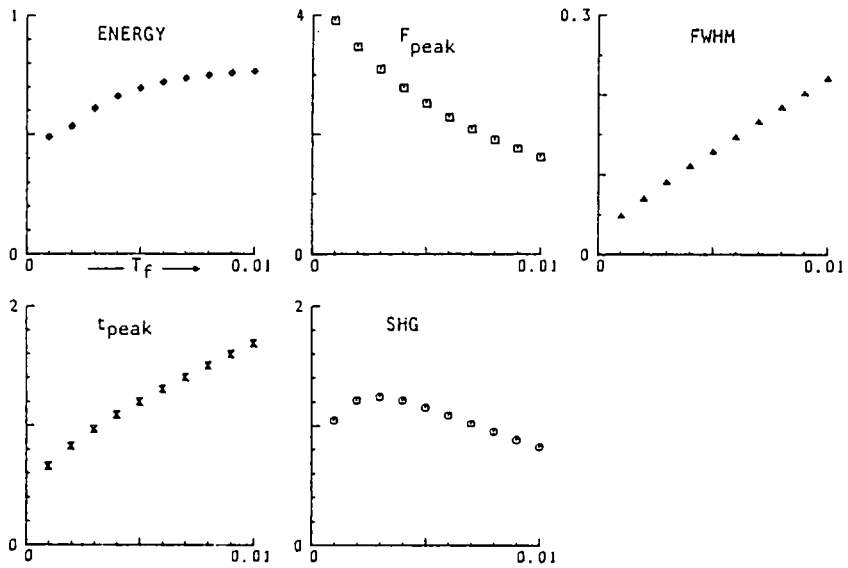
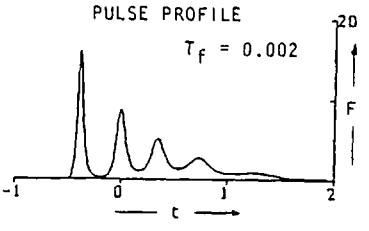
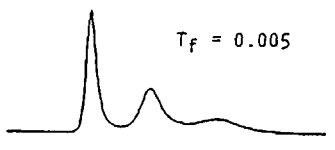


FIG. 6.7b : Dependence of parameters on bandwidth





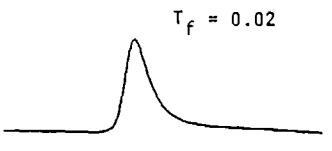
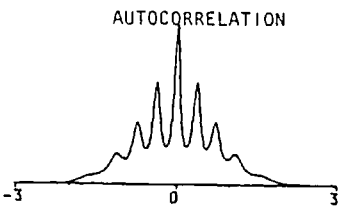
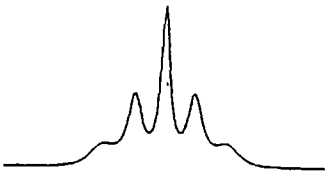


FIG. 6.8a





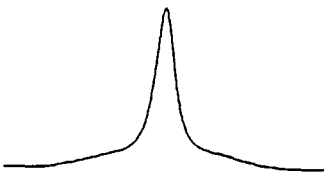


FIG. 6.8b

P = 6, Γ = 0.2, N = 10^{-5}, t_m = 0, t_e = T_f/10

INTRACAVITY
PULSE

$P\Gamma = 0.45$
$N = 10^{-5}$
$T_f = 0$
$t_m = 0.001$

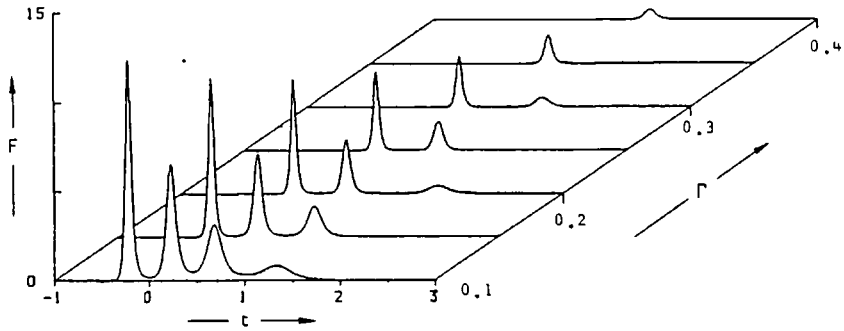


FIG. 6.9a

$P\Gamma = 0.45$

OUTPUT
PULSE

$N = 10^{-5}$
$T_f = 0$
$t_m = 0.001$

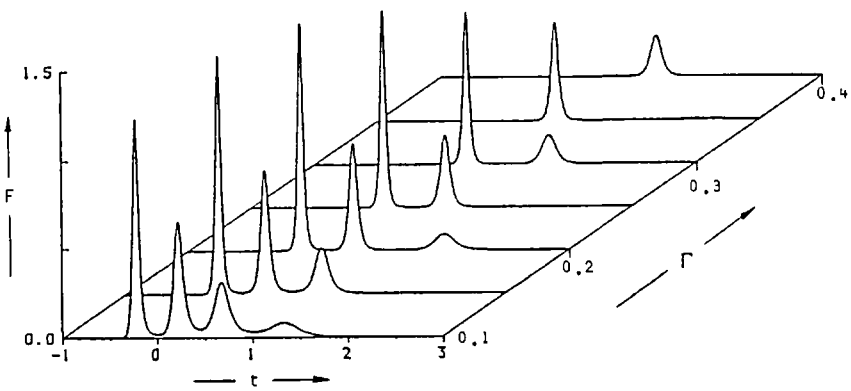


FIG. 6.9b

steady state equation reduces to

$$V(t)g(t) \simeq V(t) + t_c \dot{V} \qquad (6.1)$$

where $t_c = t_m + T_f$

The rate equation is

$$\dot{A} = -V^2 (e^A - 1) \qquad (6.2)$$

since the pumping is complete. Writing $F = V^2$ gives the simple coupled equations

$$\frac{T_c}{2} \dot{F} = F(e^{\frac{1}{2}[A-\Gamma]} - 1) \qquad (6.3a)$$

$$\dot{A} = -F(e^A - 1) \qquad (6.3b)$$

From (6.3) the pulse peak occurs at $A = \Gamma$. Using this to integrate a & b up to the peak of the pulse:

$$\int_{A_{initial}}^{A_{final}} \frac{dA}{e^A - 1} = -\int_{\theta}^{peak} F \, dt \qquad (6.4)$$

As usual, write the initial full amplification as $P\Gamma$ giving

$$\ln \left[\frac{1 - e^{-P\Gamma}}{1 - e^{-\Gamma}}\right] = J_{front} \qquad (6.5)$$

When P & Γ are small this reduces to

$$J_{front} \simeq \ln P$$

and is independent of Γ although the pump energy delivered is not.

Now solve for the peak intensity:

$$\frac{T_c}{2} \dot{F} = \frac{-\dot{A}}{(eA - 1)} (e^{\frac{1}{2}[A-\Gamma]} - 1)$$

$$\tfrac{1}{2} T_c \int_{\theta}^{PEAK} dF = \int_{P\Gamma}^{\Gamma} \frac{dA e^{-A}}{1 - e^{-A}} - \frac{e^{-\frac{1}{2}\Gamma}}{2} \int_{P\Gamma}^{\Gamma} \frac{2dA}{e^{\frac{1}{2}A} - e^{-\frac{1}{2}A}}$$

$$\tfrac{1}{2}T_c(F_{pk} - F_\theta) = \ln\left[\frac{1-e^{-\Gamma}}{1-e^{-P\Gamma}}\right] - e^{-\Gamma/2}\ln\left[\frac{\tanh(\Gamma/4)}{\tanh(P\Gamma/4)}\right] \qquad (6.6)$$

But F_θ, the intensity at threshold is negligible, so

$$F_{pk} = \frac{2}{T_c}\left[\ln\left(\frac{1-e^{-\Gamma}}{1-e^{-P\Gamma}}\right) + e^{-\frac{1}{2}\Gamma}.\ln\left\{\frac{\tanh(P\Gamma/4)}{\tanh(\Gamma/4)}\right\}\right] \qquad (6.7)$$

The inversion in the tail of the pulse A_∞, can be found from

$$\int_\theta^{PEAK} dF = -\int_{PEAK}^{\infty} dF$$

giving

$$F_{pk} = \frac{2}{T_c}\left[\ln\left(\frac{1-e^{-\Gamma}}{1-e^{-A_\infty}}\right) + e^{-\frac{1}{2}\Gamma}\ln\left[\frac{\tanh(A_\infty/4)}{\tanh(\Gamma/4)}\right]\right] \qquad (6.8)$$

The energy in the tail of the pulse is then

$$J_{tail} = \ln\left(\frac{1-e^{-\Gamma}}{1-e^{-A_\infty}}\right) \qquad (6.9)$$

For weak pumping the energy is symmetrically distributed and

$$J \simeq 2\ln P \qquad (6.10)$$

The scale width of the pulse can be found from

$$\tfrac{1}{2}T_c\int\frac{dF}{F} = \int\left[e^{\frac{1}{2}\{A-\Gamma\}} - 1\right]dt \qquad (6.11)$$

6.4 Other Theoretical Treatments

Three further analyses of the synchronous pumping problem have appeared since the gaussian solution method of Kim et al.[2]. In an elaboration of this "ansatz" approach, Herrmann amd Mottschmann [3] increased the complexity of both the rate equation and the functional form of the solution, hoping thereby to remove the restrictive approximations in [2]. At the outset, however, they state that

"[in Scavennec's] calculation, which neglects bandwidth limitation, a

steady-state regime cannot be reached and no statements about pulse duration, energy etc. can be given. For the generation of a steady-state pulse shape the influence of the bandwidth limitation by a suitable element has to be taken into consideration. Only the interaction of the pulse shortening or frequency broadening active medium and the bandwidth limiting or pulse broadening element allows a steady-state regime."

The gain was treated by explicit 4-level rate equations including pump saturation while bandwidth limitation again came from a lorentzian filter leading to the convolution with an exponential impulse function used in ch.3. The analysis was made more realistic by allowing for two passes through the active elements but the cavity mismatch and filter operations were again expanded to second order (on the assumption that the mismatch and filter response time are small compared to the pulse duration). The equation for the steady state was thus reduced to one related to that in ch.3 but with a more complicated equation for the gain. Noting that the wings of the pulse are roughly exponential, they used a cubic fit to the pulse in the vicinity of the peak and exponential fits of different scale times in the wings, matched at the half-intensity points. The system of simultaneous equations analogous to those in ch.3 contained six equations, all considerably more complicated, which were then solved for the pulse parameters.

One conclusion reached concerning mismatch is in accord with those of earlier publications and with the result presented in ch.5. A stable pulse results from the balance between the delaying action of the filter and the advance caused by the modulation of the gain by the pulse; shortening the cavity decreases the delay between the pump and dye pulses, thus reducing the available gain. They further concluded, however, that a stable, single pulse regime exists only for a limited mismatch range. For small gain, the delaying action of the filter is dominant and negative mismatch is required for synchronism; increased amplification extends the stable region to positive mismatches. The reduction in the available gain as the cavity is shortened sets a lower limit on the mismatch range for stable operation. Lengthening the cavity increases the available gain but this can only compensate for the increase in mismatch up to the point where all the gain is available (i.e. when the dye pulse arrives at the end of the pump pulse). Beyond this point stable operation is not possible. A mismatch range of 2.4mm was predicted in support of an experimental observation of 1.8mm by Kuhl et al.[4].

Good agreement was claimed with the observations on pulse duration in [4] and they predicted reciprocal dependence of the pulse width on bandwidth when the mismatch was adjusted for minimum pulse duration. At fixed mismatch, a minimum was predicted in the dependence of the pulse duration on bandwith. Decreasing the cavity loss led to a larger stable region and increased energies while "the direct influence of the variation of the total pump energy on the dye pulse energy is very small. However there is a strong indirect influence by means of an increase of the stable region." They also predicted that the dependence of the dye pulse energy, duration, intensity and shape all depend only slightly on the pump duration (at fixed pump energy) adducing in support the small pulse shortening from tandem pumping reported in [5].

These conclusions were supported by numerical evolutions (Herrmann and Mottschmann [6]), the resulting steady state pulses being within 20% of those predicted in [3]. The evolutions were started from either a flat signal (as in ch.5) or a gaussian noise burst and it was concluded that the magnitude of the starting signal was of minor importance because (for their parameters) the energy increased by an order of magnitude on each transit, the same steady state being reached within about 300 transits. For mismatches at the short end of the stable region, multiple pulsing solutions (very similar to the transition profiles in ch.5) were found. For short cavities outside the stable region they found long pulses (to which the approximation method in [3] was not applicable). The evolutions also confirmed that the pulse was unstable for large positive mismatches, reaching a limiting profile shape but moving steadily backwards in local time. They concluded that the pulse would not retain this shape because of gain relaxation and the generation of other pulses from the noise in the vicinity. They noted that the ansatz solutions of [3] had not taken into account multiple pulsing but felt that this only occurred when the main signal pulse arrived before the peak of the pump pulse which, in turn, required low output coupling and high pump power.

These results are at variance with those presented in chs.4&5 because the effect of continuous spontaneous emission into the leading edge of the pulse has been neglected. A treatment taking account of the threshold boundary value, and at the same time lifting the rate equation approximation, had already appeared. Nekhaenko [7] started from the semi-classical equations for an effective 2-level system, deriving approximate equations for the steady state as

$$I_p(L,\tau) = I_p(0,\tau)\exp[\sigma_p(G-1)]$$

$$\{t_m\frac{d}{d\tau} + (1-R)\}E(L,\tau) = \tfrac{1}{2}AP$$

$$(T_2\frac{d}{d\tau} + 1)P = E_1(L,\tau)G$$

$$T_1\frac{dG}{d\tau} = I_p(0,\tau)[1-\exp\{\alpha_p(G-1)\}]\,\alpha_p - \tfrac{1}{2}(E_1(L,\tau)P^* + c.c.)$$

As in ch.5, the system was found to be stable only for positive values of the effective mismatch . A solution was obtained for the degenerate system (i.e. when the group velocity mismatch compensated the cavity mismatch)

$$I_l(L,\tau) = \begin{vmatrix} I_{10}\,, & \tau \leq B \\ I_{10}\exp\left[\frac{2\alpha_l}{T_2\delta_L}\int_B^\tau (G-\frac{\delta_l}{\alpha_l})\,d\tau\right] & \tau > B \end{vmatrix}$$

$$T_1\frac{dG}{d\tau} = I_p(0,\tau)\{1-\exp[\alpha_p(G-1)]\}/\alpha_p - \frac{\delta_l}{\alpha_l}I_l(L,\tau)$$

where B is the threshold time and I_{10} is the intensity of the spontaneous fluorescence. Differentiation of the eqn. for I_l shows that the pulse peak occurs as the net gain passes through zero for the second time. Introducing a new variable

$$y(\tau) = \frac{2\alpha_l}{T_2\delta_L}\int_B^\tau (G-\frac{\delta_l}{\alpha_l})\,d\tau$$

gives, after some approximation, the basic equation

$$\frac{d^2y}{d\tau^2} + \gamma[e^y - \beta(\tau)] = 0 \qquad ; \qquad \gamma = \frac{2I_{lo}}{T_1T_2}\,,$$

$$\&\quad \beta(\tau) = \frac{\alpha_l(e^{\alpha_p}-1)I_p(0,\tau)}{\alpha_p\delta_L I_{lo}[e^{\alpha_p} - 1 + \exp(\xi(\tau)/T_2)]}$$

with both periodic and aperiodic solutions. Second order expansions of the intensity about the peak led to expressions for the pulse height, location and width. The last of these was found to have a minimum with pump power, the width rising exponentially for pump energies above the optimum. The coupled equations for the profile were also solved numerically. The published results, for a threshold boundary value of 10^{-8}, are similar to those from the stepping algorithm (when producing single short pulses) showing the symmetrical swing of

the gain about the loss for pumping just above threshold and the broadening of the pulse with positive mismatch.

In contrast to [3]&[7], a second treatment by Yasa [8] acknowledged the importance of spontaneous emission but omitted a bandwidth-limiting process. It was concluded that only the maintainance of the signal level before threshold by spontaneous emission allowed the existence of steady state profiles in positively mismatched cavities. The rate equation was extended to include the effect of a second pass through the amplifier. The leading half of the pulse was divided into three regions: the noise dominated region where the signal converged to reach a value I_0 (proportional to, but much greater than, the spontaneous emission level) at threshold, the unsaturated region where the growth of the pulse, in steps of the mismatch, was determined by repeated multiplications by the slowly increasing gain, and, finally, the peak of the pulse. The peak of the pulse was assumed to begin at the point when depletion exceeded the pumping, while the pump could be neglected for the duration of a picosecond pulse. This led to simultaneous transcendental equations which were solved numerically but a sech^2 approximation was also deduced for the central part of the pulse (assuming small pulse energy and neglecting the pump).

It was observed that the width and peak height of this solution "are only very slightly dependent on I_0 (and therefore on I_{sp} [the spontaneous emission power]). This is expected since as $I(t)$ increases around $t=0$, $G(t)$ does not change until the pulse attains appreciable energy in the leading edge. Hence a considerably different value of I_0 would equally well correspond to approximately the same G_0, while for a given G_0 one must still get a unique pulse shape and energy. The value of I_0 affects t_{max} resulting in an unimportant shift of the pulse peak relative to τ_0."

Numerical solutions for the parameters were obtained in a different fashion from other treatments, by using the first pass gain G_1, as an independent parameter and solving for the mismatch. The value of G_1 led to a solution for the pulse energy and hence the second pass gain and the threshold point. The published plots of the main pulse parameters against mismatch showed good agreement beween the sech^2 approximation and the numerical results. Pulse width and energy increased continuously with mismatch, the former almost linearly, the latter more slowly, while the second harmonic power showed a sharp drop towards zero mismatch, and the results, in particular this last, were felt to be in good agreement with experiment. It was concluded that subpicosecond

pulses would only be produced for mismatches of less than 2μ for a pump width of 100 ps. It was thought that fluctuations in the mismatch and the finite cavity bandwidth might result in quasistable solutions for slightly negative mismatches, "but in accordance with present results, experimental observations indicate stable modelocking in the [positive mismatch] region".

It should be noted that, providing the modelling of the finite bandwidth of the system by a linear device of response time T_f is at all valid, the use of a mismatch of 2μ to set the scale time of the pulse is unrealistic since it is equivalent to only 4 optical cycles.

Chapter 6 : References

1 van Stryland,E.W. - Opt. Commun., **31**, 93 (1979)

2 Kim,D.M., Kuhl,J., Lambrich,R., von der Linde,D. - Opt Commun., **27**, 123, (1978)

3 Herrmann,J., Motschmann,U. - Appl. Phys. B, **27**, 27 (1982)

4 Kuhl,J., Lambrich,R. von der Linde,D. - Appl. Phys. Lett., **31**, 657 (1977)

5 Heritage,J.P., Jain,R.K. - Appl. Phys. Lett., **32**,101, (1978)

6 Herrmann,J., Motschmann,U. - Opt. Commun. **40**, 379, (1982)

7 Nekhaenko,V.A. - Sov. J.Quant. Electron. **11**, 446 (1981)

8 Yasa,Z.A. - Appl. Phys. B, **30**, 135 (1983)

7

STEPPING MODEL EXTENSIONS

7.1 Introduction

The stepping approach succeeds because the self-reproducing equation relates values on the profiles through an operator which is causal for $t_m > 0$; that is, the action of the cavity elements is a function only of that part of the pulse which is ahead in local time and has therefore already been mapped out. Successful iteration of the algorithm also requires that the step be small enough to allow the time integration of the operations and that the boundary conditions are known. The first condition has not so far been a problem in the rate equation approximation and the latter is satisfied if residual effects from the previous round trip can be neglected. The equations used so far have been greatly simplified by the partial integration of the rate equation and by the simple form of the filter. In principle, however, the stepping model can accomodate much more complicated cavity processes while the latter restriction above can be lifted by adopting simple iterative methods.

This chapter presents several modifications and extensions to the simple ring stepping model. The first of the above restrictions is investigated through the form of the filter while the effect of residual gain storage is handled by iterative solution, allowing extension to standing wave cavities and giving insight into the modelocking of systems such as colour centre lasers. Finally the cavity processes are elaborated to give an exact treatment of hybrid modelocking and brief consideration of colliding pulse effects.

7.2 The Etalon Filter

It was assumed in ch.4 that the etalon spacing would not affect the nature of the solution providing that the spacing was less than T_f and that the filter bandwidth was much broader than that of the pulse. The latter condition apears to be true (except under strong gain saturation) - the pulses are typically 10 to 100 times longer than the scale time t_m+T_f. That the effect of the filter on the pulse is small under these circumstances is demonstrated in fig.7.1 which shows the pulse profile at different stages in the ring cavity. The different profiles are generated from the normal stepping equation (GAIN-

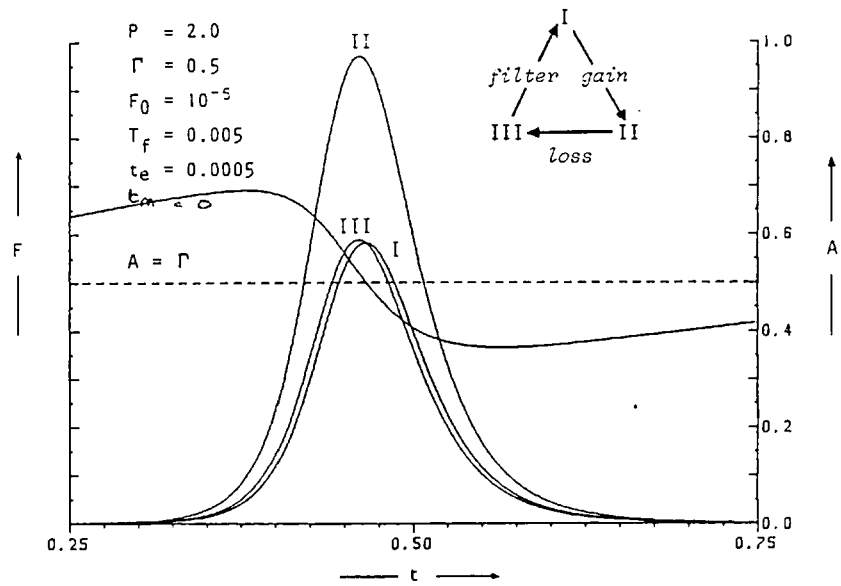

P = 2.0
Γ = 0.5
$F_0 = 10^{-5}$
T_f = 0.005
t_e = 0.0005
t_m = 0
A = Γ
II
III
I
I
filter
gain
III
II
loss
F
A
1.0
0.8
0.6
0.4
0.2
0.0
0.25
0.50
0.75
t

FIG. 7.1

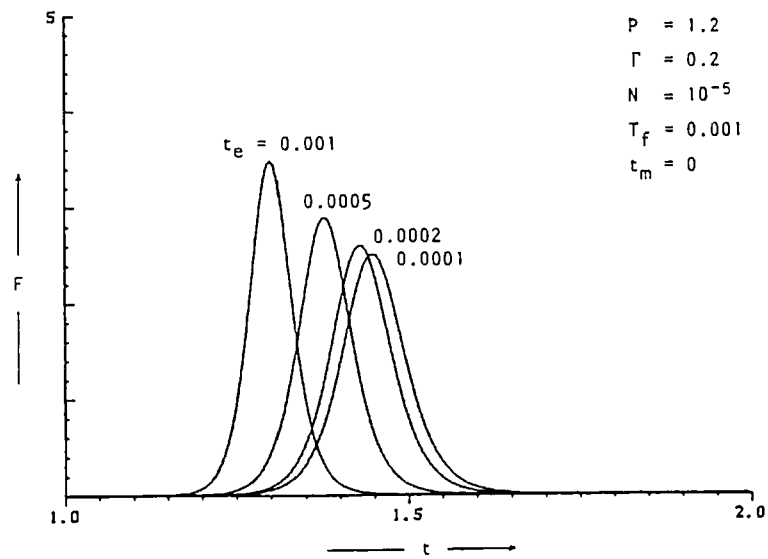

5
P = 1.2
Γ = 0.2
N = 10^{-5}
T_f = 0.001
t_m = 0
t_e = 0.001
0.0005
0.0002
0.0001
F
1.0
1.5
2.0
t

FIG. 7.2

LOSS-FILTER) by multiplying by the appropriate value of the gain and then by the loss. The bulk of the pulse shaping is done by the gain saturation.

This assumption about the bandwidth ignores the phase, however: the imaginary part of the filter spectrum changes rapidly at the centre of the profile and is sensitive to the f.s.r. The stepping algorithm profiles for $t_m=0$ are affected by the etalon spacing until t_e is small compared to T_f (fig.7.2). For this reason, most of the zero mismatch profiles presented so far have been generated with a value of T_f/t_e of at least 5. The variation immediately casts doubt on the ability of the stepping algorithm to describe the effect of mismatches of order T_f (which is the reason for the cursory presentation in ch.4). As $t_m \rightarrow T_f$ the filter ceases to operate. The algorithm can be reformulated to keep the finesse constant as t_m increases but at the expense of increasing complexity. Fixing the etalon spacing at a small fraction of T_f, stepping relations can be written for integral multiples of t_e as

for $t_m = 2t_e$

$$V_{i+1} = RV_i + (1-R)V_{i-1}g_{i-1}$$

for $t_m = 3t_e$

$$V_{i+1} = R(1-R)V_{i-3}g_{i-3} + (1-R)V_{i-2}g_{i-2} + R^2V_{i-1}$$

. .

More initial values are needed as the order increases. The profile for "stepping by 2" is sensitive to the ratio of the initial values, but not greatly so. For $t_m<0$ the new equation is as intractable as the old:

for $t_m = -2t_e$:

$$V_{i+1} = \frac{V_{i-1} - RV_{i-2}}{(1-R)g_{i+1}}$$

7.3 Feedback & Iteration

a) Incomplete gain relaxation

The evaluation of the initial gain value for a stepping profile has so far been simplified by assuming that the residual inversion relaxes fully before the next pump pulse. Accordingly, the pumping strength has been defined in terms of the level required to reach threshold in a single pulse. The results from the stepping model have shown that a significant fraction of the total gain delivered is not extracted by the steady state pulse, particularly at low pumping levels. This residual gain will increase the effective pump power when the cavity round trip time is not large compared to T_{1a}. When the dye pulse is both weak and arrives at the end of the pump, the gain evolution is anti-symmetric about Γ and the effective pump parameter P' is easily determined. The dye pulse passes through the amplifier after the pump pulse when the inversion has reached $P'\Gamma$. Providing that the effective pump is also weak, the residual inversion is $(2-P')\Gamma$ which relaxes by a factor $\rho = \exp[-T_{ring}/T_{1a}]$ during a round trip. The inversion delivered by the pump is still $P\Gamma$ hence

$$P' = P + \frac{(2-P)\rho}{1+\rho}$$

There is no simple solution when these ideal conditions do not obtain. The stability of the stepping equations suggests that a self consistent solution may be found by iterating the algorithm, using the gain at the end of one stepping profile to modify the initial gain value for the next. When the noise term is included and the profile is started before threshold, this simply means adding the feedback term $A_{final} \times \rho$ to A_{start}. For moderate feedback - $T_{ring} \simeq T_{1a}$ - the iteration converges rapidly, often within 5 passes. (If the stepping profile is seeded each time with a small noise value, the iteration converges even when the profile starts too late in the pump and the asymptotic value of the gain at the start is above threshold). Figs. 7.3a&b show the final profiles for several cavity lengths. The effect is equivalent to raising the pump power.

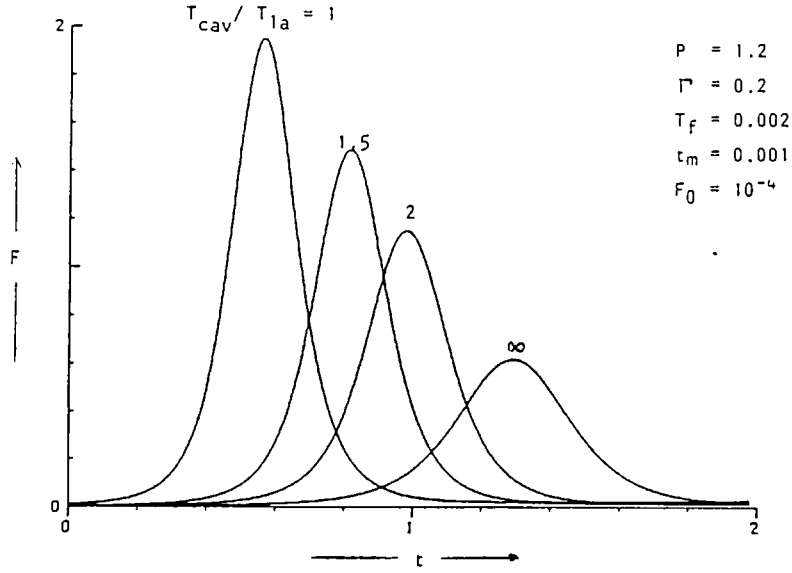


FIG. 7.3a

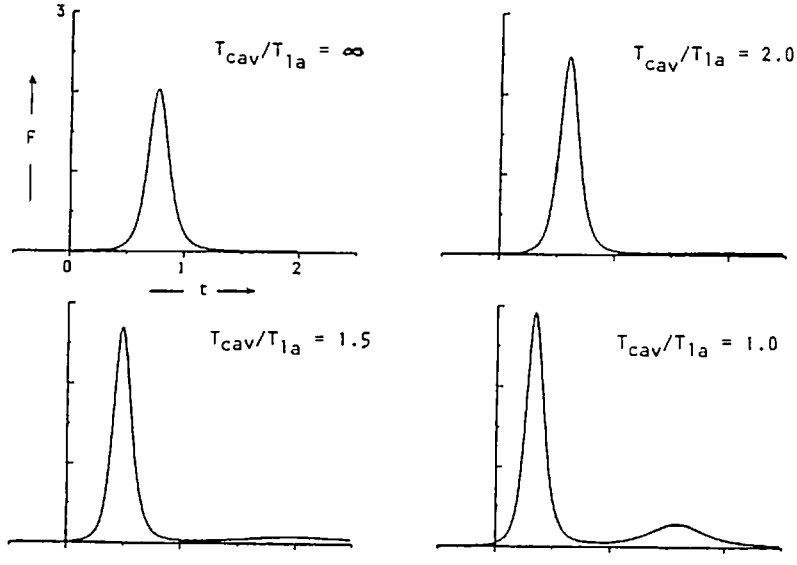


FIG. 7.3b P = 1.5, Γ = 0.2, T_f = 0.002, t_m = 0.001

b) Colour Centre Lasers

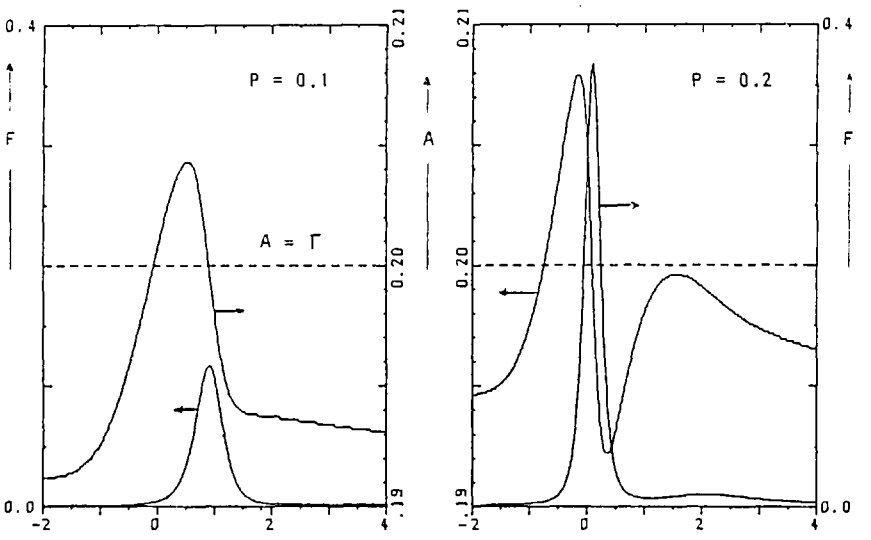
The recent successful modelocking of colour centre lasers presents a system which is very similar to typical synchronously pumped dye lasers but with a population relaxation time which is long compared to the cavity round trip time. F-centres in alkali halides have wide homgeneously broadened emission bands and allow efficient absorption of continuous optical pumping. Modelocking of $KF:F_2^+$ was reported by Mollenauer and Bloom [1] using a Nd:YAG pump giving ~100 ps pulses at 100 MHz at approximately 5 w average power. The length of the colour centre laser was 1/3 of that of the pump. Pulse widths were measured by continuous autocorrelation using a shaker assembly. The effect of cavity length tuning was remarkably similar to that in synchronously pumped dye lasers: reducing the length narrowed and enhanced the correlation until a maximum was reached. The shortest pulses were obtained with the cavity a few μ shorter than this, and further shortening usually produced satellites a few tens of picoseconds from the main pulse. The authors suggested that "only the gain cross-section (about the same in both dye and color center) and not the spontaneous emission rate (slower in the color center) is of significance to the modelocking." Pulse widths of 3-5 ps ($sech^2$) were obtained over a wavelength range of 1.25-1.45 μ. The spectra were often close to the bandwidth limit for pulses of ca. 5 ps, but were occasionally several times wider (which was attributed to maladjustment). Conversion efficiency was similar to that in CW operation - 55% using 50% output coupling. Pulses of ca. 4ps were also obtained from $LiF:F_2^+$ pumped by Kr^+.

In a second paper, Mollenauer et al. [2] observed that modelocked operation with a gain storage time much longer than the round trip time led to a pulse width dependence on pump power and cavity loss which was significantly different from that in dye lasers. The gain medium comprised $Tl^0(1)$ (neutral thallium with a single perturbing vacancy) colour centres in a KCl host giving a gain cross-section of 1.3×10^{-17} cm^2, a radiative lifetime of 1600 ns and a half-power bandwidth of 650 cm^{-1}, peaked at 1.52 μ. The absorption bandwidth was 1300 cm^{-1} peaked at 1.04 μ. The cavity length in this system matched the pump laser (1.5 m). A birefringent filter was neccessary for bandwidth-limited pulses. CW operation gave a slope efficiency of 20% for 34% output coupling, reaching a maximum output of 1.2 w for 6 w pumping (threshold = 185 mw). For 12% and 24% output couplings the slope efficiency were 9% and 16%. Under synchronous pumping there were two thresholds - the first for laser action

itself and the second for full modelocking. Below the second threshold the autocorrelations had a peak at least 25 ps wide on an even wider pedestal. Above the modelocking threshold the correlations lacked a coherence spike. The pulse widths decreased monotonically with pump power, reaching ca. 8 ps at 5 w, and, in contrast to typical dye laser results, the width increased with increasing output transmission at fixed pump power. This was attributed to improved pulse compression arising from increased gain modulation, either from increased pump power or increased intracavity power with lower output coupling.

Synchronous pumping of a colour-centre laser further into the infra-red was reported by Isganitis et al. [3]. Ar^+ pumping (5145 A, 150 ps, 70 MHz, >1 W) excited F_A(II) colour centres in Li-doped KCl which were tunable from 2.5 μ to 2.87 μ in continuous operation. The cavity, with a length 1/4 that of the pump, was operated with 2 or 4% output both with and without a birefringent tuner (1 mm sapphire). Spectral broadening indicated the onset of modelocking as the cavity length was adjusted and the pulse duration was measured by cross-correlation with the pump pulse, giving a minimum pulse width of 75 ps (nearly bandwidth limited). Satellites or extended background radiation were seen only when the pump itself had a trailing pulse. The position of the colour-centre pulse relative to the pump was found to be much more sensitive to cavity length (16 ps/μ) than had been observed for a dye laser (0.5 ps/μ) by Frigo et al.[4]. This sensitivity was attributed to the reduction of the gain modulation arising from the long fluorescence time ($\sim$ 75 ns compared with a round trip time of 3.6 ns and a pump period of 14.7 ns).

For pulsed pumping in the presence of gain storage, the threshold pump parameter is given by $[1-\exp(-T_{cav}/T_{1a}) - T_{cav}/T_{1a}]$. The modelocking threshold power reported in [2] was about 10 times the laser threshold, giving a pump parameter of $P \simeq 1/16$. The modulation of the gain by the pump and laser pulses is therefore much smaller than the values seen so far for dye systems. The stepping algorithm iterations nevertheless converge rapidly for these parameters providing that the gain is given an appropriate initial value. Assuming that the laser is operating under "positive-type" conditions, the residual gain is such that one pump pulse takes the net gain from just below to just above the loss. A reasonable initial value is therefore $\Gamma - P\Gamma/2$. Fig.7.4 shows the profiles for $P = 0.1$ & $0.2, \Gamma = 0.2$, $t_m = 0.001$, $T_f = 0$ and $T_{ring}/T_{1a} = 0.01$. Convergence takes 5 iterations and is stable even though the feedback term (=99% of the residual gain) is much larger than the pump.



$\Gamma = 0.2$, $N = 10^{-5}$, $T_f = 0$, $t_m = 0.001$, $T_{cav}/T_{1a} = 0.01$

FIG. 7.4

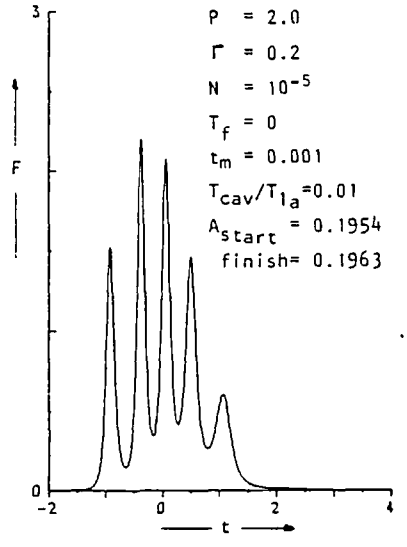


FIG. 7.5

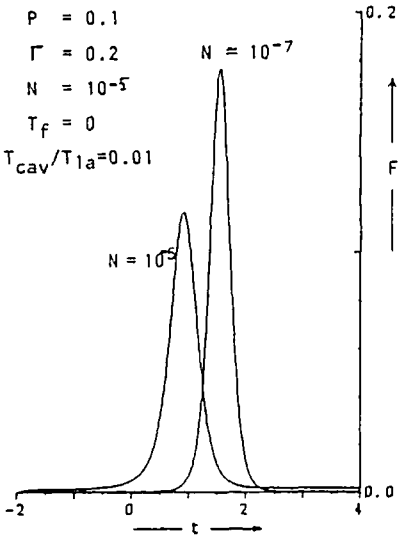


FIG. 7.6

The gain must be below threshold at the end of the pulse so the feedback becomes less important as the pump is increased. Fig.7.5 shows the satellites produced by pumping far above threshold (with a single pump pulse now sufficient to exceed the loss). In spite of the high pump power, the initial and final values of the gain are still very close to threshold. If, on the other hand, the pump is reduced towards the first threshold, the stepping algorithm becomes unstable. At P=.02 alternate iterations produce a broad weak pulse while the others fail to exceed threshold. Although the observation of very broad autocorrelations in [2] might simply indicate weak pulse compression, the claimed second threshold and the limit cycle of the stepping algorithm suggest that the system is actually unstable. It was shown in ch.4 that both the noise power and the excess gain (when close to threshold) significantly affect the pulse. The observation in [1] that the level of the spontaneous emission does not affect the pulse may not be justified: the long storage time substantially reduces the gain modulation (for the parameters of [1], at least) and, in consequence, the pulse compresssion. The noise power is also reduced by a factor ~100 and it may be this which allows the formation pulses of a few ps in duration. Fig.7.6 shows the effect of this reduction on the pulse in fig.7.4a.

c) Second pass

In a standing wave cavity the pulse makes two passes through the gain medium on each round trip and can receive significant secondary amplification from the second pass if the gain has not relaxed. There is direct evidence for this in the careful fluorescence measurements of Frigo et al. [4], which showed the two dips in the spontaneous emission from the amplifier as the pulse passed. The half-nanosecond delay corresponds to the distance between the jetstream and the focussing mirror, and the magnitude of both the delay and the second dip suggest that the effect is not due to a satellite.

The second pass is equivalent to adding a second amplifier providing that the pulse does not overlap with itself so that the two depletion processes are independent. The second amplifier is not pumped, and the initial state, given by the residual gain in the first, is again determined by iteration. To start with, we ignore the filter (through which the pulse also makes two passes) and write the new stepping algorithm as

$$F(t)\ g(t)\ h(t)\ \exp(-\Gamma') \quad = \quad F(t+t_m)$$

where g is the net amplitude gain coefficient of the first amplifier and h that of the second. The rate equation for the first pass is as before while that for the second contains the amplified flux

$$dH / dt \quad = \quad -F' \left[e^{H} - 1 \right] \quad , \quad F' \ = \ Fe^{G}$$

The initial secondary amplification is set equal to the residual primary amplifcation from the last iteration multiplied by a relaxation factor (to allow for the return delay). The iteration again converges rapidly (fig.7.7).

The double pass can be combined with finite cavity length in an exactly similar fashion. Providing the system is sufficiently above threshold, the iterations are stable. The results agree with numerical evolutions (ch.8) and there does not seem to be any "trapping" of the iteration in a solution which is only metastable. The form of the filter convolution means that a second pass through the etalon can easily be included.

7.4 Hybrid Modelocking

The addition of small quantities of saturable absorber to the amplifier in synchronously pumped systems has repeatedly been reported as improving the pulse stability and reducing satellites. This seems a natural addition to the picture of the synchronously pumped steady-state as a "giant pulse", with the saturable absorber helping to "Q-switch" the profile in the same way as a low noise boundary value. The absorber can be incorporated into the stepping equations in the same way as the second pass through the amplifier. If the absorber is isolated from the amplifier in a second jet stream, the basic stepping equation becomes

$$F_{i+1} \quad = \quad F_i \ \exp(\ A_i - B_i - \Gamma)$$

and the rate equation for the absorber is

$$dB/dt \quad = \quad - F' \ s \ [e^{B} - 1] \ - \ B/T_{1b} \quad , \quad F' \ = \ F \ e^{A}$$

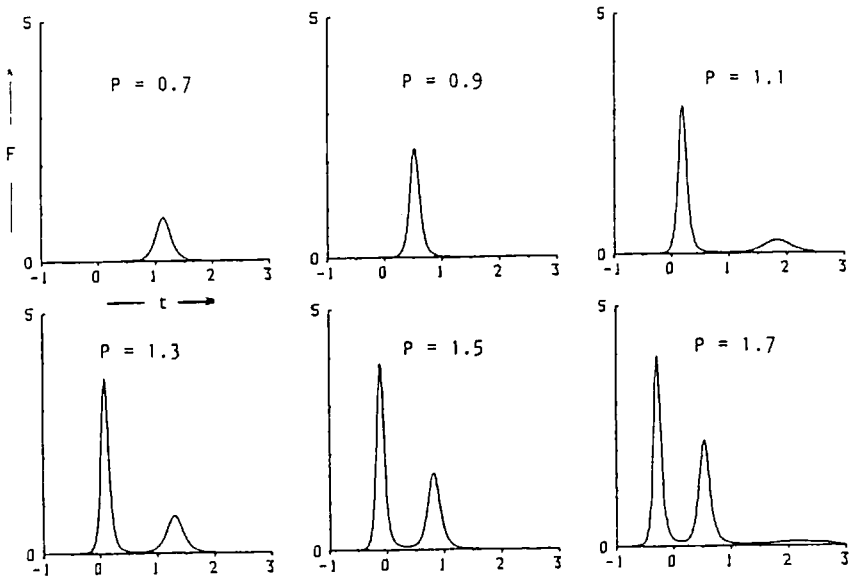


FIG. 7.7 $\Gamma = 0.2$, $T_f = 0.002$, $t_m = 0.001$, $F_0 = 10^{-5}$

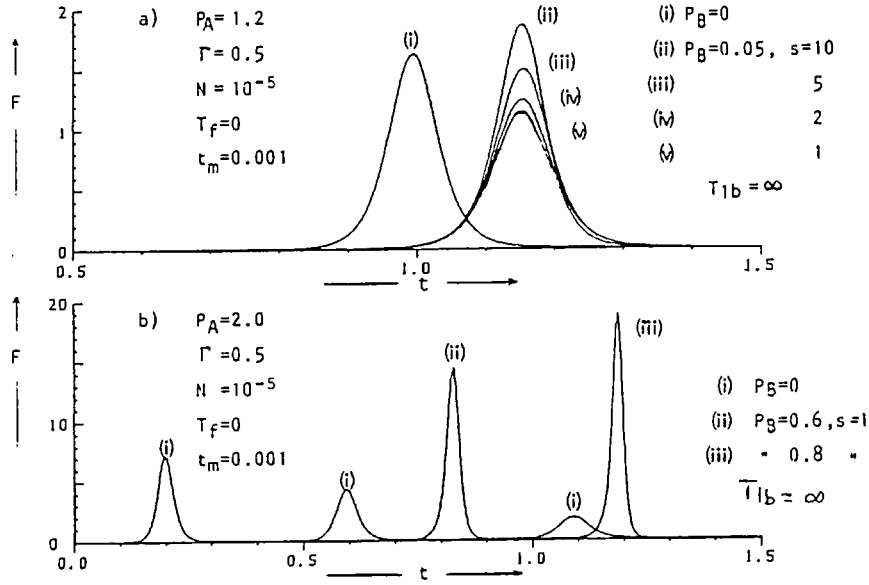


FIG. 7.8 : Hybrid stepping profiles

where the relative cross-section factor, s , allows for telescoping to enhance the preferential saturation of the absorber (New,[5]). The fluorescence lifetime, T_{1b}, may be fast enough in some dyes to affect the pulse. We define the unsaturated absorption level relative to the linear loss as $B_u = P_B \Gamma$, and, initially, assume that $T_{1b} << T_{ring}$. At low pump powers the absorber can actually suppress the pulse (fig.7.8a) needing large values of s before there is any improvement. When the pump is increased, however, cross-section enhancement may not be neccessary (fig.7.8b).

The equations can be iterated, as before, to accomodate finite absorber recovery during a round trip. The result appears simply to be depression of the absorber. On the other hand, very fast recovery can lead to enhancement of a satellite train under extreme conditions (Fig.7.9), and, if the parameters are further distorted, can produce erratic satellite bursts in which the spacing is very sensitive to the time variation of the pump (the onset of erratic behaviour of the coupled rate and time delay equations is considered again in ch.8).

Although the stepping technique can easily accommodate this extra nonlinear process while already complicated analytic solution methods would be made appreciably more so, it is clear that the results presented above do not explain the characteristic experimental features - (low absorber molarities (typically 1-10% of that of the amplifier), operation without large s values and the removal of autocorrelation spikes. The problem of absorber recovery is considered again in the next chapter.

7.5 Active modelocking

The stepping approach is appropriate when an external periodic drive imposes a self-reproducing condition with a known time delay. We have so far neglected the simplest form of modulation - active loss modulation. Although there was an early report of active modelocking of a pulsed dye laser (Ferrar [6]), simultaneous reports of active loss modulation (Dienes et al. [7]) and of phase modulation (Kuizenga [8]) marked the start of CW dye laser modelocking. The loss modulation produced appreciably better results than the phase modulation, giving pulse durations down to 55 ps. The argon and dye systems of the former shared the same folded resonator and the quartz AOM, operated at a depth of several per cent, modulated but did not modelock the pump. Modelocking was achieved at the fundamental rate (75 MHz) and at the third harmonic.

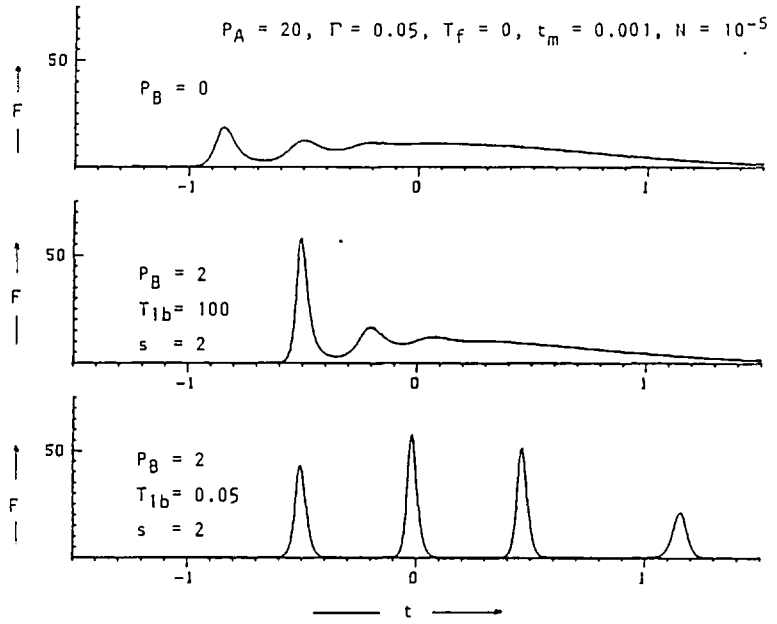


FIG. 7.9

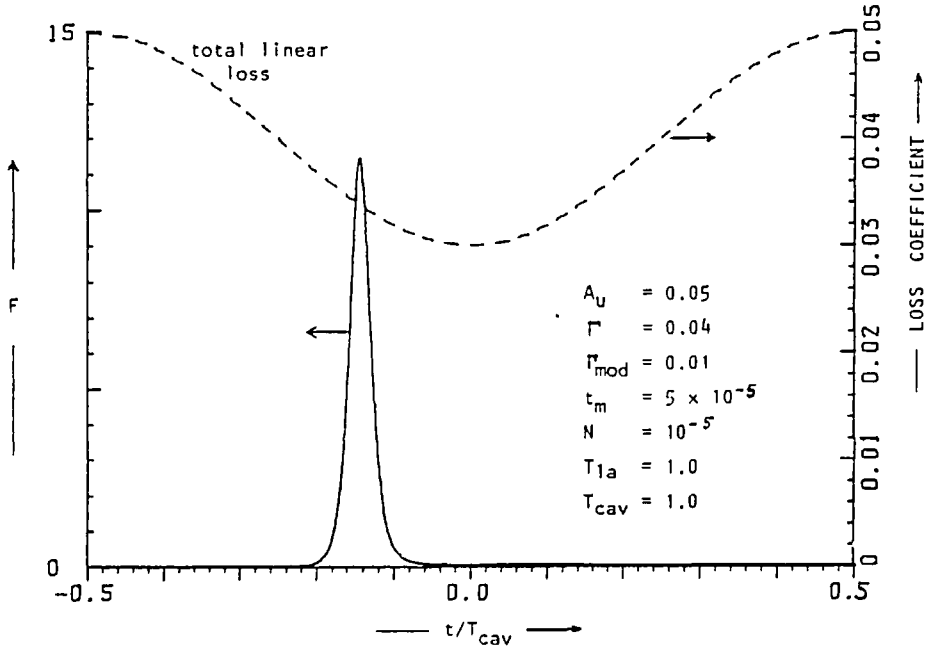


FIG. 7.10: Active Modelocking

spite of the increased modulation depth at 250 MHz, the shortest pulses were obtained at 500 MHz: under optimum conditions, the pulse duration fell as the modulation depth was increased, low modulation giving a 35 ps (gaussian) pulse and an autocorrelation with a coherence spike which eventually merged into the main profile as the modulation was increased. Excess spectral width was attributed to chirping. The best pulse durations obtained were 10 ps while operation at increased power broadened the pulses considerably.

The application of simple stepping equations to the case of loss modulation is complicated by the fact that the system is pumped continuously. While it seems resonable to expect that the pulse still arrives after tnreshold for +ve mismatch, the location of threshold depends on the gain recovery and hence on the pulse energy unless the cavity is long, and the algorithm must again be iterated. Although the "hard" loss modulation could, in principle, be responsible for the net loss required on the tail of a "positive-type" profile, it is likely that this is again achieved by gain saturation. The range of the modulator transmission values in Scavennec's work was typically 0.96 to 1.0 which was large compared to the quoted output coupling of 2%. Fig. 7.10 shows a pulse generated by the stepping method without a filter. The stepping range extends over the whole cavity – the gain is pumped continuously and there was no artificial relaxation factor between iterations (A_u is the steady-state value of the gain in the absence of a deleting signal intensity). The mismatch is equivalent to ca. 50u for a 1 m ring cavity. For pumping reasonably well above threshold, convergence of the stepping iterations is again stable, while preliminary results have again shown limit cycles for pumping very close to threshold.

Kuizenga's phase modulation experiment [8] was much less successful than the loss modulation in [7], modelocking being "difficult and sometimes impossible". The aqueous solution of Rh-6G was contained in a 0.5 mm contacted dye cell, focussed by a thick lens, on one of the cavity mirrors. The cavity length could be adjusted from 20 to 60 cm. The threshold pump power was 180 mW and typical operation was at 1 W giving 50 mW output which fell to 20 mW with the incorporation of the $LiNbO_3$ phase modulator. The free running spectrum had a width of 6.5 nm and showed structure which was attributed to an etalon effect in the dye cell. The modelocked spectrum was similar but the etalon structure was substantially reduced. A sharp central spike, which was

attributed to a fully locked cluster of modes, scanned across the main spectrum as the modulation frequency was tuned. Photodiode measurements showed two pulses of about 0.5 ns duration in the cavity (one at each phase extremum) but with considerable fine structure at the detector limit. The incorporation of a 90 μ etalon gave a broadened free-running spectrum dominated by the etalon transmission peaks. The changing distribution of the modelocked spectrum between these peaks as the modulator was tuned was accompanied by changes in the complicated phase structure. Although a stepping equation can, in principle, be formulated for phase modulation (assuming that the profile is either strictly self-reproducing or that any systematic drifting in the phase profile is known) the approach seems to be invalidated by the very poor modelocking observed.

Chapter 7 : References

1 Mollenauer,L.F., Bloom,D. - Opt. Lett., **4**, 247 (1979)

2 Mollenauer,L.F., Vieira,N.D., Szeto,L. - Opt. Lett., **7**, 414 (1982)

3 Isganitis,L., Sceats,M.G., German,K.R. - Opt. Lett., **5**, 7 (1980)

4 Frigo,N., Hemenway,C., Mahr,H. - Appl. Phys. Lett., **37**, 981 (1980)

5 New,G.H.C. - I.E.E.E. J. Quant. Electron., QE-**10**, 115 (1974)

6 Ferrar,C.M. - I.E.E.E. J. Quant. Electron., QE-**5**, 550 (1969)

7 Dienes,A., Ippen,E.P., Shank,C.V. - Appl. Phys. Lett., **19**, 258 (1971)

8 Kuizenga,D.J. - Appl. Phys. Lett., **19**, 260 (1971)

9 Scavennec,A. - Opt. Commun., **20**, 335 (1977)

10 Scavennec,A. - Opt. Commun., **17**, 14 (1976)

8

NUMERICAL EVOLUTIONS - PERTURBATION & INSTABILITY

8.1 Introduction

The noise-free evolutions presented in ch.5 suggested that even a complicated pulse with several satellites formed in a well-controlled manner, with the cavity mismatch and the filter diffusing the structure and balancing the tendency of the pulse to approach equilibrium with the pump. Experimental results show fluctuations on widely differing timescales, however. Much of this may be associated with spontaneous emission: the leading edge of the pulse evolves continuously from threshold and it remains to be seen to what extent the fluctuations are smoothed out as the mismatch drives the structure across the pulse envelope. Nevertheless, the extreme sensitivity of the pulse to the cavity length and the fact that the pulse could be thought of as having several degrees of freedom - the position and energy of each satellite - suggests that the response to external perturbation might be erratic.

This chapter presents attempts to disturb the evolution by slow perturbation of the main parameters, by radical alteration of those parameters, by using strong saturable absorbers, and, finally, by feeding in a random noise signal. The system proves to be very stable under moderate perturbation but large distortion of the parameters reveals further analogies between the local time profile of the synchronous pulse and the real time behaviour of other systems. The introduction of saturable absorbers gives insight into the role of recovery times in optimum pulse formation while at high absorber levels two new self-pulsing modes are found.

8.2 Pump & Loss Modulation

Figs.8.1-3 show the effect on the pulse evolution of a harmonic modulation of $\pm 5\%$ in the pump power for moderate pumping. The pulse follows the perturbation closely but the depth of modulation is a function of the period and can be greater than that of the pump. The pumping is here close to threshold and a change of 5% in the total pump power represents a much larger change in the excess gain (it was shown in ch.7 that the pulse energy is proportional to the excess when close to threshold). The increased modulation depth is not,

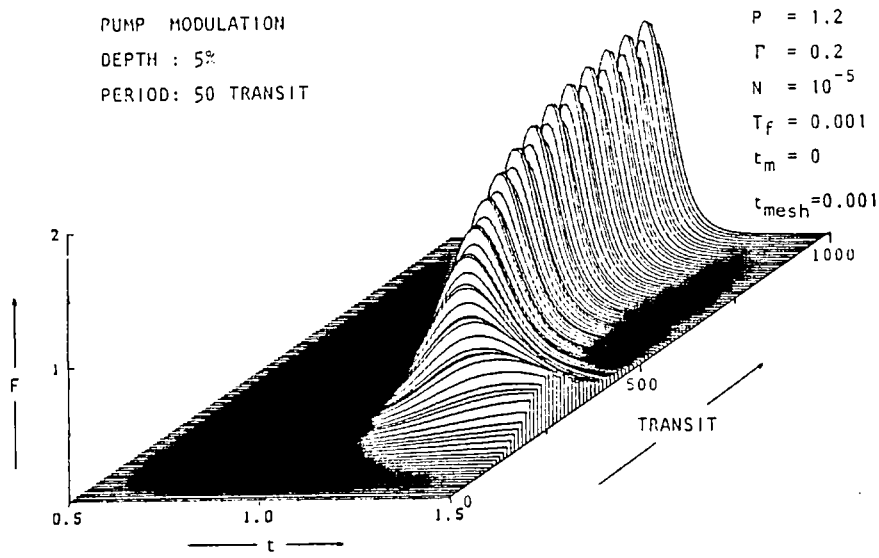


FIG. 8.1: Modulation of pump power

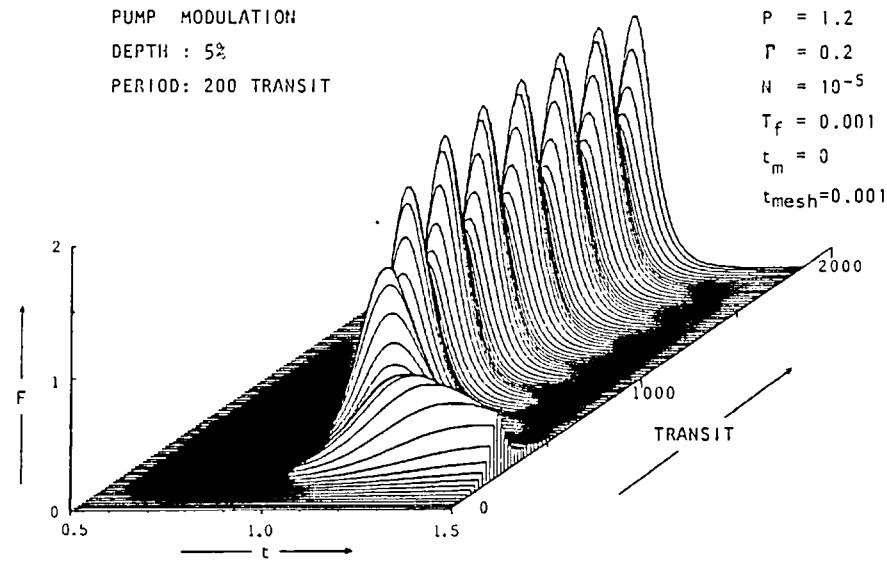


FIG. 8.2

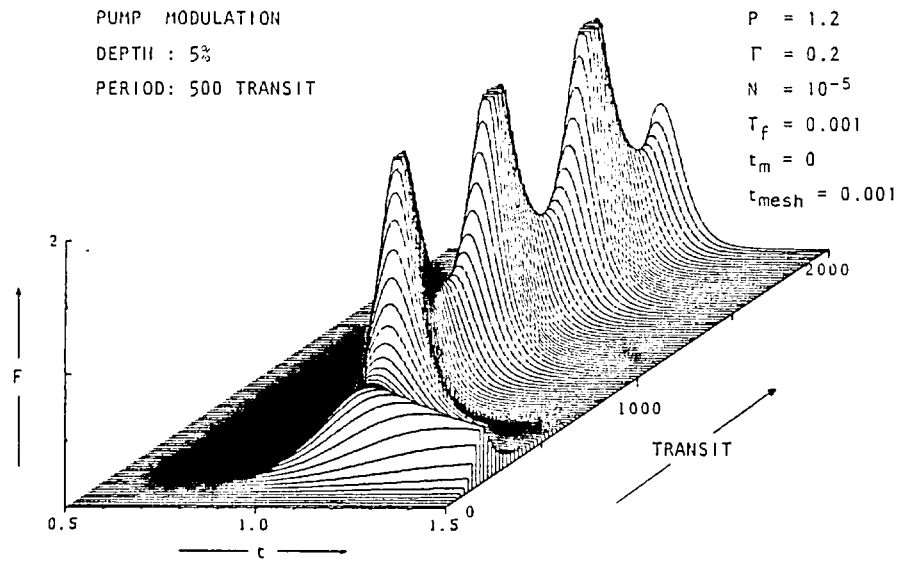

PUMP MODULATION
DEPTH : 5%
PERIOD: 500 TRANSIT
P = 1.2
Γ = 0.2
N = 10⁻⁵
T_f = 0.001
t_m = 0
t_mesh = 0.001
2
F
0.5
1.0
1.5
t
0
1000
2000
TRANSIT

FIG. 8.3

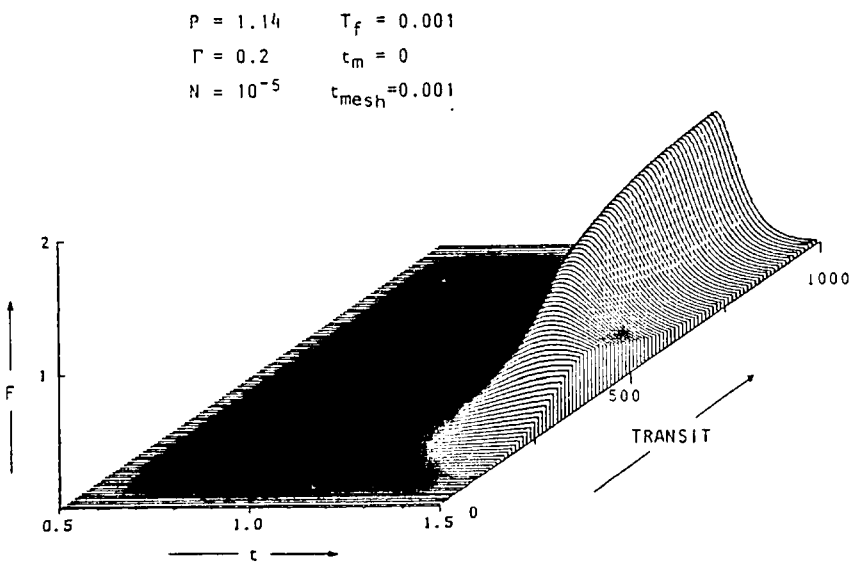

P = 1.14
Γ = 0.2
N = 10⁻⁵
T_f = 0.001
t_m = 0
t_mesh=0.001
2
1
F
0.5
1.0
1.5
t
0
500
1000
TRANSIT

FIG. 8.4

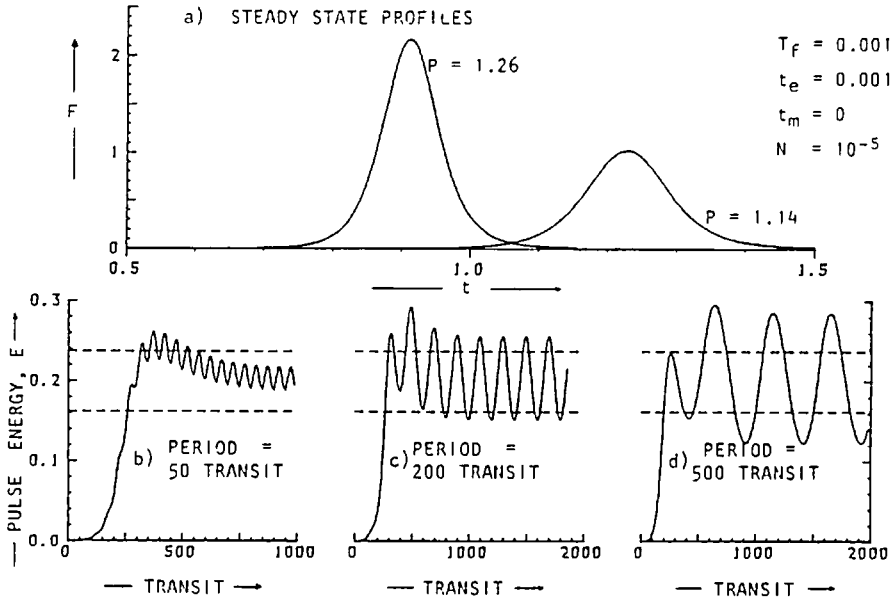

a) STEADY STATE PROFILES
P = 1.26
P = 1.14
T_f = 0.001
t_e = 0.001
t_m = 0
N = 10^{-5}
F
t
PULSE ENERGY, E
b) PERIOD = 50 TRANSIT
c) PERIOD = 200 TRANSIT
d) PERIOD = 500 TRANSIT
TRANSIT

FIG. 8.5

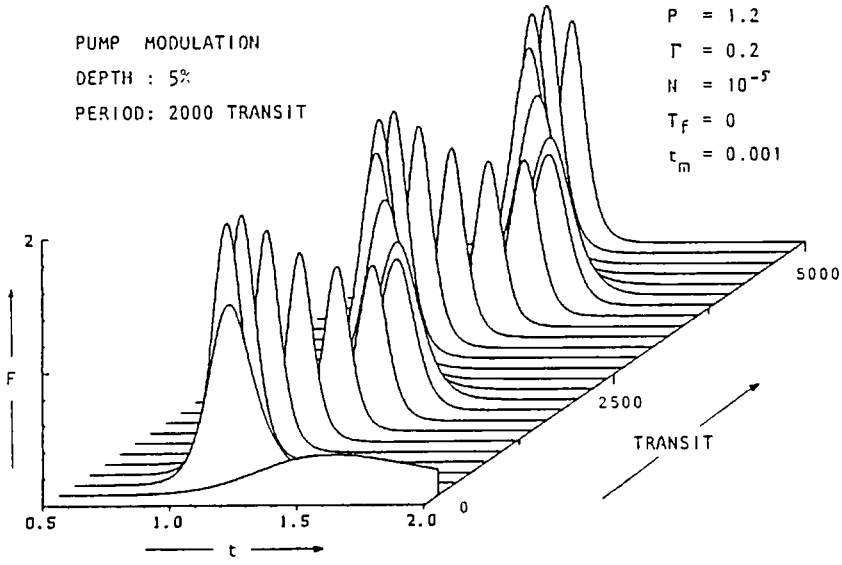

PUMP MODULATION
DEPTH : 5%
PERIOD: 2000 TRANSIT
P = 1.2
Γ = 0.2
N = 10^{-5}
T_f = 0
t_m = 0.001
F
t
TRANSIT

FIG. 8.6

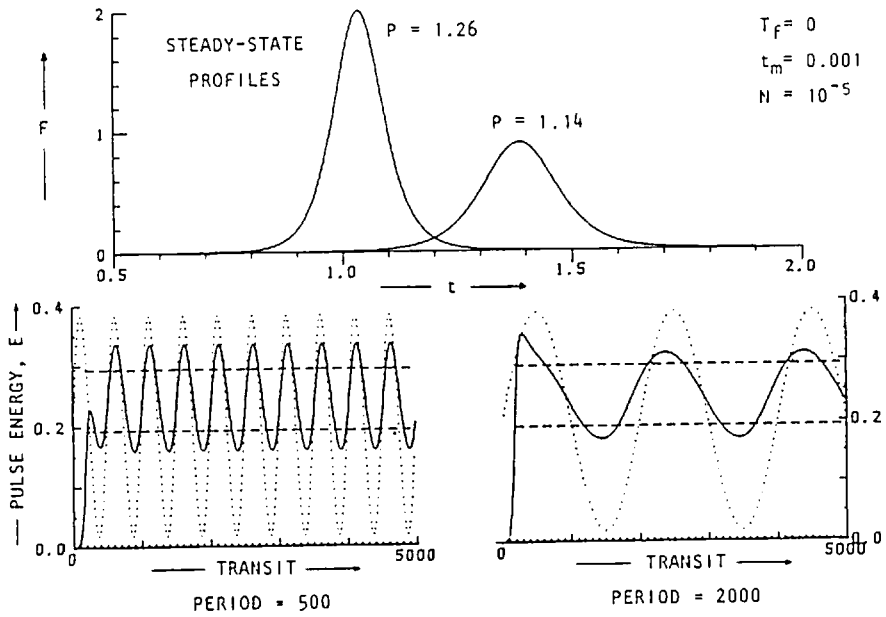


FIG. 8.7 (Dotted lines show modulator phase)

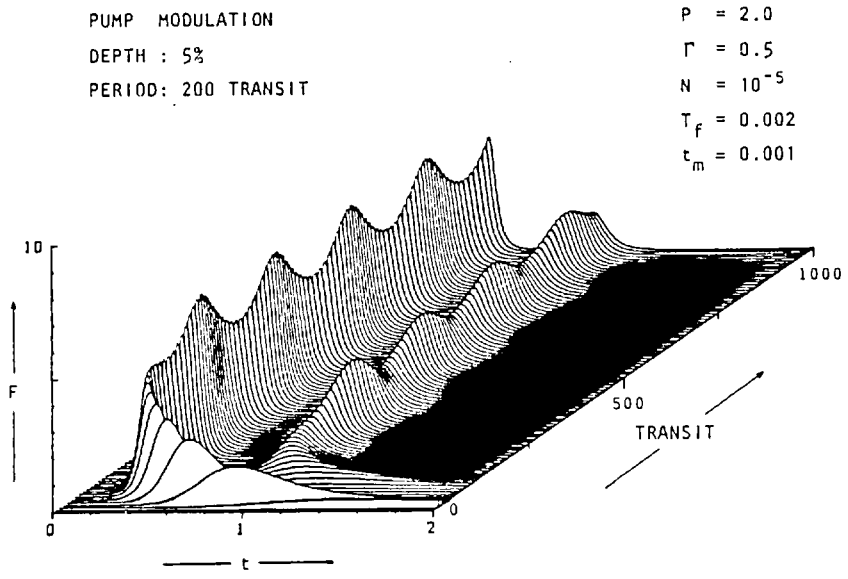


FIG. 8.8

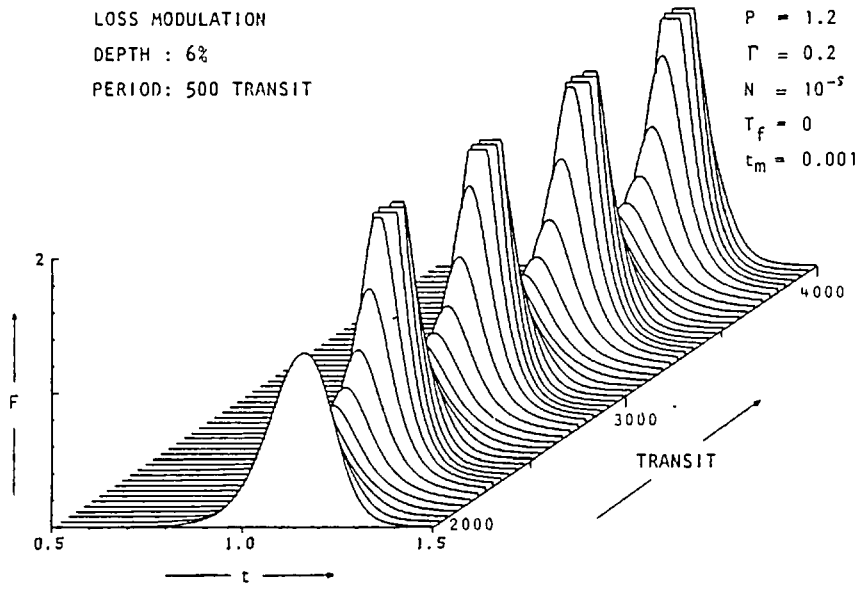

LOSS MODULATION
DEPTH : 6%
PERIOD: 500 TRANSIT
P = 1.2
Γ = 0.2
N = 10^-5
T_f = 0
t_m = 0.001
2
F
0.5
1.0
1.5
t
2000
3000
4000
TRANSIT

FIG. 8.9

however, caused by closer approach to adiabatic operation as the perturbation frequency is reduced. Without modulation the approach to steady state takes 1000 transits or more (fig.8.4), but at a modulation period as low as 200 transits the energy range exceeds that of the steady state solutions (the dashed lines in fig.8.5b–d). The quasi–static solutions for this range of pump powers span a significant local time range (fig.8.5a) but the perturbed pulse is unable to move fast enough in local time and becomes trapped at the "early" end of the range of the steady–state solutions. The longer the period, the greater the effect on the energy until the perturbation is slow enough to allow the pulse to move (fig.8.6). The energy modulation begins to decrease again as the perturbation becomes adiabatic (fig.8.7).

Fig.8.8 shows the same relative modulation at increased pump power. The modulation on the satellite is out of phase with the main pulse but again the change is cyclic and stable. When the cavity mismatch is negative the result is just a small, uniform modulation of the whole profile.

The effect of slow loss modulation is similar (fig.8.9).

8.3 Modulation of t_m

The combined action of the gain and filter displace the steady state pulse by an amount that is exactly compensated for by the cavity mismatch. For the values of the gain coefficient used so far, the pulse is much longer than t_m or T_f and the relative displacement of the pulse on each transit is very small. This "magnification" of t_m in the pulse width is one reason why the mismatch is critical. The evolutions of ch.5 suggest that the approach to steady state may take thousands of transits while the stationary nature of the perturbed pulses in §8.2 suggests that the pulse may be difficult to displace on a shorter timescale. In view of this, what happens if the mismatch is subjected to fast periodic modulation, particularly if the range encompasses a change in sign? If the pulse remains almost stationary in local time during the modulation period then the mismatch error will accumulate during a half period resulting in a significant displacement of the pulse relative to the pump. Figs.8.10 & 11 show the effect of small relative modulations in positive and negative values of the average mismatch. The pulse is again held stationary in the pump frame by displacing the profile by 1 or more mesh points on each transit while the perturbation is applied by moving the origin of the pump itself. The profiles are plotted in the unperturbed pump frame, the oscillation

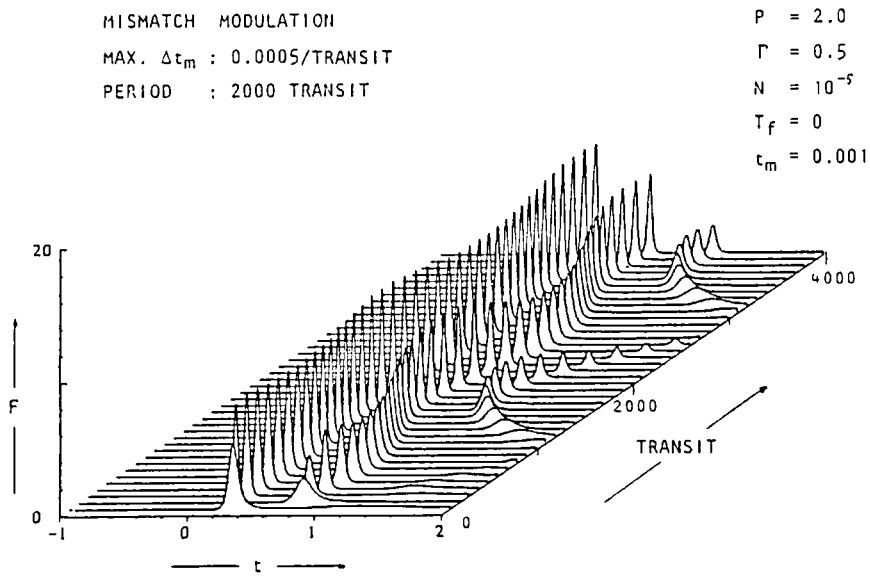


FIG. 8.10

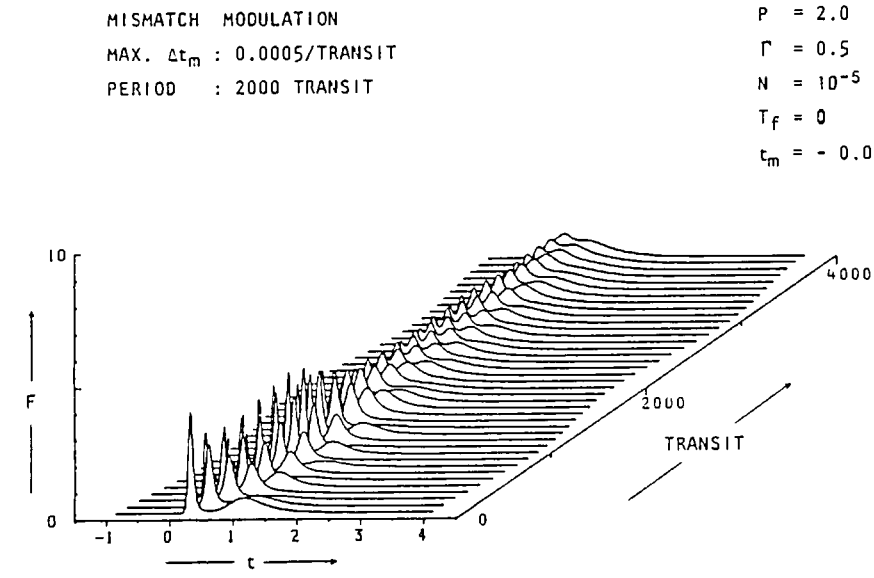


FIG. 8.11

FIG. 8.12a

AUTOCORRELATION ℘

TRANSIT 4000

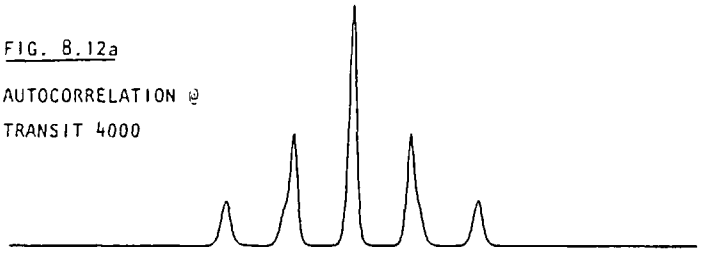
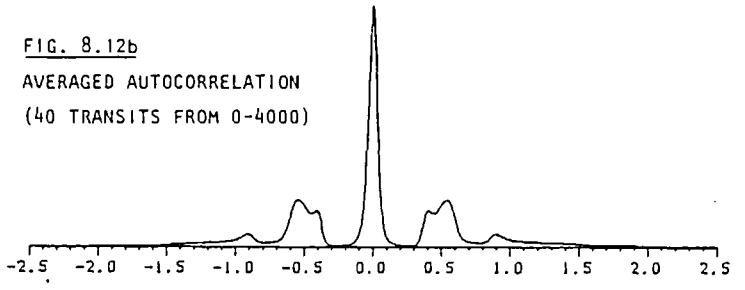
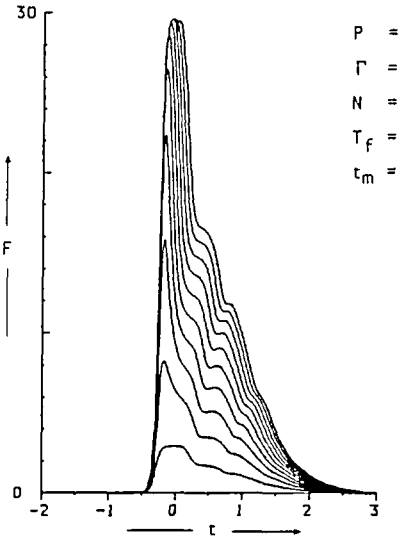


FIG. 8.12b

AVERAGED AUTOCORRELATION

(40 TRANSITS FROM 0-4000)





P = 50

Γ = 0.01

N = 10^{-5}

T_f = 0

t_m = 0.005

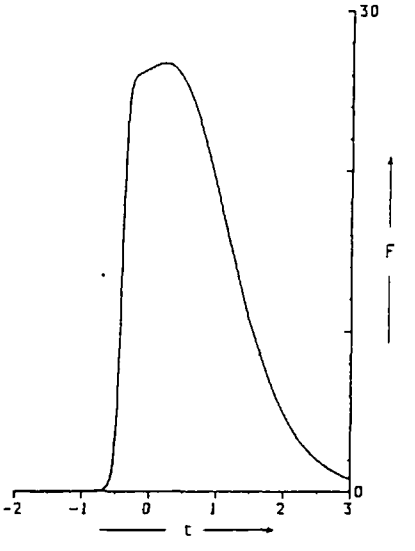


FIG. 8.13a : STEADY STATE CAVITY-DUMPING CYCLE (90%, 100 TRANSITS)

FIG. 8.13b : STEADY STATE PROFILE

of the end points in fig.8.11 indicating the size of the accumulated mismatch error. For $t_m > 0$ the evolution is surprisingly sensitive but the response is still cyclic. The maximum deviation of the mismatch is only half of the average value but, if the pulse shows significant local time "inertia", the pulse lag accumulates to give a maximum dislocation relative to the pump roughly equal to [modulation period/2]x[max. deviation] – in this case approximately 0.5.

Fig.8.12a shows the simple autocorrelation of the pulse at 4000 transits. The sharply defined satellites are much reduced in the average autocorrelation shown in fig.8.12b (averaged only over the plotted profiles). Although the value of t_m used here is probably ten times too large (.0005 x 100 ps >15μ = 7μ in mirror position) the effect may be significant at realistic mismatches.

8.4 Cavity Dumping

The best experimental performance reported for continuous cavity-dumped operation has been good pulses of a few ps, dumped about every 100 transits. Although the growth from noise to a saturating signal is rapid for strong pumping, the approach to steady state slows as the saturated gain approaches equilibrium. The slow evolution will also involve the gradual narrowing of the noisy spectrum by the finite bandwidth of the system. Evolution is periodically restarted when the system is cavity-dumped but spectral narrowing will probably continue since even efficient dumping – say 99% – will leave a seed pulse which is well above the noise level. The seed pulse, however, has only 100 transits of reshaping before being switched out again. More importantly, the use of high-Q cavities suggests that the pulses may suffer badly from satellites or long tails. This is evident in fig.8.13a which shows the steady state cycle of a pulse from one cavity dump to the next in a low loss cavity. The pump power is similar to that used for much of the preceeding work, $P\Gamma=0.5$, but the fixed cavity loss is now only 1%. 90% of the energy is dumped on each 100^{th} transit. The cycle has reached a steady state by 400 transits with the peak energy increased by a factor ~100 over typical values for the earlier results. The steady state profile without dumping (fig.8.13b) shows that critical damping of the stepping algorithm oscillations can occur for $t_m > 0$. The cavity-dumped profile represents a curious distortion of the equilibrium solution and is far from producing picosecond pulses. The latter stages of the cycle were almost unchanged when the dumping efficiency was increased to 99%. Although a large value of t_m was used to speed the computation, the steady

state profile for much smaller mismatch values is still a broad equilibrium profile.

8.5 Substantial Parameter Modifications

a) Short Cavity Feedback

In spite of the "degrees of freedom" that the pulse has through satellite structure, the evolutions studied so far have been strongly damped. As a pulse with several satellites evolves, the total energy, and therefore the gain extracted, oscillates slowly. What happens if this perturbation is fed back by incomplete gain relaxation during a round trip? Evolutions for cavities as short as $T_{1a}/10$ (fig.8.14) have proved completely stable for both positive and negative mismatches. The gain storage raises the effective pump power and the results for positive mismatch appear to agree with the iterated stepping model. As the storage time is increased and the gain modulation by the pump pulse itself is reduced, the satellite structure diminishes and the evolution becomes, if anything, faster and better damped. The stability seems to be maintained when the feedback comes from the pulse itself. For large mismatches and long storage times the intensity is well above the noise throughout local time and the strong signal before threshold reduces the gain modulation which allows the formation of the "giant pulse". (The whole cavity must then be modelled, not just the local time range of the pump. To be practicable, the characteristic times must then be distorted and are no longer appropriate to normal synchronously pumped dye systems but are closer to those of, for example, colour centre lasers).

The balance between pumping and depletion keeps the tail of a negatively mismatched pulse close to threshold. In a long cavity, however, relaxation eventually pulls the gain well below threshold. Numerical evolutions with an artificially short value of T_{1a} suggest that the pulse then just decays and the signal fed into the centre of the pulse is kept at a low level. Neither this nor the artificial fixing of the feed at a very low level are apparently sufficient to disturb the balance (although it should be noted that the mismatches in these tests were always very large).

b) Synchronous pump and loss modulation

The pulse stability has also been investigated with modifications to the

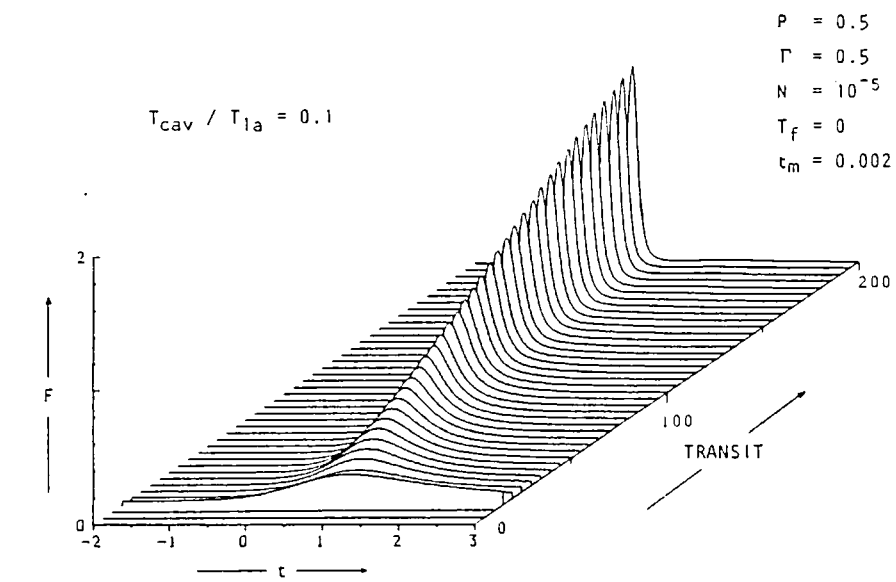


FIG. 8.14

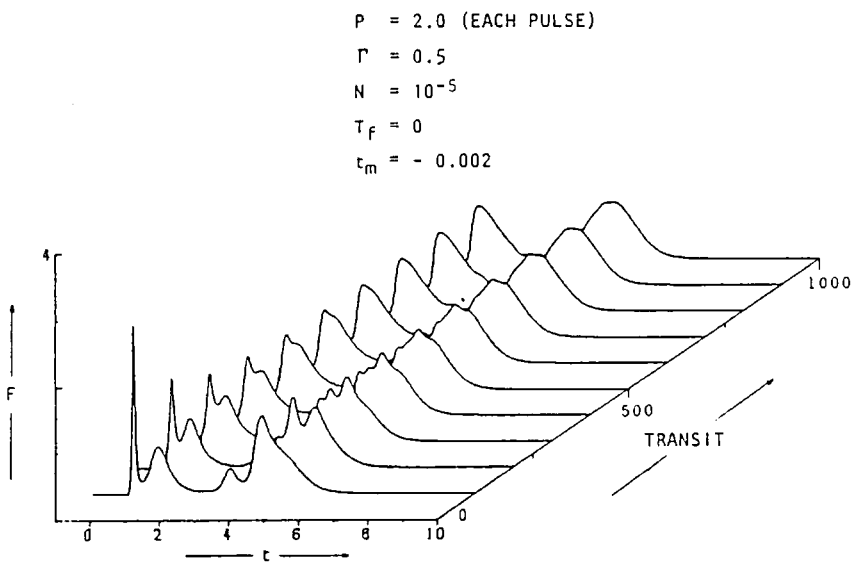


FIG. 8.15 : EVOLUTION WITH DOUBLE PUMP PULSE (CENTRES AT t=0&4)

pumping. The stepping model can be iterated successfully to incorporate the effect of a second pass through the residual gain. The conclusion that, with moderate gain relaxation, this just raises the pump power is borne out by the numerical evolutions (the pulse was assumed to be short compared to the delay and was therefore just fed back through the residual gain). A larger perturbation was provided by adding a second pump pulse a few t_p after the first. The pulses for both positive and negative mismatch appear to be stable and the stepping model can therefore be used for positive mismatch. An evolution for $t_m < 0$ is shown in fig.8.15. The incorporation of a synchronous loss modulation with the loss minimum located either ahead or after the peak of the pump also appeared to have little effect on a negatively mismatched pulse.

c) Extreme modulation: subharmonic oscillations

A pulse with satellites has several characteristic timescales – the combination of mismatch and inverse bandwidth which scales the satellite duration, the satellite spacing which is determined by the satellite energy and the pump rate and the long delay times T_{1a} and T_{cav}. Although this seems to offer the possibility of unstable interactions, the parameters of a typical synchronously pumped dye laser are orders of magnitude away from those yielding chaotic operation. The formation of well-modulated satellite bursts requires a sharp rise in the gain before the pulse. The attempt to perturb the equilibrium through strong gain storage tends to remove this and hence the satellites themselves.

To reach the regime of self-sustaining nonlinear oscillations the gain storage time must be increased substantially and the pumping reduced. The operation then becomes continuous with weak modulation by the synchronous pump. The required increase in T_{1a} is available from CW gas lasers with cavity dimensions comparable to the dye lasers considered so far. Experimental observations of subharmonic behaviour and erratic operation in a CO_2 laser have recently been presented by Arrecchi et al. [1]. The large ratio of T_1 to T_2 (0.4 ms to 0.01 μs) means that the single mode dynamics can again be reduced to a rate equation. The third degree of freedom neccessary for chaos was added by an electro-optic loss modulator. The interesting modulation frequencies for the CO_2 system were around 100 kHz and therefore easily accessible. Taking a simple view, the onset of erratic behaviour can be expected when the driving frequency is of the same order as the natural relaxation

oscillation frequency, the nonlinearity leading to more complicated response than simple resonance and distortion. Following [1], we now modify the dye laser parameters substantially, retaining the synchronous pump and noise injection but shortening the cavity and reducing P, greatly increasing T_{1a} and increasing the depth of the slow loss modulation (the travelling wave assumption is retained).

Normalising to the round trip time, the coupled equations are

$$\dot{E} = E\,(A - \Gamma - \Gamma_{mod}(t)) \qquad (8.1)$$

$$\dot{A} = P\Gamma - E\,A - A/T_{1a} \qquad (8.2)$$

where the energy, E, of the system is characterised by $F \times T_{cav}$. The linearised frequency is

$$\Omega_0 = \frac{1}{2}\sqrt{\frac{P^2}{\Gamma^2} - 4(P - \Gamma/T_{1a})} \qquad (8.3)$$

Figs. 8.16a–e show the evolution for $T_{1a}=2000$, $P=.03$, $\Gamma=0.5$ (again with a noise term of 10^{-5}). The undriven relaxation oscillation is shown in (a). In (b) the modulation (±50% of the linear loss) is too fast and simply perturbs the output with the natural oscillation still visible. Reducing the frequency (c) results in "capture" with stable output modulation at half the drive frequency. Halving the frequency again gives deep modulation at the fundamental period (d). The oscillation stays at the fundamental when the period is doubled again (e). The type of oscillation is very sensitive to the pump power, sometimes showing transient subharmonic oscillation (a slow transition from the type in (c) to that in (d). The onset of erratic behaviour is shown in figs. 8.17a–f, where the parameters have been further modified ($P=.01$, $T_{1a}=8000$). Fig. 8.17a shows strong subharmonic spiking but when the modulator frequency is increased the motion suddenly becomes more complicated – the output periodicity is greatly increased if not infinite. The system is now much more sensitive and a change of 2% in the drive frequency produces significantly different results. The frequency differs by only 0.2% in fig. 8.17d (although the noise level has been reduced). The phase portrait, $[E_{i+1} - E_i]$ v E_i, is shown in (e). Fig. 8.17f shows the restoration of periodic spiking by adding a slow (T_{cav}, $T_{mod} \ll T_{1b} \ll T_{1a}$) saturable absorber.

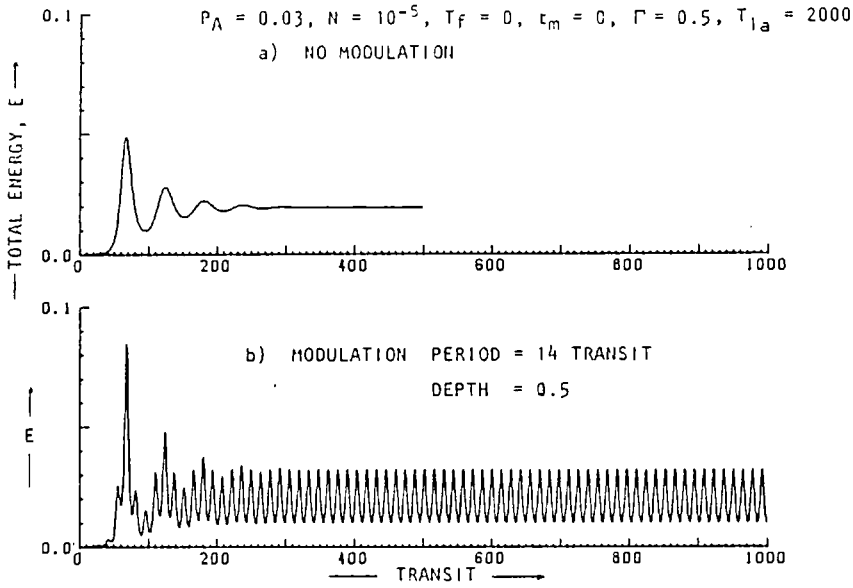


FIG. 8.16

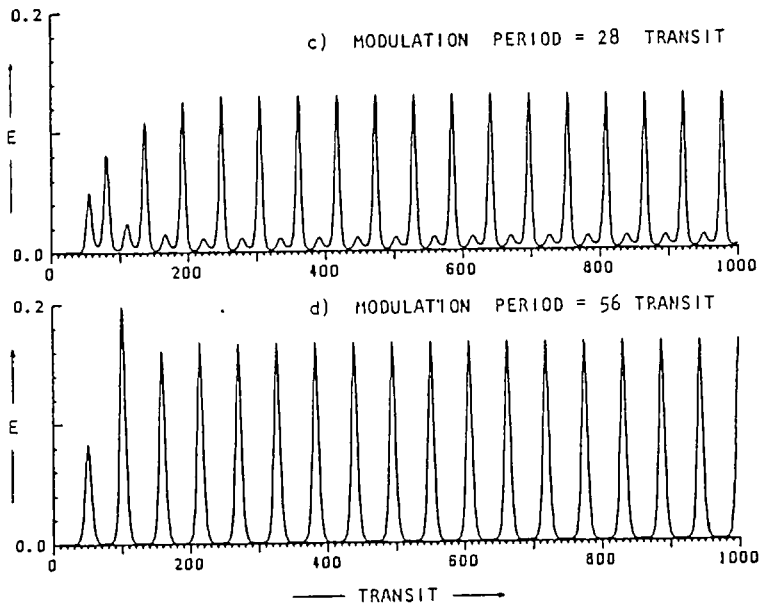


FIG. 8.16

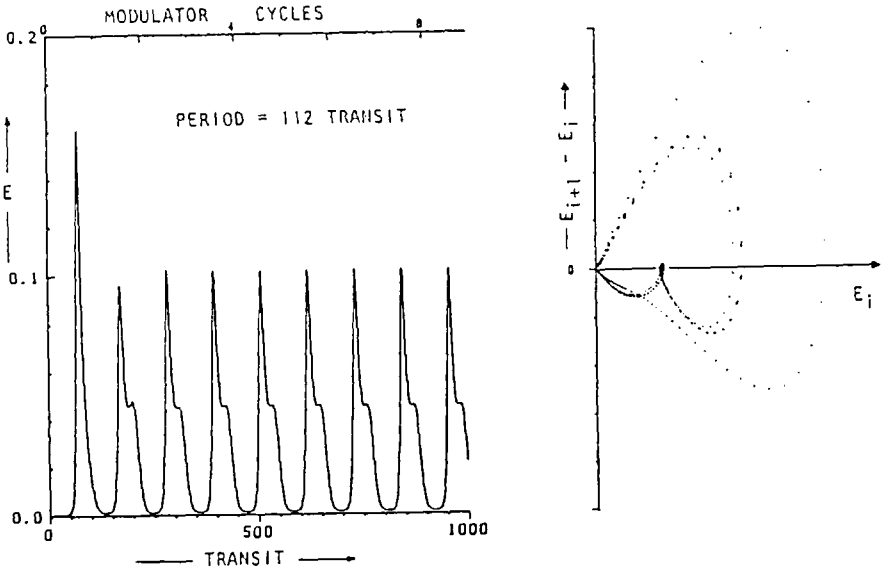


FIG. 8.16e

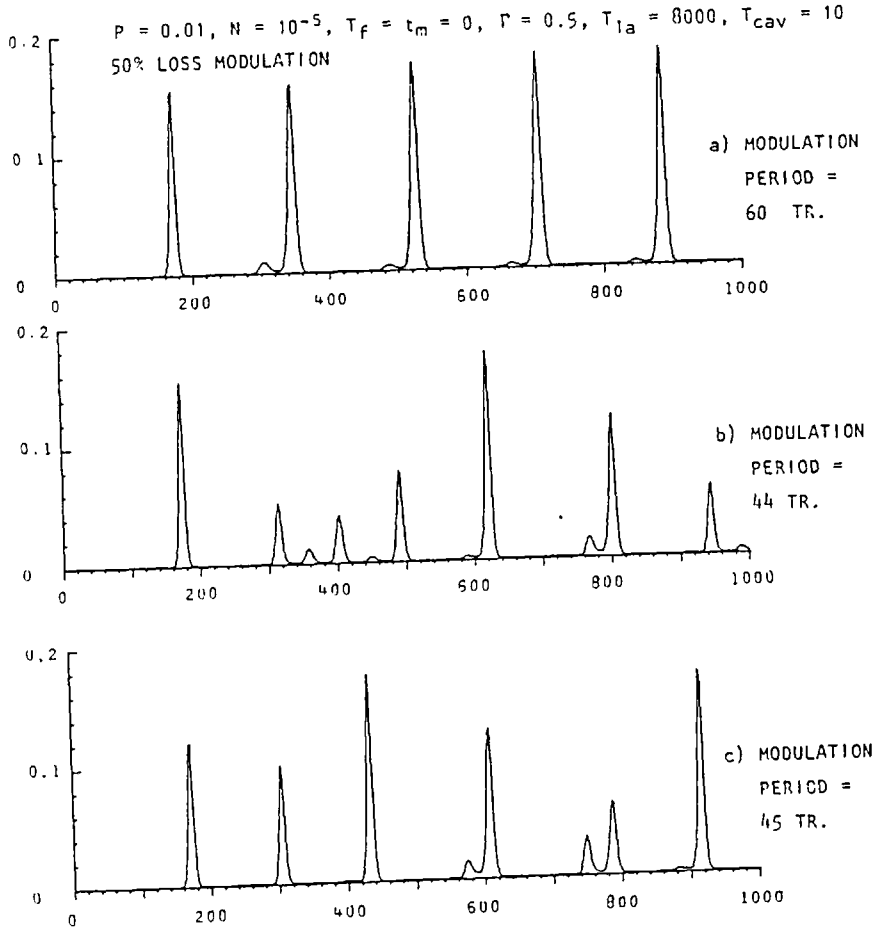


FIG. 8.17 a-c

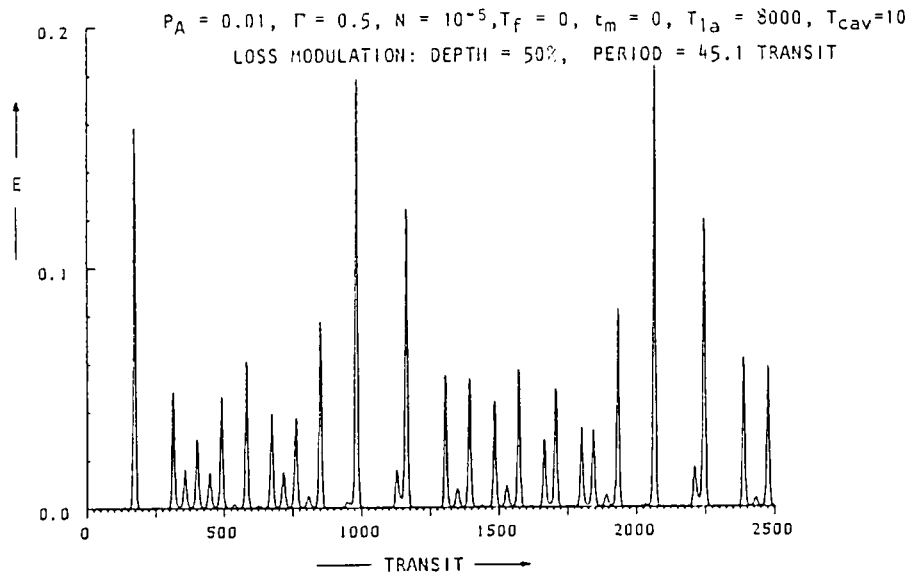


FIG. 8.17d

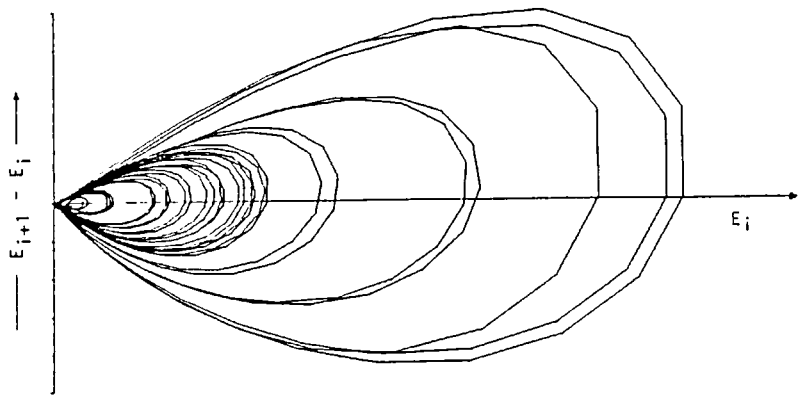


FIG. 8.17e

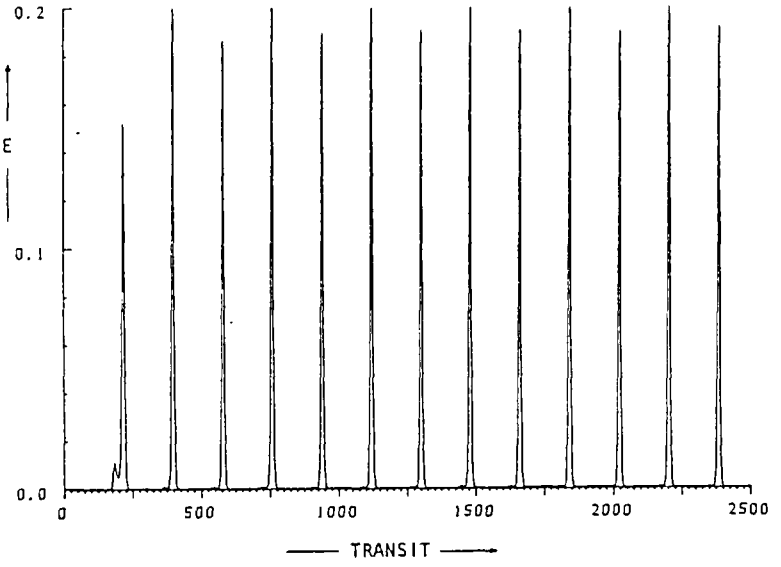


FIG. 8.17f : ADDITION OF ABSORBER (P_B = 0.6, T_{1b} = 800)

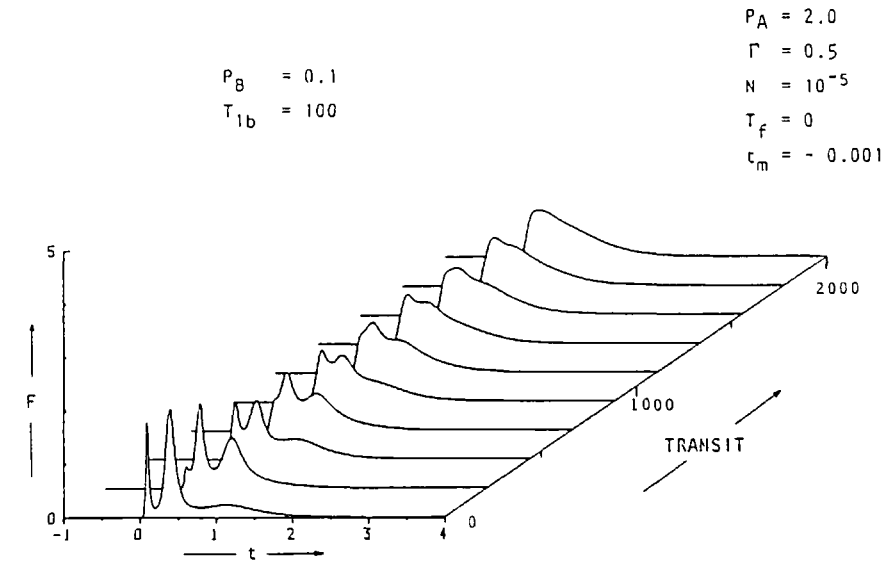


FIG. 8.18a

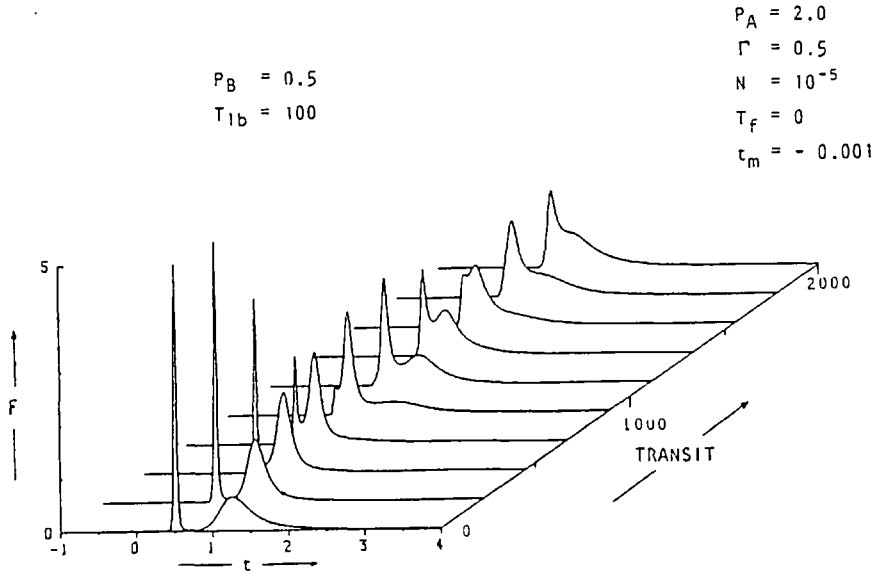


FIG. 8.18b

8.6 Hybrid Modelocking and Self-pulsation

a) Transition to negative mismatch

The hybrid stepping model appears unable to explain the improvement in performance claimed for addition of small amounts of absorber. Although the absorber does delay threshold, the effect is only significant when the amount of absorber is itself significant and the result is often a drop in the pulse intensity without any compression, particularly if the saturation is not enhanced by telescoping. It is also difficult to see why a pulse in this regime should be stabilised by the absorber. Under the conditions of the stepping model, with gain on the leading edge, the pulse is not in the strong compression regime of passive modelocking. Does the absorber have a different effect when negative mismatch forces the pulse to arrive before threshold?

Figs.8.18a&b show the effect of weak and moderate "slow" absorbers on negatively mismatched pulse evolution. The spike in (b) suggests that transient passive compression occurs, but the short pulse is not stable and the final result is again the equilibrium solution (neither evolution has fully converged). The gain in the tail is just below unity and, although the leading edge has been delayed and sharpened slightly, the main effect is a reduction of the pulse energy.

The results in chs.4 & 5 suggest that for $|t_m| < T_f$ the pulse profile is largely governed by T_f and that a small mismatch can be viewed as a perturbation on T_f. In view of this, the consistently reported mismatch tolerances - as small as 0.5μ in one case - are difficult to understand. Even if the figure represents a just detectable change in the autocorrelation, it is very small since 1μ = 3 fs and 1 optical cycle = 2 fs. For a bandwidth of 100 nm, $\frac{1}{\Delta\omega} >$ 10 fs and the tolerance has been reported for pulses which are much longer. The results in ch.6 show that the final collapse of the pulse occurs for mismatches between about $-3/4\,T_f$ and $-T_f$: i.e. just beyond the point where the matrix solution fails and there is no longer gain on the leading edge of the pulse. It is just at this point that the mismatch best compensates for the dispersion of the filter: increasing the mismatch from 0 to $-T_f/2$ has little effect on the pulsewidth, although satellites may increase, but should reduce the spreading of noise structure through the pulse which will take place at t_m=0.

This leads to a picture of the "best modelocked" pulse delicately balanced

at a mismatch perhaps $T_f/5$ from complete collapse, with the reduced gain saturation compensated by the large mismatch. Does the absorber now become more effective? Fig.8.19a(i)&(ii) shows the effect of adding a small amount of absorber (4%). Although the pumping is weaker than that in ch.5, a satellite pulse still forms as the collapse begins (curve (i)). Adding the absorber with a saturation factor of $S = 2$ (a(ii)) just delays threshold and reduces the energy. The width of the main pulse is hardly affected.

The preferential saturation of the absorber alone is apparently not enough to compress the equilibrium solution for $t_m < 0$ or to destabilise it. The absorber introduces a further degree of freedom, however - the recovery time T_{1b}. While this does not have much effect on many of the stepping model solutions, it actually determines the pulse duration in "slow absorber" modelocking. When the mismatch is such that the pulse is beginning to collapse, the gain depletion by the pulse is close to equilibrium with the pumping. Under these conditions even a small amount of extra loss, arising from fast absorber recovery, can bring the tail of the pulse well below threshold. Fig.8.19a(iii) shows the depression of the satellite which occurs when T_{1b} is reduced to $t_p/5$. The recovery is slow enough for the main pulse to be unaffected. Without the absorber, the pulse still arrives after the ideal threshold time ($\theta = 0.6841$), and the absorber, while increasing the loss on the front of the pulse, does not bring the pulse into the regime of strong passive modelocking where a large leading edge loss is important for pulse compression. A small increase in t_m still brings the pulse over the transition point and the profile collapses (fig.8.19b). A large value of T_f has been used so far giving pulse widths of approximately $t_p/10$. Fig.8.20 shows the result of halving both t_m and T_f, keeping the absorber parameters fixed. The pulse duration halves but the recovery is insufficient to control the satellite.

We have already remarked that the dispersion of noise "information" should be at a minimum under these circumstances. It follows, then, that the profile shoud be insensitive to the size of the noise feed. Fig.8.21 suggests that this is so. Once the value of N is small enough for the noise dominated part of the signal to be well below the saturation flux, the profile is little affected by the magnitude (although these evolutions were well converged, they should be treated with caution. The feed values in the tail of the pulse were allowed to "float" - i.e. the values in the tail were fed in. The plots show the full extent of the profile in the evolution and the feed values were therefore substantial).

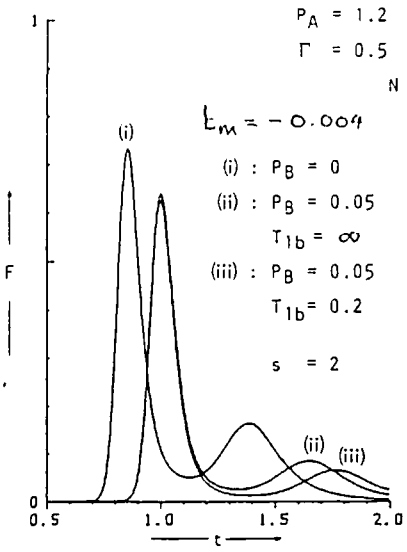


FIG. 8.19a

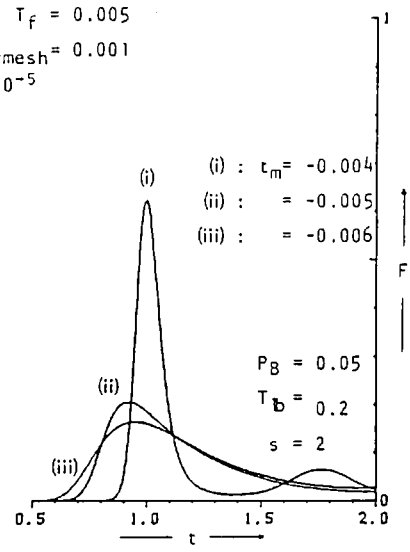


FIG. 8.19b

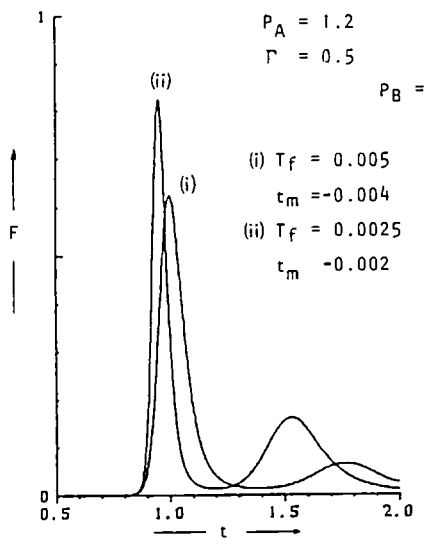


FIG. 8.20

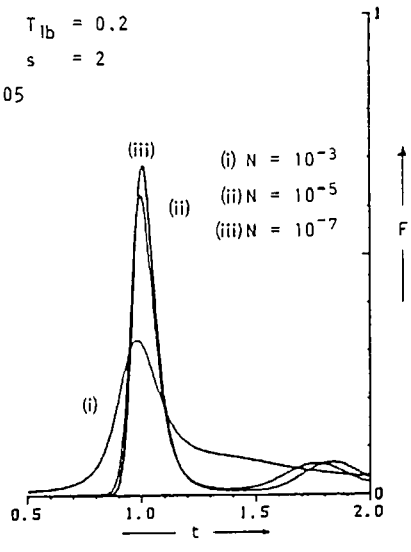


FIG. 8.21

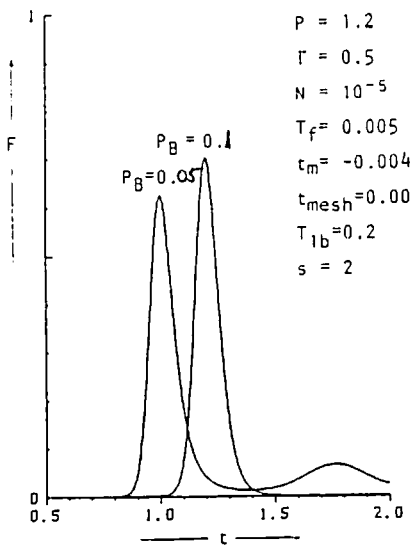


FIG. 8.22

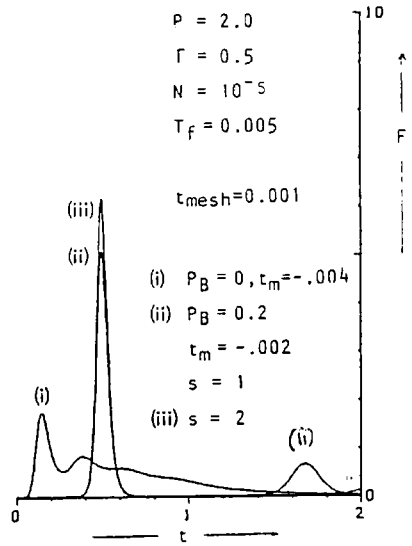


FIG. 8.23

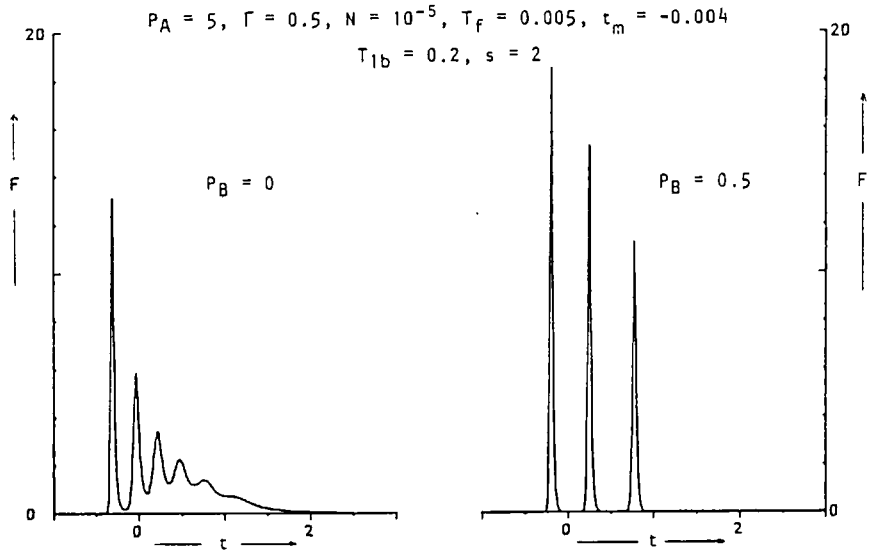


FIG. 8.24a

FIG. 8.24b

When P_B=0.05 the absorber offsets 25% of the net gain and the effect on the pulse is small. Doubling the absorber level (fig.8.22) brings a substantial improvement. It was remarked above that even at low pump power satellites were present when the pulse was close to collapse. At higher pumping the pulse is closer to collapse for the same values of t_m and T_f, and absorber level of P_B = 0.05 has even less effect (fig.8.23(i)). Reducing the mismatch slightly and raising the absorber level to 10% again brings a substantial improvement (fig.8.23ii&iii). In most experimental reports of hybrid modelocking, the absorber is added to the amplifier jet stream and therefore cannot benefit from the enhanced saturation achieved by telescoping in typical passively modelocked systems. Fig.8.23 also shows that the action of the absorber under these circumstances does not need the saturation enhancement, although it benefits from it.

At very high pump power and a mismatch of -.004 the profile is an enhanced relaxation oscillation (fig.8.24a) which the fast absorber, at a level of 10%, further enhances, giving the intense satellites in fig.8.24b.

b) Negative mismatch and self-pulsation

We now return to the speculation of ch.5: is the profile stable for large negative mismatches? The evolutions in that chapter suggested that for a wide range of parameters the steady state is stable and takes the form of an over-damped relaxation oscillation once t_m exceeds $-T_f$. Beyond the transition point the pulse arrives before threshold and the resulting reduction of the gain modulation raises the tail of the pulse and completely removes any modulations in the profile. The introduction of a slow absorber of moderate strength appears not to disturb the balance between tbe signal and the pump. With the extra degree of freedom introduced with T_{1b} the picture is altered and in fig.8.24b the equilibrium has clearly been broken. The profile remains stationary because the filter still just balances the mismatch.

Figs.8.25a-h show the onset of instability as the concentration of "fast" absorber is increased for mismatches beyond the transition point. At low levels the evolution to the equilibrium solution is just perturbed (fig.8.25a) but at a threshold absorber level a self-sustaining oscillation starts (b),(c). The threshold appears to depend on both the noise level and the absorber lifetime. As the absorber level is increased the operation moves towards passive mode-locking and the constraint on T_{1b} weakens. Fig.8.25g shows the stability of

$P_A = 2.0$	$T_f = 0$	$T_{1a} = 1.0$
$\Gamma = 0.5$	$t_m = -0.01$	$T_{1b} = 0.2$
$N = 10^{-5}$	$s = 2$	$T_{cav}/T_{1a} = 1.0$
		$T_{cav}/T_{1b} = 1000$

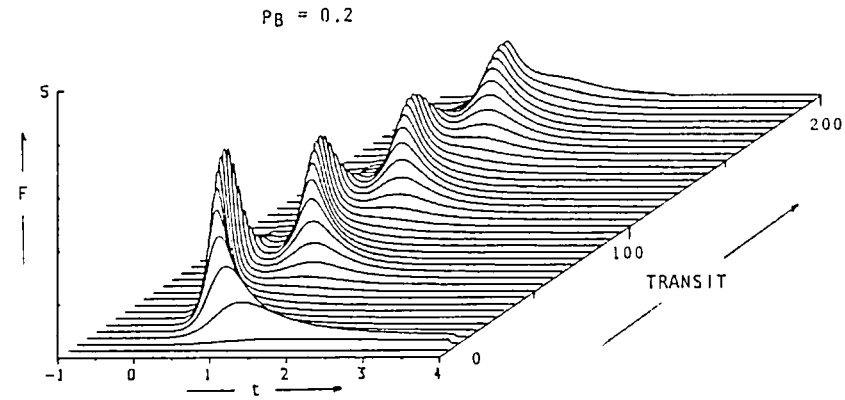


FIG. 8.25a

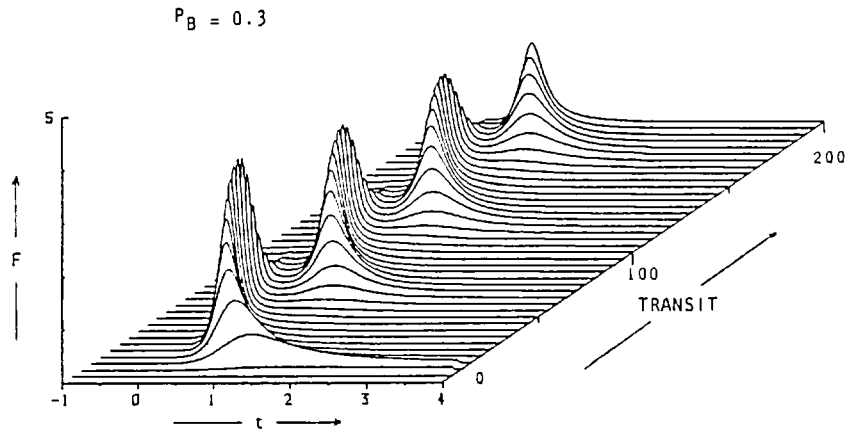


FIG 8.25b

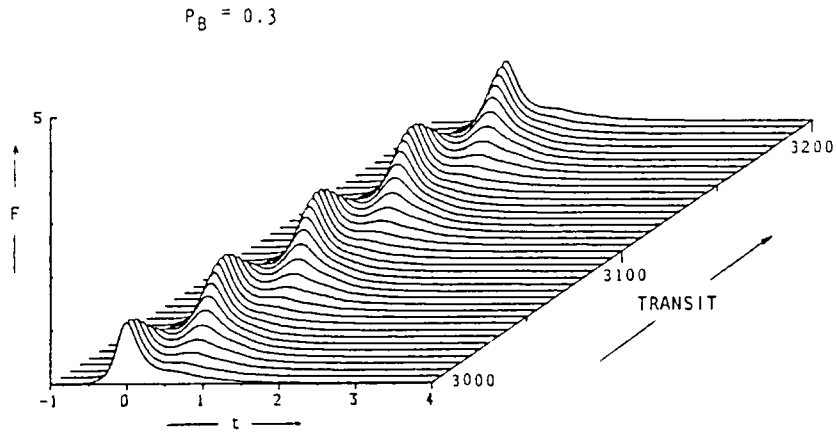


FIG. 8.25c

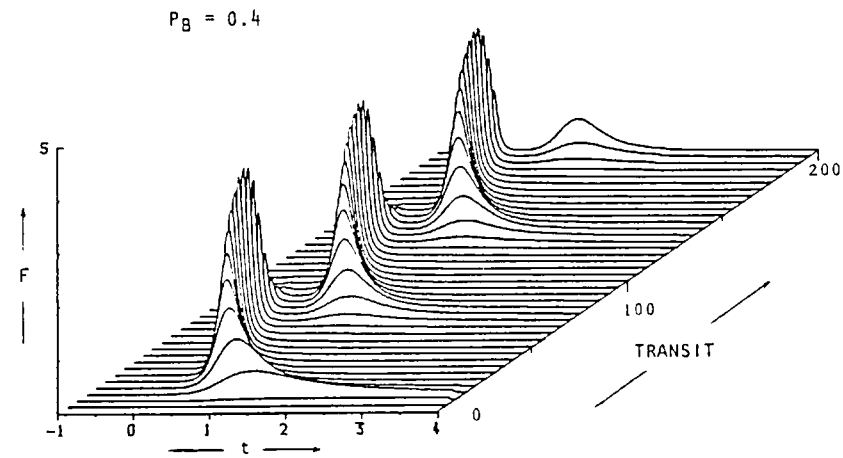


FIG. 8.25d

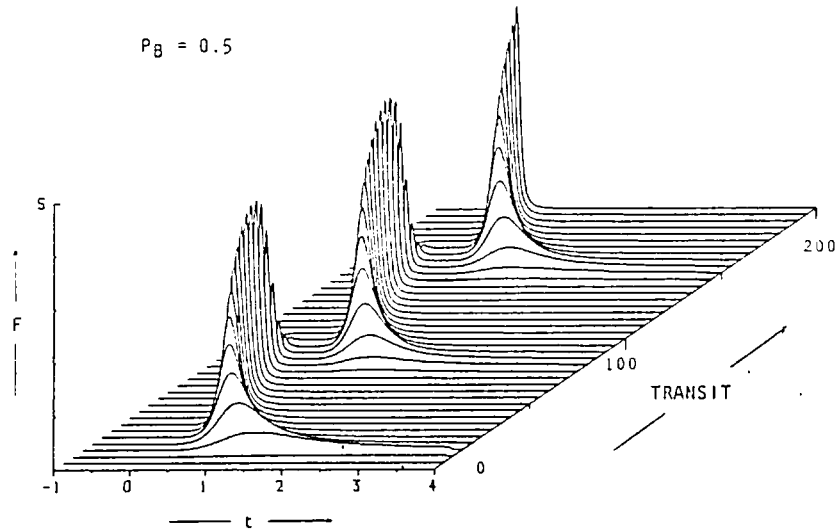


FIG. 8.25e

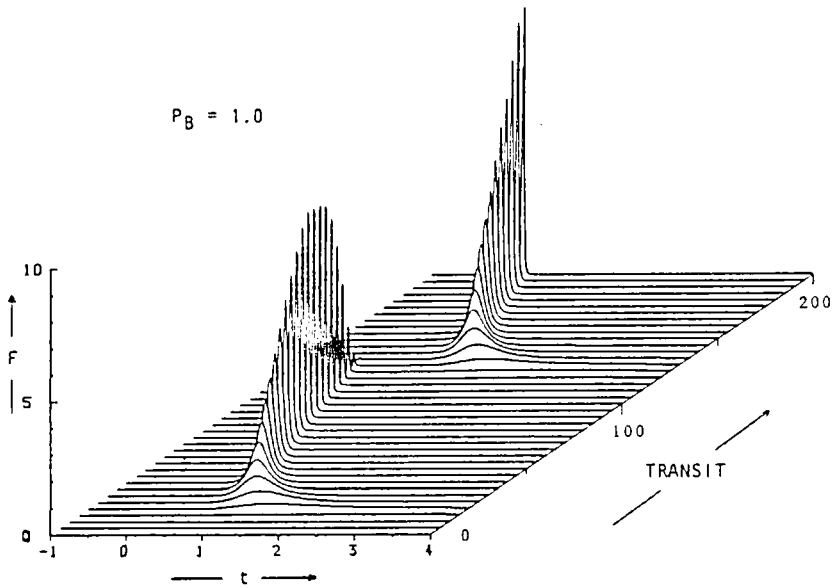


FIG. 8.25f

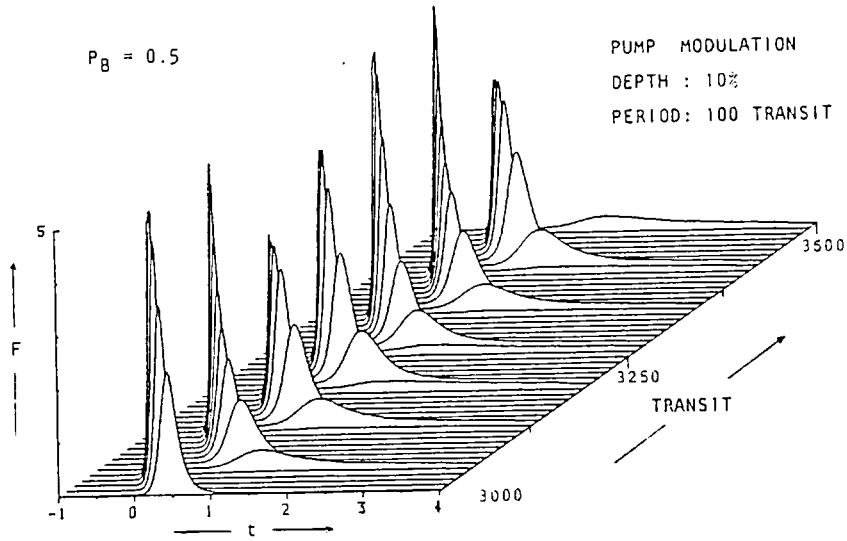


FIG. 8.25g

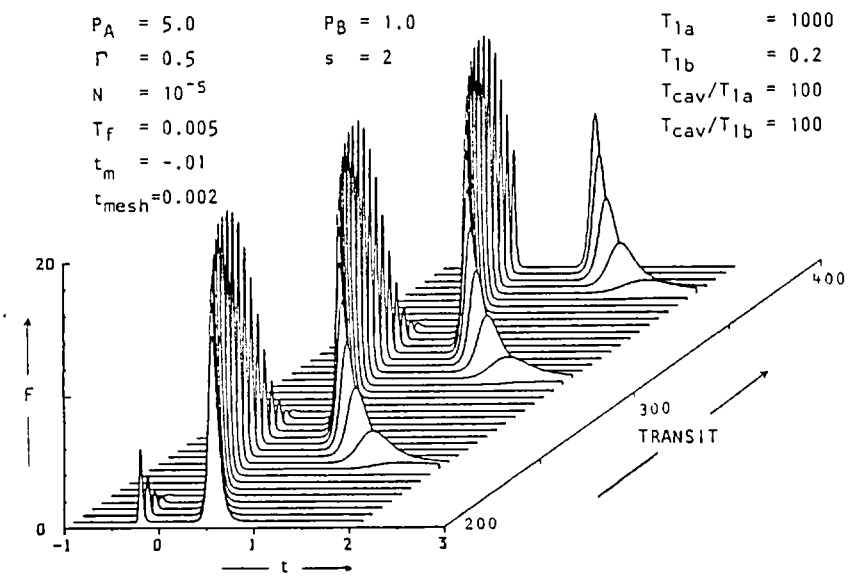


FIG. 8.25h

the pulsation in the presence of pump power modulation. To further perturb the evolution, and for comparison with the result of the next section, the amplifier recovery is incomplete ($T_{cav}=T_{1a}$). To reduce the computation, the filter was absent from (a)-(g) but its restoration does not effect the pulsation (fig.8.25h). Preliminary results suggest that at high pump powers a "revolving" burst of satellites, like the stationary profile in fig.8.24b, can be sustained.

c) Strong hybrid and positive mismatch

The pulsation described above occurs when strong absorption "gates" the tail of the pulse while the large mismatch advances the pulse relative to the pump. What happens when the mismatch is of opposite sign? As the absorber level is increased in a long cavity, the stepping algorithm solution appears later and later in the pump until the absorption is high enough to prevent the system exceeding threshold ($P_B > P_A - 1$). In a continuously pumped, passively modelocked laser, CW operation is unstable for certain combinations of the main parameters (characteristic times, cross-sections etc). In the "static compression" regime, a strong absorber causes net loss on the leading edge of the pulse while incomplete recovery of the depleted amplifier ensures that there is also loss on the tail. The net gain is only greater than unity near the peak of the pulse. By choosing appropriate pump and absorber levels and fixing $T_{cav} \simeq T_{1a}$, $T_{1b} \ll T_{cav}$, the gain only rises above the unsaturated loss as lasing begins. Once the pulse is intense enough to saturate the gain, partial amplifier recovery combined with full absorber recovery ensures that there is loss on the leading edge.

The inclusion of the etalon filter and background noise term of the present work, which were not present in New's study, do not affect the most important conclusion (v.i. ch.9). Because the pulse is very much shorter than the recovery rates of both the amplifier and absorber, it is not sensitive to the way in which the two parameters recover, only to the values after a delay of one round trip. It is likely, therefore, that the main principle can be carried over to strong hybrid modelocking. There are two important differences, however. First, a short cavity length leads to incomplete amplifier recovery under continuous pumping but the storage increases the gain under impulsive pumping. Second, the passively modelocked pulse determines its own velocity in the cavity but in a synchronously pumped system a steady state pulse must be locked to the

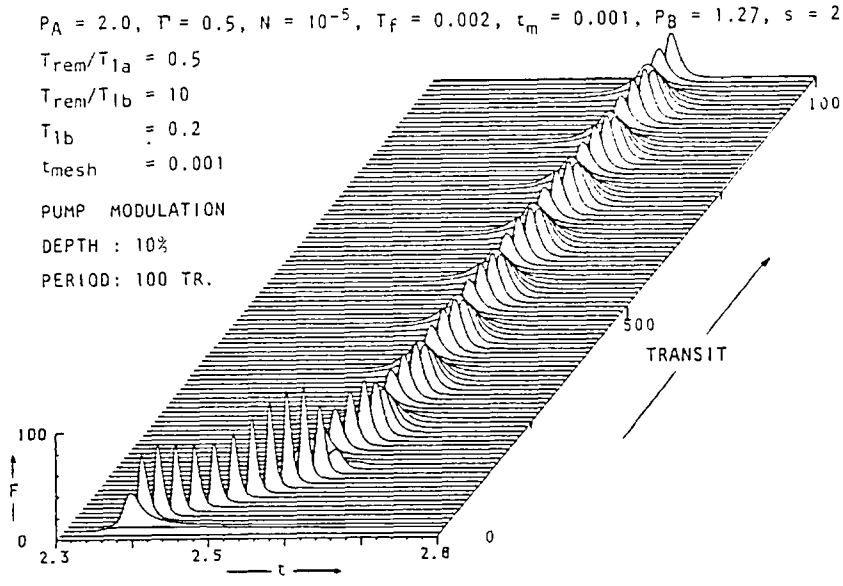


FIG. 8.26a

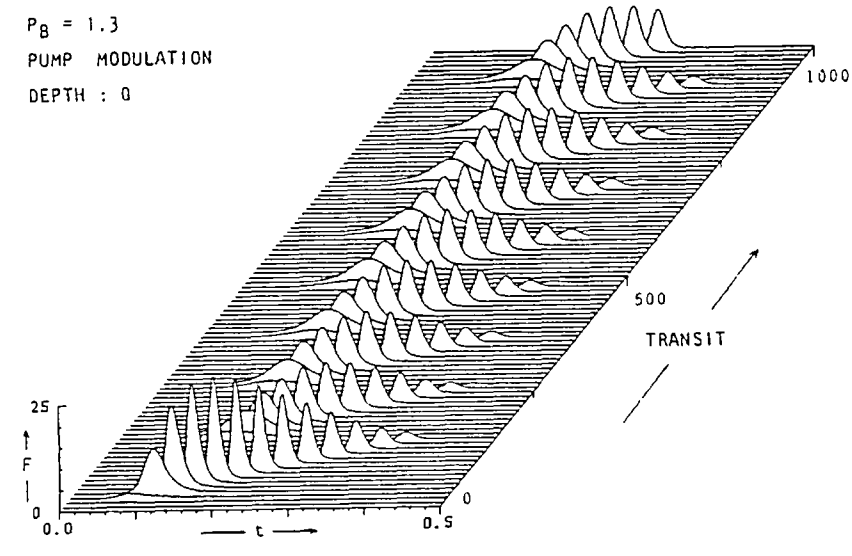


FIG. 8.26b

pump frequency. A pulse sustained under the conditions described above must be moving backwards in local time since both the absorption and the filter remove energy from the front of the pulse (the necessary "gain" on the tail comes only from the energy released by the filter). What happens if these conditions are maintained in a synchronously pumped cavity with positive mismatch so that the pulse is further retarded?

Fig.8.26a shows the pulse evolution in a positively mismatched system with finite amplifier relaxation, pump modulation and an absorber level just below the passive threshold. The intense pulse stabilises at the end of the pump and responds stably to the fairly rapid modulation. A small increase in P_B takes the system into "strong" passive modelocking. Fig.8.26b shows that the operation does indeed show the characteristics of "static compression". The pulse forms very rapidly, reaches a minimum duration determined only by the filter, and starts to move backwards in local time, arriving later and later after the pump. As it drifts backwards relaxation slowly reduces the gain remaining when it arrives. With $T_{cav}=T_{1a}$, the gain relaxation during a cavity transit, although not complete, is substantial. For a long time the falling gain reduces the pulse energy without altering the drift rate. The fall in energy reduces the gain depletion, however, and the gain at the end of the pump pulse comes closer to threshold on each transit. As the gain exceeds threshold a new pulse forms rapidly at the end of the pump and the old pulse dies away as the gain at that point is reduced. The cycling is completely stable – the pulse cannot become balanced half way down the gain decay. The absorber recovery between the two pulses is not neccessary – in contrast to the effect shown above for $t_m<0$, the instability is not caused by absorber "gating". The recovery of the absorber within the range of the collapse merely hastens the transition (it must of course recover during the rest of the round trip).

The deep modulation of the energy and second harmonic is shown in fig.8.26c. Reducing the mismatch to zero increases the period of the oscillation: note that it is the decay time of the pulse, not the reformation time, which is extended. Figs.26d & e show the response of the oscillation to a 10% pump power modulation at frequencies close to the first and second harmonics of the natural frequency. The energy variation (figs.26f & g) show that the oscillation locks to slow perturbations. In fig.8.27 the parameters have been altered to slow the natural oscillation and the 10% variation just perturbs the energy without apparently pulling the frequency. If the filter is

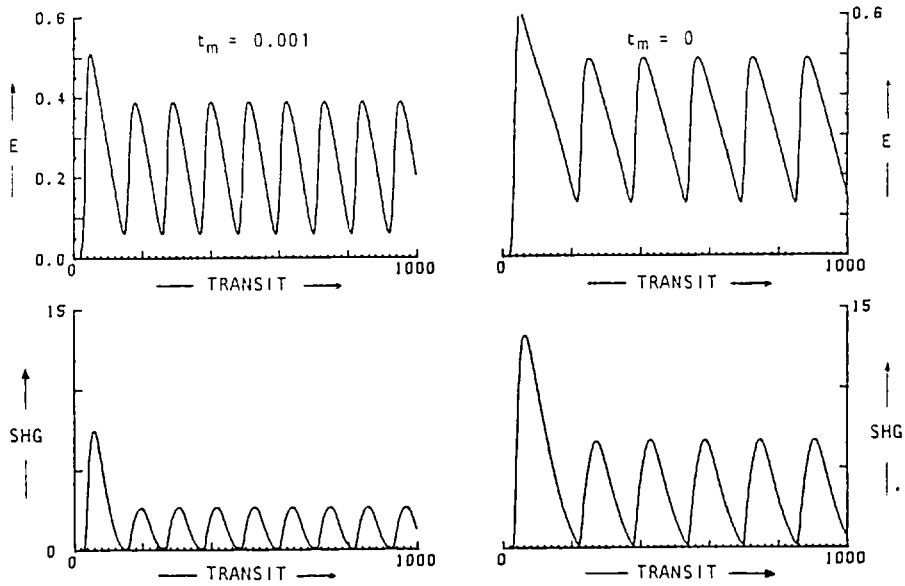


FIG. 8.26c

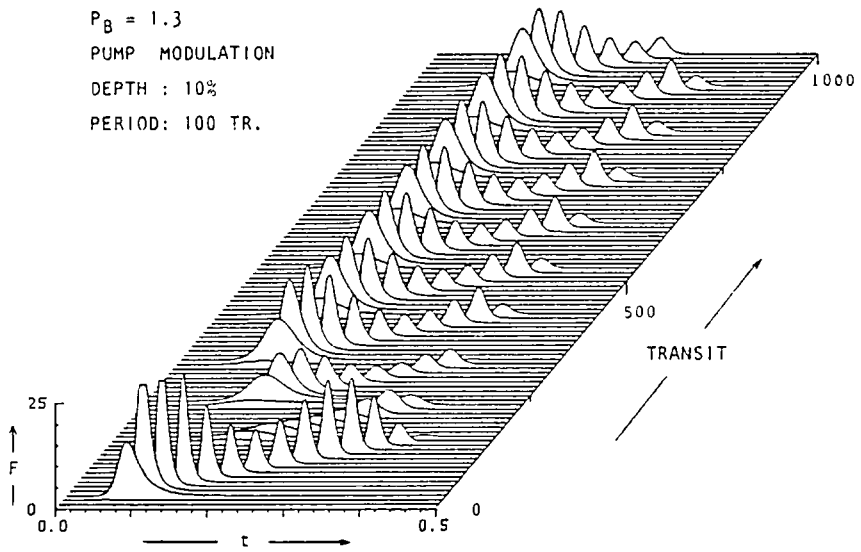


FIG. 8.26d

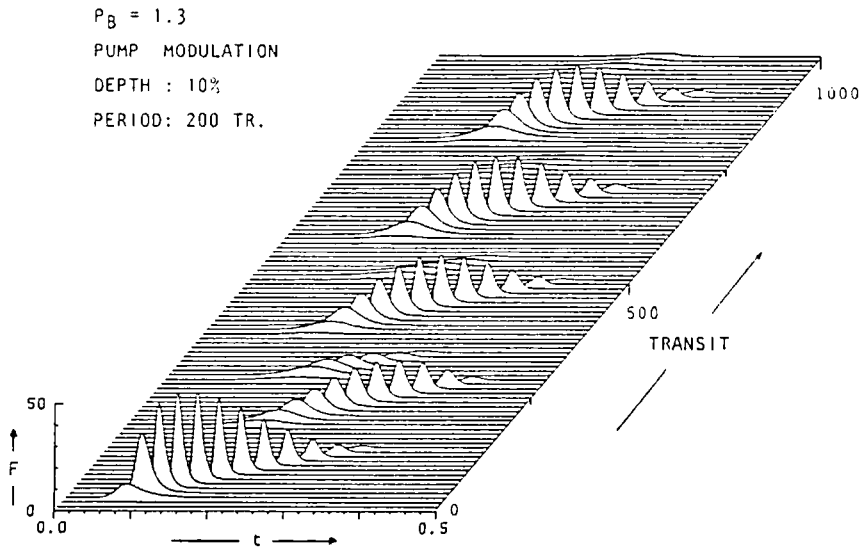


FIG. 8.26e

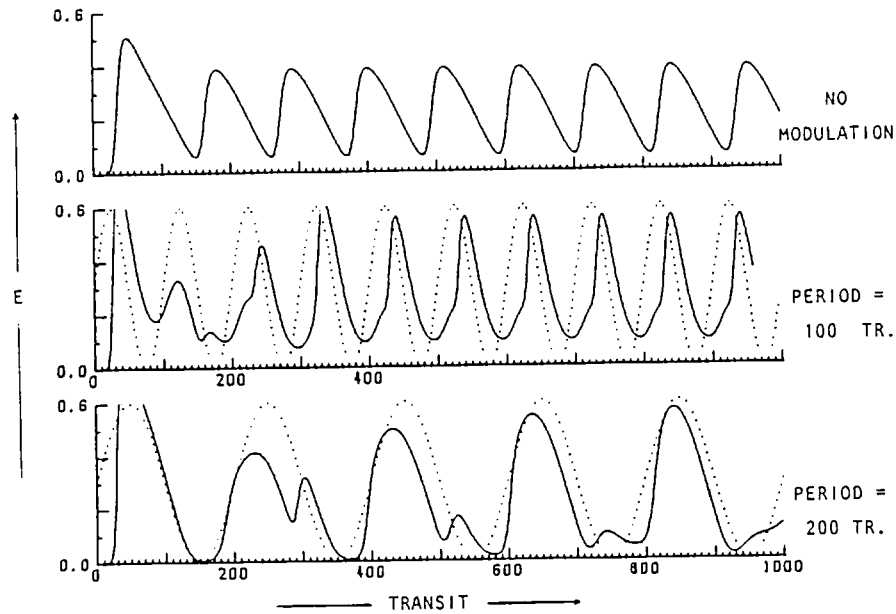


FIG. 8.26f

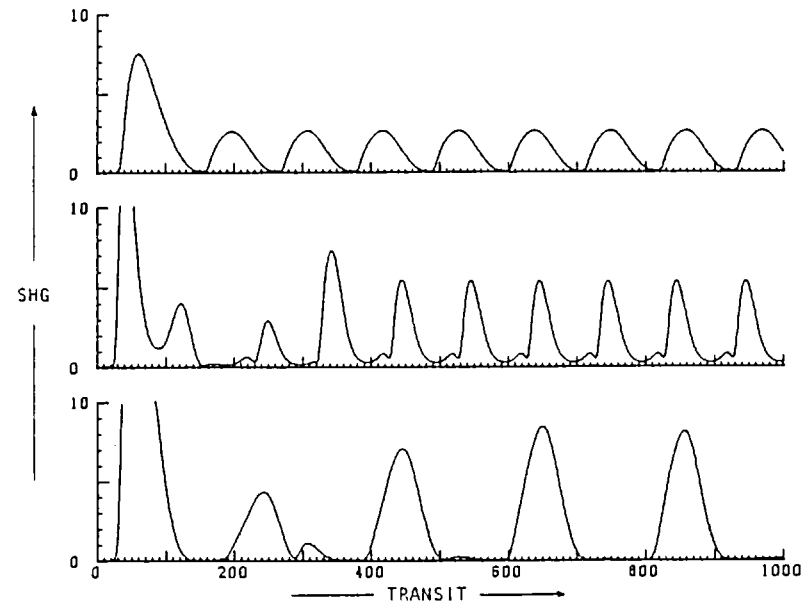


FIG. 8.26g

removed from the model, the pulse compresses indefinitely. (The evolution of a gaussian noise burst under these conditions is shown in the next section.)

This asynchronous hybrid modelocking (which does not seem to have been noted before) offers an elegant way of investigating cavity mismatch, quite different from the difficult autocorrelation studies of McDonald et al. [2]. The shift per transit due to the pulse reshaping must be less than the width of the pulse (the results in ch.9 suggest typically 20%). If pulses with durations less than 100 fs are produced the intrinsic drift rate will be very small, and by adding the cavity mismatch to this the cycle period can be adjusted at will. The microscopic drift cannot be measured easily, of course, but, through the energy variation, the cycling can. The reformation of the pulse may take several hundred transits under real conditions but the cycle period, limited ultimately only by the cavity stability, may be orders of magnitude longer. The pulse will therefore appear to be well modelocked. The reproducibility of the cycle will depend on where the pulse reforms each time, but if this is always close to the pump then the regular self-starting of modelocking, at a rate which is slow for detectors such as streak cameras, could provide a novel way of studying the onset of modelocking. This self-excitation at a rate given, roughly speaking, by the ratio of the largest and smallest times in the system appears to be unlike anything previously associated with modelocked dye lasers. In contrast to some of the results presented earlier, the effect should depend little on the detailed physics of the model.

The stepping model is clearly inappropriate to this regime: it is not a steady state and, as will be shown in ch.9, even if the intrinsic drift rate were known, the stepping approach cannot be used to predict the pulse itself. The hybrid stepping profiles in ch.7 showed significant pulse compression (above threshold power and loss levels) up to very high absorber concentrations. Finite gain relaxation increases the effective pump power and allows the absorber level to be increased to give still more pulse compression. For moderate increases of this kind, the stepping iteration converges readily to give the profiles in fig.8.28. Above a critical absorber level (between $P_B = 1.2$ & 1.22 in this case) the operation changes to the strong passive modelocking seen above, with loss on the leading edge of the pulse. There is now no synchronous steady state and the iteration of the stepping algorithm no longer converges, changing suddenly to a limit cycle. As usual, the stepping profiles are evaluated in the region of the pump but the local time range of

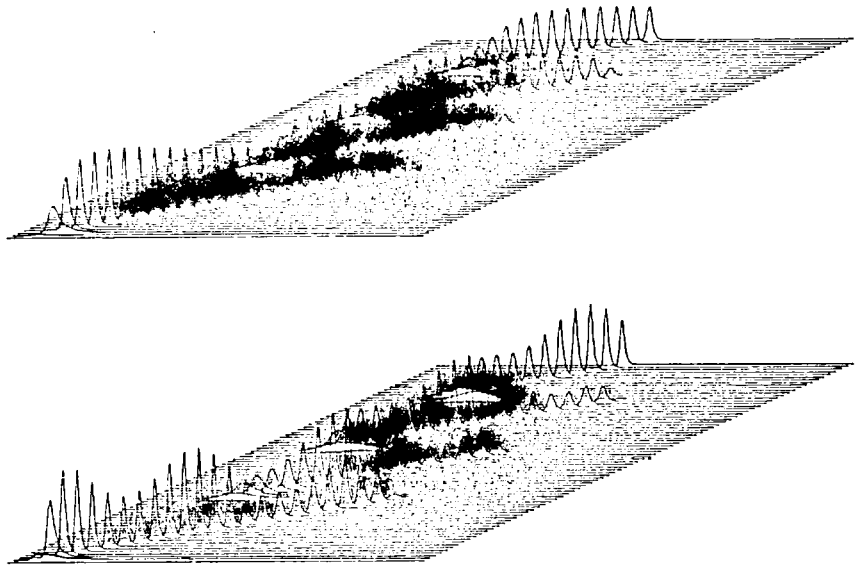


FIG. 8.27

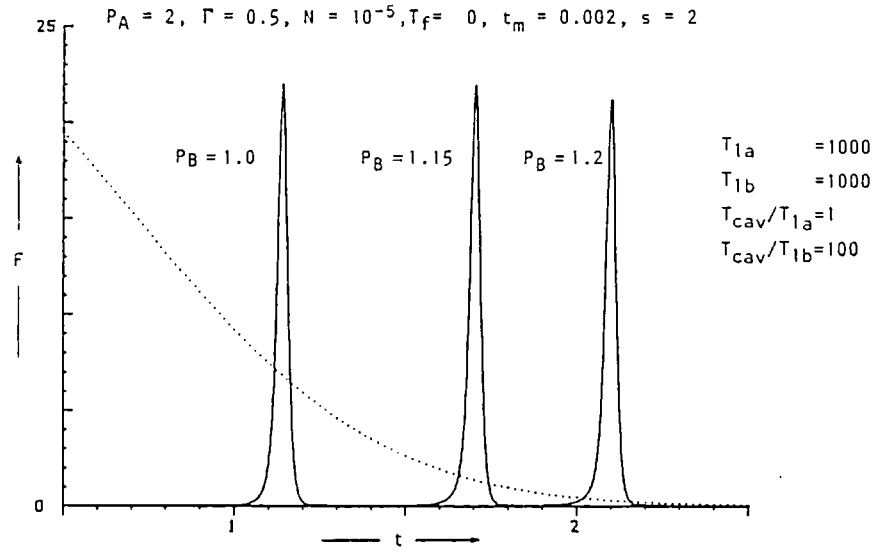


FIG. 8.28

each iteration must be long enough to ensure that the gain at each end of the range is below threshold. For these parameter values at least, the limit cycle stabilises very quickly - in less than 10 iterations - and does not seem to be affected by the initial value of the gain (the gain does not rise above threshold on the first iteration and can be given an arbitrary head start). The period of the cycle does depend on the parameters values but all the values used so far have yielded simple, single period, cycles.

8.6 Noise burst evolution

The constant noise addition term is probably the worst approximation of this rate equation treatment, particularly when a narrow band filter is included. A reasonable simulation of the evolution from noise, even in the rate equation approximation, requires a substantial increase in computation. Accurate integration requires that there be several mesh steps across the fastest fluctuation, while continuous noise injection probably needs complex amplitude treatment. A simulation with realistic values for the different characteristic times would need tens or even hundreds of thousands of mesh points. To reduce the problem, we remove both the filter and the noise injection and investigate only the stability of the evolution in the presence of continuous intensity fluctuations from a noise feed.

The evolutions were started from a noise burst, and (for $t_m \neq 0$) further noise values were fed in at one end of the profile. The initial gaussian noise burst was created by fourier synthesis, the spectrum having a gaussian amplitude distribution with random phases. (The spectrum was normally defined for positive freqencies only, up to 1.5 x the width and sufficient equally spaced harmonics were taken to make the initial burst non-periodic. The problem of generating fresh noise values for the mismatched feed was avoided simply by using the initial burst as a source and restarting from a random location in the array when the end was reached).

The noise burst and its simple autocorrelation are shown in figs. 8.29a&b. The triangular envelope in (b) is the correlation of the square envelope of the burst itself. The "contrast ratio" between the peak of the autocorrelation and the maximum value of the envelope is too large and shows that the sampling rate is too low for the autocorrelations to be accurate. Figs. 8.30a&b show the evolution for positive mismatch under the strong pumping conditions used previously. Although the profile fluctuates wildly, the average distribution of

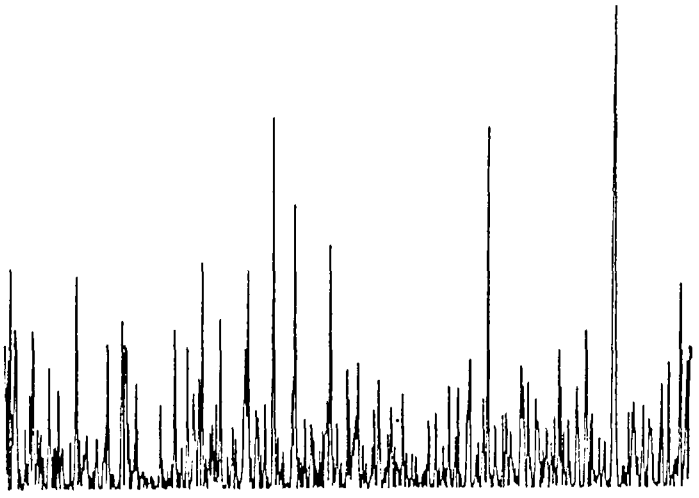


FIG. 8.29a

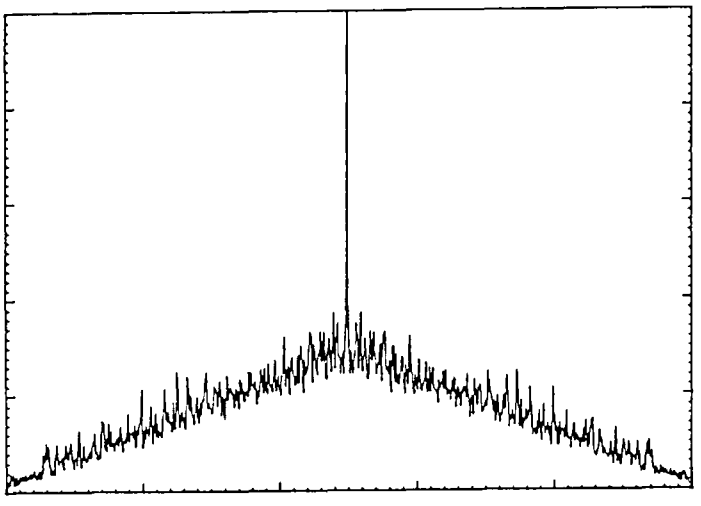


FIG. 8.29b

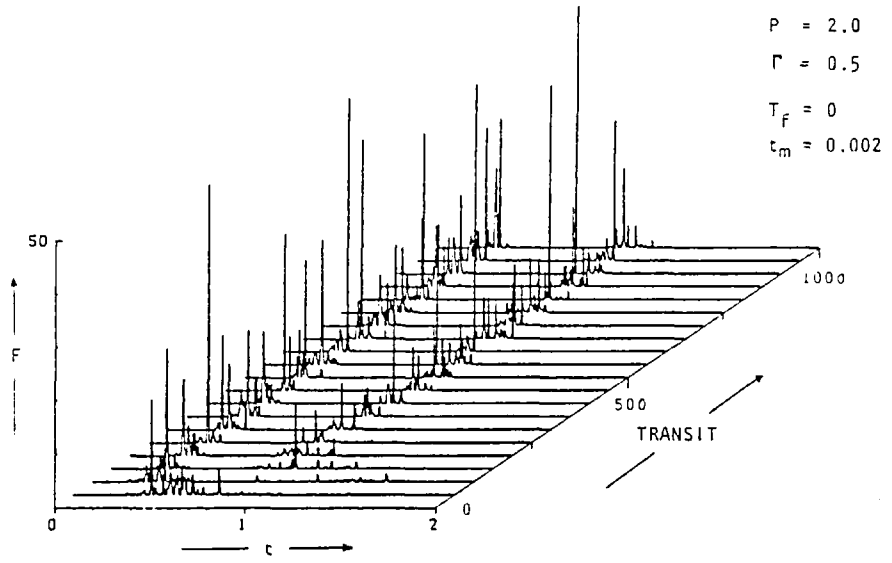


FIG. 8.30a

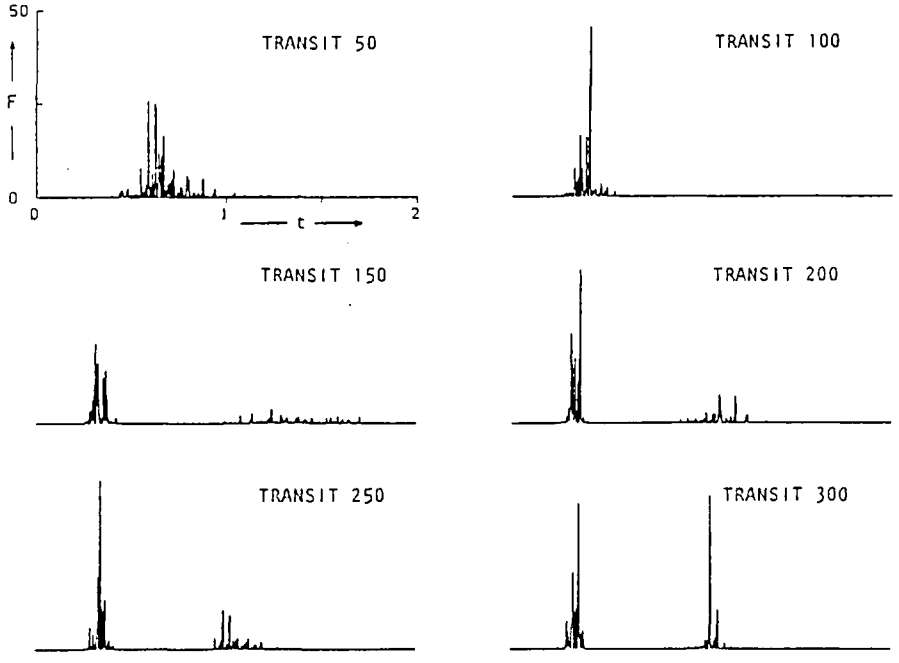


FIG. 8.30b

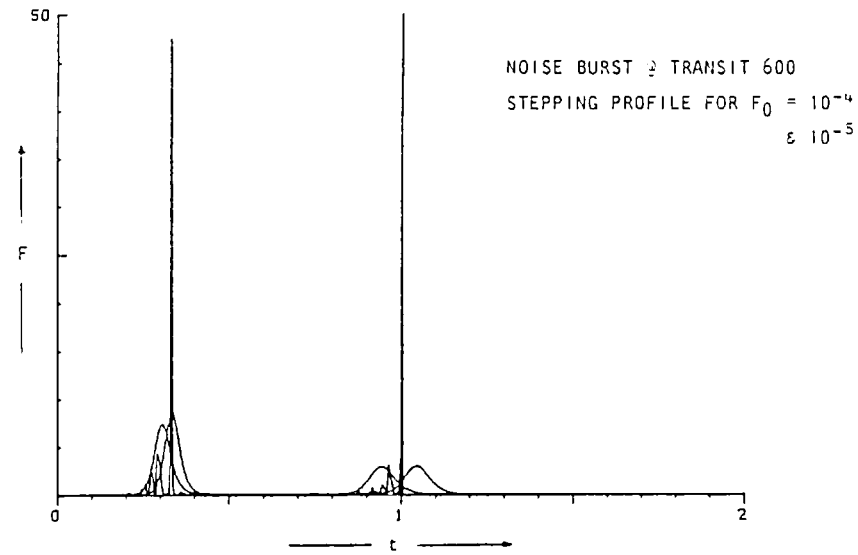


FIG. 8.31a

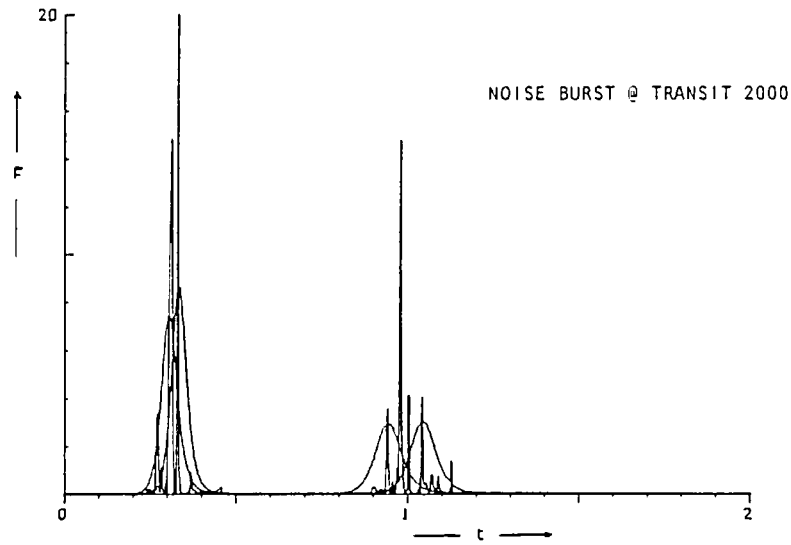


FIG. 8.31b

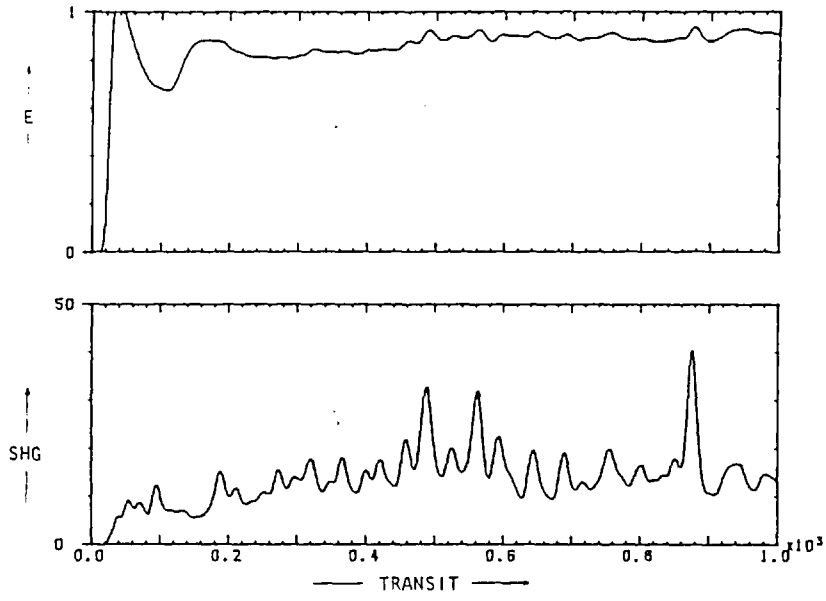


FIG. 8.32

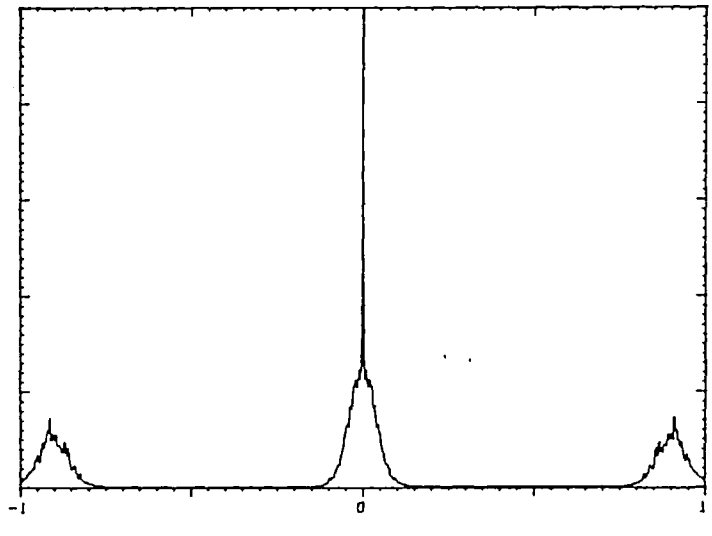


FIG. 8.33

$P_A = 2.0$, $P_B = 0.5$, $\Gamma = 0.5$, $T_f = 0$, $t_m = 0.002$

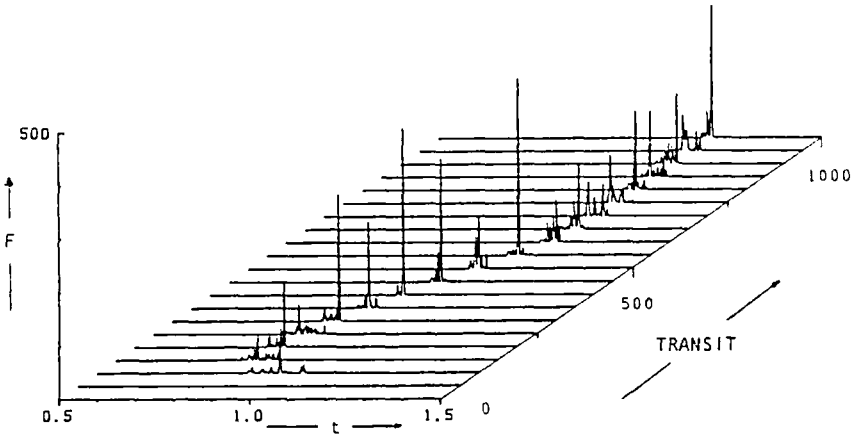


FIG. 8.34

$P_A = 2.0$ $T_{1a} = 1000$
$P_B = 1.3$ $T_{1b} = 1000$
$s = 2$ $T_{cav}/T_{1a} = 1$
$T_f = 0$ $T_{cav}/T_{1b} = 100$
$t_m = 0.002$
$\Gamma = 0.5$

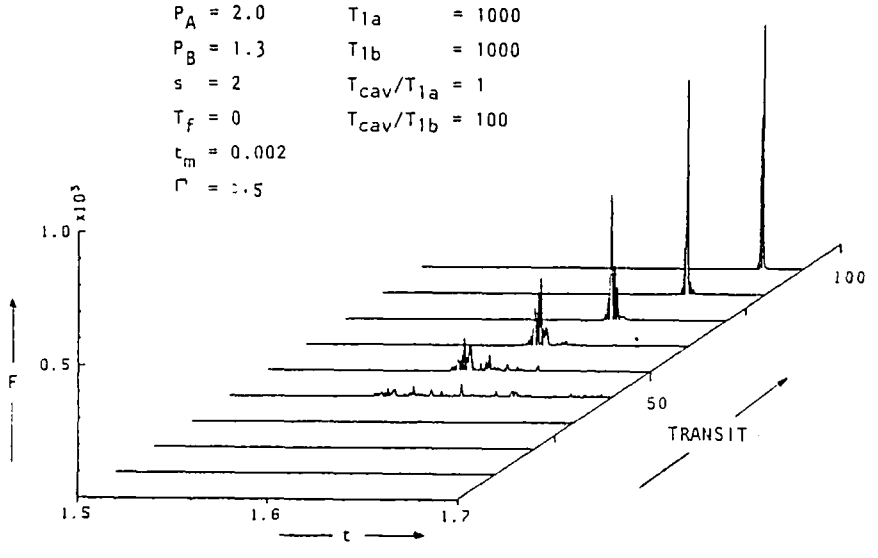


FIG. 8.35

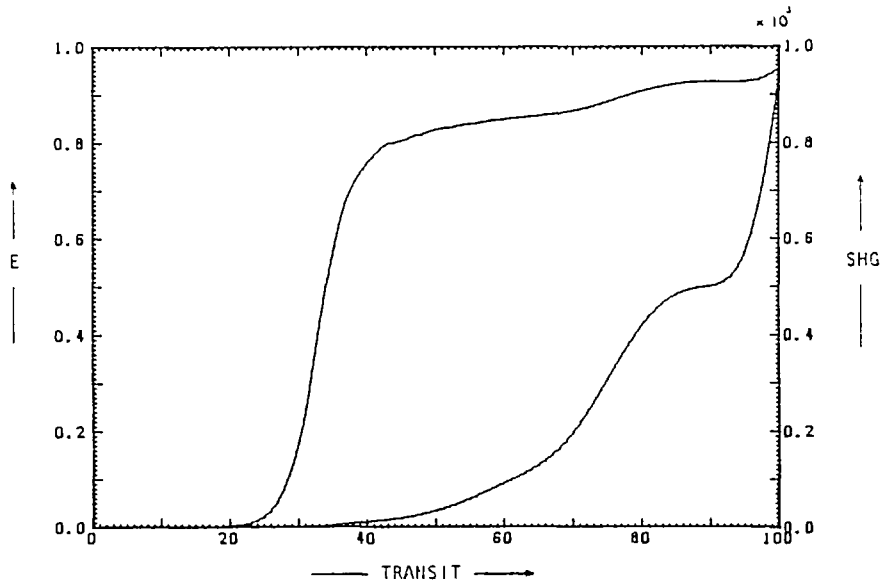


FIG. 8.36

$P_A = 2.0$, $P_B = 0.5$, $T_f = 0$, $t_m = -0.01$, $s = 2$,

$T_{1a} = 1000$
$T_{1b} = 0.2$
$T_{cav}/T_{1a} = 1$
$T_{cav}/T_{1b} = 1000$

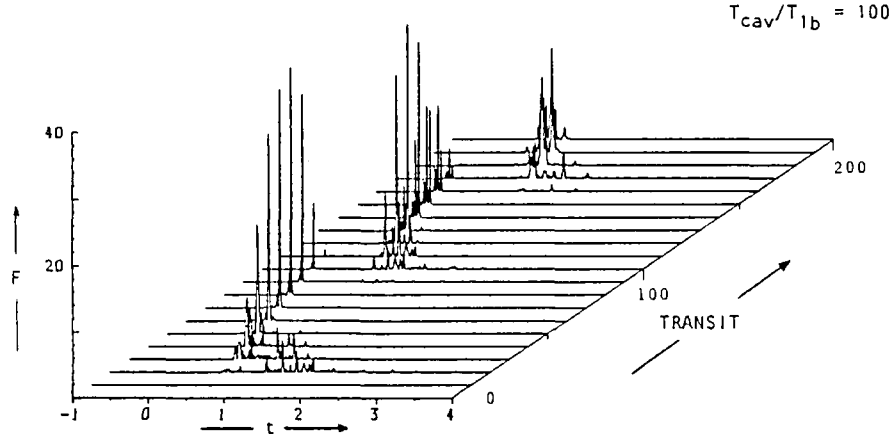


FIG. 8.37

energy is in good agreement with the stepping model. The average intensity level of the noise feed is 10^{-5} and fig.8.31a&b show the pulse at 600 & 1000 transits together with the stepping profiles (without continuous noise addition) for this and a higher noise level. The variation of the fundamental and second harmonic energies is shown in fig.8.32 and the autocorrelation, averaged over 1 in 10 profiles, in fig.8.33.

The hybrid stepping results show that a moderate saturable absorber level can appreciably enhance the "Q-switching" providing that the pump is strong enough. The resulting pulse compression will not neccessarily be accompanied by the claimed increase in stability, however. For distinct positive mismatch the noise fluctuations will be fed across the stepping model envelope. The absorber simply compresses the envelope and does not select and maintain a single noise spike. Consequently, if the absorber compresses the envelope down to the width of a noise spike the fluctuations in the energy may actually get worse. Fig.8.34 shows the evolution in the presence of a moderate absorber. The location of the pulse agrees roughly with the stepping model. The intense compression in the "strong" regime, with a large value of the absorption, is shown in fig.8.35, up to the point where the integration of the rate eqution breaks down, and the energy in fig.8.36. The weaker compression acting in the self-pulsation in a negatively mismatched cavity is seen in the stable oscillation in fig.8.37.

Chapter 8 : References

1 Arecchi,F.T. Meucci,R., Puccioni,G., Tredicce,J. - Phys. Rev. Lett., **49**, 1217 (1982)

2 McDonald,D.B., Waldeck,D., Fleming,G.R. - Opt. Commun., **34**, 127 (1980)

9

CONCLUSION

A general solution of the coupled differential/time delay equations for the steady-state pulse shape appears to be difficult. Abandoning the search for "analytic" solutions, the profile has been studied as a nonlinear oscillation in local time, showing different types of behaviour depending on the conditions. This numerical approach gives a clearer picture at moderate computational cost. The numerical studies of the evolution form a consistent picture, showing the control of the evolution by both the mismatch and the filter response time. The inclusion of a process with a finite memory time in the stepping equations is, however, only possible when the mismatch time is much less than T_f: that the general case remains unsolved reflects the difficulty of extrapolating a time evolution for a period longer than the characteristic times of the system. As we have already remarked, this does not seem to be a serious problem as far as the noise-free profiles are concerned.

The problem lies in the incorporation of noise fluctuations. A fluctuating profile cannot be predicted by a steady-state algorithm but it is neccessary to consider under what, if any, circumstances the pulse can be fully modelocked and to what extent the steady-state algorithm can predict the time average of the fluctuating envelope. For mismatches longer than T_f the pulse duration is roughly proportional to t_m and the transit time of a fluctuation across the profile is independent of mismatch. If this is too short for the filter to smooth out the fluctuation, then it will be so for all positive mismatches. When the cavities are matched, noise structure will still diffuse across the profile. As remarked in ch.8, the diffusion only becomes stationary as $t_m \rightarrow T_f$ and the envelope is on the verge of collapse.

Although the general picture of the transition from broad profiles at long cavity lengths through increasing satellite formation to the very long pulse solution for negative cavities is in general agreement with experimental observation, some important aspects remain in doubt. The noise level used for most of the results was based on a very crude estimate of the fluorescence power fed back by the mirrors. If the pump is assumed to be around 100ps long, very

few of the pulse profiles shown for this value are as short as 1 ps and satellite formation appears to be inevitable: the position would be much improved by reducing the initial value by several orders of magnitude. We have also argued that the pulse should only be "modelocked" - i.e. the noise fluctuations are fully controlled - when the mismatch is slightly negative. However, there have been several reports that properly modelocked autocorrelations were seen only when the cavity length was longer than that at which satellites formation was apparent. It will be neccessary to simulate the effect of noise fluctuations properly before the autocorrelation results can be interpreted with confidence. The satellites seem to be sufficiently evenly spaced to show in the autocorrelations but the perturbed mismatch evolution in ch. 8 showed marked suppression of the satellites in the average autocorrelation. On the other hand, the deep modulation of the pulse in the presence of pump perturbation has almost no effect on the autocorrelation. It should be noted that measurements averaged under sinusoidal perturbation are weighted in favour of the extreme values in contrast to random distributions.

The treatment has also ignored the possibility of inhomogeneous broadening. Kuhl et al. [1] remarked that "peaks or modulations in the pulse spectra were found to indicate the presence of multiple pulses or pulse substructure (under which conditions the autocorrelation had a broad shoulder) and this raises tne possibility that satellite pulses might be centred in different parts of the spectrum. We may also note that when the pulse contains sharply modulated satellites each reforms from the noise in isolation from the others. If the mismatch is large enough for the noise to diffuse across the pulse, then the satellites will to some extent be decorrelated from each other.

The stepping approach can be extended to include processes not so far considered. When these do not involve a fast relaxation time, extension will be simple: for example to rate equations which include pump saturation effects. Of greater significance will be the lifting of the rate equation approximation. The field and polarisation equations in the slowly varying amplitude and phase approximation

$$\dot{P} + \frac{P}{T_{2a}} = -iAE\frac{c\varepsilon_o}{T_{2a}\omega_o}$$

$$\dot{A} + \frac{A}{T_{1a}} = \text{Pump} - \frac{\sigma}{\hbar} Im(EP^*)$$

$$\left[\frac{\partial}{\partial z} + \frac{1}{c}\frac{\partial}{\partial t}\right]E = \frac{i\omega P}{2\varepsilon_o c} - \frac{1}{2}E\Gamma$$

$A_u = 1.2$ $T_{1b}/T_{cav} = 0.2$
$B_u = 0.2$ $T_f/T_{cav} = 0.004$
$\Gamma = 0.2$ $t_{mesh}/T_{cav} = 0.002$
$N = 10^{-5}$
$s = 5$

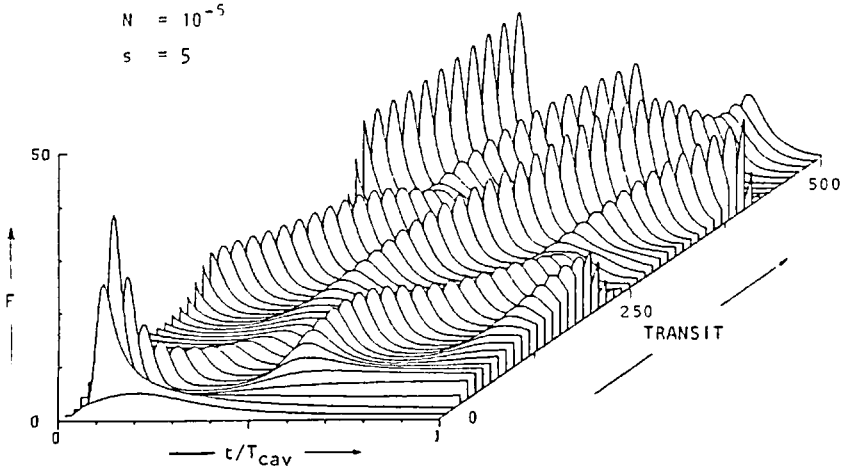


FIG. 9.1 : Passive modelocking (ring cavity, sech start)

$A_u = 1.2$ $T_{1b}/T_{cav} = 0.2$
$B_u = 0.8$ $T_f/T_{cav} = 0.004$
$\Gamma = 0.2$ $t_{mesh}/T_{cav} = 0.002$
$N = 10^{-5}$
$s = 5$

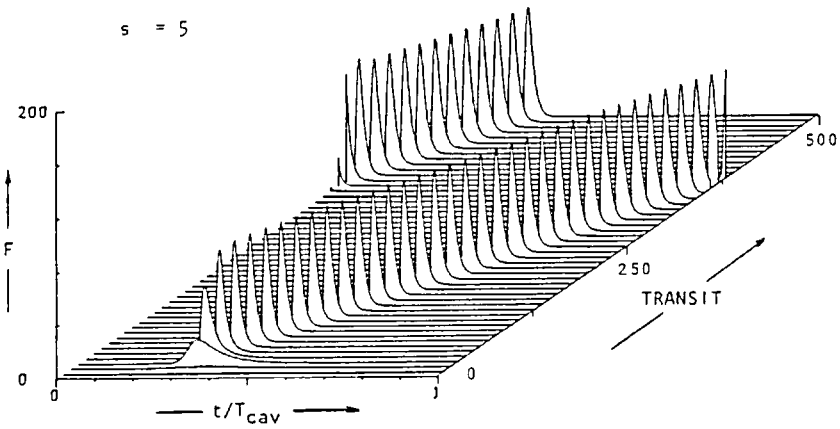


FIG. 9.2

$A_u = 2.0$ $T_{1b}/T_{cav} = 0.2$
$B_u = 0.8$ $T_f/T_{cav} = 0.004$
$\Gamma = 0.2$ $t_{mesh}/T_{cav} = 0.002$
$N = 10^{-5}$
$s = 5$

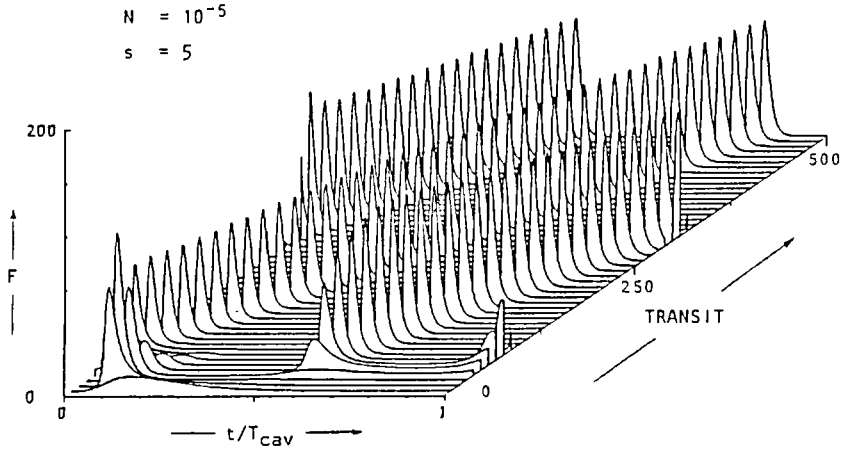


FIG. 9.3

can be subjected to the stepping method when $t_m << T_{2a}$. There is now an extra degree of freedom, however: while the intensity envelope may be self-reproducing the phase profile may not. Chirped behaviour was obtained by Mourou and Sizer [2] in a synchronously pumped system producing pulses of less than 100 fs. A preliminary investigation, treating the profiles as strictly self-reproducing and using a very crude integration, has produced stable results which are very similar to the stepping model. The fabry-perot etalon can be retained, and, in the complex amplitude treatment, extended to the off-resonant case simply by adding a phase factor.

The analogy between the steady-state equations and the evolution of a giant pulse has already been drawn by Khandokhin et al. [3] for the case of passive modelocking, although it was noted that the requirement that net gain precede the pulse was contrary to the requirements for stable passive modelocking. The etalon filter can be incorporated into the rate equation model of passive modelocking but it appears not to be possible to derive a stepping model for the steady state. Figs.9.1a-c show the evolution of the pulse from a small $sech^2$ start pulse. In (a) there is insufficient absorber and pulsed operation is unstable. In (b) increased absorber level leads to strong compression, showing the rapid backwards drift of the pulse, while high amplifier and absorber levels lead to stable double pulsing (c). For the parameter ranges investigated so far, operation under the conditions in (b) often results in a pulse of width $\sim 5 \times T_f$ and a slip/transit of as much as $T_f/2$. If this is generally the case then the operator expansions and perturbation treatments used in much of the literature may be invalid.

The results for strong hybrid modelocking presented in ch.8 show that the synchronous steady state is unstable in the presence of strong nonlinearity. Long period relaxation oscillations have already been reported for a passively modelocked dye laser by Diels et al. [4]. In a carefully optimised Rh-6G/DODCI system producing pulses as short as 60 optical cycles, it was observed that minimum pulse duration was associated with a relaxation oscillation near 50 KHz. By applying a pulsed modulation at the frequency (or a submultiple) of the oscillation, the evolution of the pulse during the cycle could be studied. The very long period of the strong hybrid oscillations occurred through a small slip relative to a fixed clock. This reference is not present in the passively modelocked system, but there might possibly be other "memory" mechanisms, for example a continuously varying phase perturbation on the pulse. A simple

consideration of the conditions for the maintainance of a stable pulse in the presence of spontaneous emission suggests that loss on both the leading and trailing edges is neccessary. If the absorber recovers fairly quickly, however, it may be possible to sustain pulsed operation with net gain on the immediate trailing edge. The pulse would then be continuously drawn backwards into a short interval of net gain, controlled by the absorber recovery, just as the synchronously pumped pulse is drawn forwards. Throughout this interval fluctuations would grow from the noise and their relative importance would depend on how long the main pulse took to catch up with them. For absorber recovery times which were not quite fast enough the growth of fuctuations in the tail of the pulse might lead to erratic restarting of the pulse.

Chapter 9 : References

1 Kuhl,J., Klingenberg,K., von der Linde,D. - Appl. Phys., **18**, 279 (1979)

2 Mourou,G.A., Sizer,T. - Opt. Commun., **41**, 47 (1982)

3 Khandokhin,P.A., Khanon,Y.I., Matorin,I.I. - Opt. Commun., **27**, 111 (1978)

4 Diels,J.-C., Menders,J., Sallaba,H. in "Picosecond Phenomena II" ed. Hochstrasser,R., Kaiser,W. SHank,C.V. (Springer Verlag, Berlin, 1980)

ACKNOWLEDGMENTS

This work could not have been carried out without the extended patience of my supervisor, Prof. G.H.C. New, and the support given by my parents, and by T.E.A. and D.A.: to them all I am most grateful.

It is a pleasure to acknowledge the encouragement given by many members of the optics section, in particular Dr. P.M. Radmore, who collaborated on some parts of the work, and Dr. P.L. Knight.

I am also particularly grateful to Prof. E.M. Freeman (Electrical Engineering Dept., Imperial College) for the organisation of financial support and, with Dr. C.F. Bryant, the extension of substantial computing facilities.

Finally, the work owes its completion to G.K. Beckmann and M.A.R. Hardwick, who made their microcomputer facilities freely available and gave more than generously of their time and effort during the final weeks.